26+ Year Old Photovoltaic Power Plant: Degradation and Reliability Evaluation of Crystalline Silicon Modules – North Array

by

Jonathan Belmont

A Thesis Presented in Partial Fulfillment
Of the Requirements for the Degree
Master of Science in Technology

Approved April 2013 by the
Graduate Supervisory Committee:

Govindasamy Tamizhmani, Chair
Mark Henderson
Bradley Rogers

ARIZONA STATE UNIVERSITY

May 2013

ABSTRACT

The object of this study was a 26 year old residential Photovoltaic (PV) monocrystalline silicon (c-Si) power plant, called Solar One, built by developer John F. Long in Phoenix, Arizona (a hot-dry field condition).

The task for Arizona State University Photovoltaic Reliability Laboratory (ASU-PRL) graduate students was to evaluate the power plant through visual inspection, electrical performance, and infrared thermography. The purpose of this evaluation was to measure and understand the extent of degradation to the system along with the identification of the failure modes in this hot-dry climatic condition.

This 4000 module bipolar system was originally installed with a 200 kW DC output of PV array (17^{o} fixed tilt) and an AC output of 175 kVA. The system was shown to degrade approximately at a rate of 2.3% per year with no apparent potential induced degradation (PID) effect. The power plant is made of two arrays, the north array and the south array. Due to a limited time frame to execute this large project, this work was performed by two masters students (Jonathan Belmont and Kolapo Olakonu) and the test results are presented in two masters theses. This thesis presents the results obtained on the north array and the other thesis presents the results obtained on the south array. The resulting study showed that PV module design, array configuration, vandalism, installation methods and Arizona environmental conditions have had an effect on this system's longevity and reliability. Ultimately, encapsulation browning, higher series resistance (potentially due to solder bond fatigue) and non-cell interconnect ribbon

breakages outside the modules were determined to be the primary causes for the power loss.

ACKNOWLEDGMENTS

I am extremely grateful to my advisor, Dr. Govindasamy Tamizhmani, for his expertise and leadership. It is truly an honor to learn from such a knowledgeable icon in the solar world. It has been an excellent experience to work with him and the Arizona State University Photovoltaic Reliability Laboratory (ASU-PRL).

I would like to express my appreciation to committee members Dr Henderson and Dr Rogers for their patience with this thesis development. Their example and "Global Resolve" was a profound influence for expanding my ideas of community and energy.

I cannot thank Martha Benton enough for her support. She has been a valued irreplaceable asset to me and many other grad students. She has been there since the day that I applied for grad school and has assisted me throughout the process.

My sincere appreciation also goes to Bill Kazeta, who patiently assisted our team on the Solar One site. His years of experience were an invaluable resource for us.

I would also like to thank the Salt River Project team for giving PRL and our research team the opportunity to study this site.

The John F. Long's home owners association of the Solar One sub division along with Stanley Pellow were excellent hosts for letting us on the site to review their power plant.

I would like to thank the John F. Long Foundation for the photos and history information. They were instrumental in my quest for the hidden history of Phoenix and the interesting influence that John F. Long had on the future of solar energy.

I would also like to thank Joseph Kuitche and the PRL crew that assisted us with gathering the data and with research. They helped to focus the laborious effort of collecting array data efficiently. It was an enjoyable experience working with Sai Tatapudi, Suryanarayana Vasantha Janakeeraman and Jaya Mallineni.

I cannot forget to include the wordsmith expertise of Richard Starling. He helped solidify the writing flail. Thank you very much to my final thesis checker and great friend, Joanne Swann, thank you for your eagle-eye error-catching astuteness.

Lastly I would like to thank Kolapo Olakonu for his work on the south array and for his expertise for infrared photography and all the additional lab work on this project.

DEDICATION

This thesis is dedicated to my daughter Kayla. We dedicate our work to your green energy future!

TABLE OF CONTENTS

Page

CHAPTER Page

CHAPTER Page

CHAPTER Page

LIST OF TABLES

Table Page

LIST OF FIGURES

Figure Page

Figure Page

Figure Page

LIST OF VARIABLES

A= Current in Amperes

In^2 = Square Inches

W/m^2= Watts / $Meter^2$

kW = *Kilowatts*

V = Voltage

I = Current

I_{sc} = Short Circuit Current

V_{oc} = Voltage Open Circuit

MWh = Megga Watt Hour

FF = Fill Factor

STC = Standard Test Conditions (25^oC, 1000 W/m^2)

CHAPTER 1

INTRODUCTION

1.1 Background

Solar photovoltaic (PV) industry is one of the fastest growing industries in the world. Degradation and reliability assessments of existing field aged PV systems are important to study to see the long term factors affecting modules, strings, and the system. These studies of the past can help us understand and reinforce current construction and assembly design to create a better PV modules and system.

John F Long was a pioneer developer and builder in Phoenix, Arizona. He built affordable residential homes and was on the cutting edge with his building techniques and his realization of the benefits of solar applications in his neighborhood developments.

Reprinted by authorization of John F. Long Foundation

Figure 1- John F. Long Solar Rooftop

In the 1980's Mr. Long worked with the Department of Energy developing the groundwork for power quality analysis technology [1]. The inverter harmonic analysis that was developed was intended to be used for rooftop photovoltaic solar systems The cost of rooftop systems at the time proved to be not cost effective [2]. This helped to launch Solar One residential PV power plant, a 17^{o} fixed tilt south facing array.

The Solar One array system is located at N 71st Ave & W Osborn Road in West Phoenix and was installed November of 1985 to serve 20 houses in the adjacent Solar One neighborhood to the north.

Beginning in the summer of 2011, the Solar One power plant was our topic of study. Salt River Project (SRP) electric company requested assistance from the Arizona State University Photovoltaic Reliability Lab (ASU-PRL) to investigate the Solar One PV power plant to evaluate its current state of operation and efficiency. This project was directed by Dr Govindasamy Tamizhmani and site supervised by Bill Kazseta.

The study of such a power plant is important from many respects. Since the array has had many years of operation, SRP would like to determine the state of degradation with any issues that are important such as shock hazard safety. Additionally, lessons learned from the past can be applied to the present.

Reprinted by authorization of John F. Long Foundation

Figure 2- Solar One Residential Power Plant in Phoenix in 1986

1.2 Statement of Problem and Scope

Degradation is a natural process of a photovoltaic (PV) system. Once modules and systems degrade to a significant level the energy output of the system is greatly affected. Evaluating and pinpointing the extent of this degradation and failures of Solar One was the team's goal.

The team's study was a co-operative effort between Kolapo Olakonu and Jonathan Belmont with Bill Kazseta as on site advisor and supervisor. The array was split into north and south sections Kolapo Olakonu and Jonathan Belmont worked side by side performing tests on the entire Solar One array. The same analysis was used for the north

array and south arrays. Kolapo Olakonu was assigned the south array and presented his Thesis November 2012. The following findings presented here are of the north array.

The entire array contains 4,000 frameless 50W M54 Arco modules. We were to review electrical performance of the modules, along with visually inspecting and photographing the modules using both a standard camera and an infrared thermography camera. We were also to investigate Potential Induced Degradation (PID) since this could be a cause of deterioration on the positive ground side of a bipolar array.

The DC side of the array was the focus of the study. We did not do any in-depth review of the inverter or the AC side of the output.

The entire investigation would have to be non-intrusive without disrupting or damaging modules. Evaluation of the system could only be performed through analyzing groups of accessible data. These groups would entail sub-arrays, panel groups and individual modules. However, only "new" stored modules for possible replacement separate from the array were possible to test.

1.3 Scope of Study

- Determine the state of the system
- Review causes of anomalies
- Review any performance degradation of the system and determine the possible causes for degradation and failure modes.
- Report results to SRP for their overall evaluation of the system.
- Report the results to the Solar PV industry illustrating degradation and performance issues resulting from design and cyclic weathering.

1.4 Scope of Project

The Solar One array is made of 8 sub-arrays composed of 100 panel groups with a total of 4000 (50 Watt) modules. Splitting the system in half, the electrical performance system was tested first by taking current- voltage (I-V) curves over the north 4 sub-arrays and 50 panel groups.

Additionally we were to:

- Study new modules for baseline performance curves
- Perform low light testing with uniformly shaded modules
- Record I-V curves for sub-arrays and panel groups
- Normalize I-V curves for relative comparative analysis
- Conduct Megger testing to record leakage current
- Review possible temperature gradient differences along the length of the array
- Compare output results of each section while reviewing causes of possible accelerated degradation and failure modes.

Since many of the modules have been replaced, reassembly alignment and faulty sealing materials may have accelerated the interconnect ribbon breakage from thermal expansion. Water intrusion added to corrosion and further degradation. It is hypothesized that ribbon design and site assembly methods along with stone-throwing vandalism may have contributed to the 40% power difference between the lower performing East array and the better performing West array.

Potential Induced Degradation (PID) was found to be not a factor since the arid conditions of Arizona are not favorable for PID and/or the cell technology had a different

anti-reflective coating (titanium dioxide as opposed to current silicon nitride). However, it was found that the dry desert environment resulted in an extensive browning effect of the encapsulate.

Reprinted from Google Maps

Figure 3- Solar One Residential Power Plant in Phoenix in 2012

CHAPTER 2

LITERATURE REVIEW

2.1 Previous Studies of the Solar One Power Plant

There were a few early reports recording details of the Solar One power plant [2] [3] that were helpful supplements for our study. These studies were performed during the first 10 years of operation. One report even included a detailed failure analysis of a similar system in Austin Texas [4] that confirmed some of our conclusions. These reports are important because they can give us a snapshot of the past in terms of design and data.

Examining this original data, we can extract and plot out points and compare them to today's values. From this data we can determine the degradation rate and explore other issues that may have played a part in the decline of the system. The Austin study was a great find since it validated our hypothesis and previous findings that the premature failure of the non-cell conducting ribbons from the modules to the copper busbar contributed significantly to system deterioration.

2.1.1 Austin Solar Power Plant Report

We discovered the Austin study a few weeks before this thesis was released. The report was titled, "Module Field Experience with Austin's PV Plants" and written by John E. Hoffner [4]. The Austin PV Plant was comprised of the same modules and panel group design as Solar One. It was installed in 1987, two years following the installation of Solar One. Hoffner's findings contributed significantly to our Solar One investigation.

The Hoffner report substantiates our hunch that the failure of the conductive ribbons was a major cause of system decline

This plant contained a total of 6160 modules of the same module and panel design as Solar One. A team studied The City of Austin's Electric Utility Department power plant as it was being constructed. Tests were conducted by the New Mexico Solar Energy Institute. The testing procedure consisted of shading one to three modules while measuring the current through each bypass diode.

During installation they found 39 modules that were non-functioning. Within three months after installation the total of failed modules increased to 100. This failure quantity was high enough to convince Arco to assign a special task force to investigate the failure.

Arco attributed the failure of the ribbons to the busbar expansion. They found that most of the shearing was located at the spot welded point on the busbar. Arco suggested cutting the plastic to prevent the different rates of expansion between the copper and the plastic busbar cover.

The Austin inspection team could physically remove and investigate the causes of module failure as it happened. This was not possible for us since this would have been a destructive investigation years after the fact of failure. Instead, we used an infrared detection method.

The Hoffner report found:

- Ribbon shear is due to thermo cycling of the busbar

- Seal cementing held ribbons in place, causing a lack of flexibility which contributed to shearing forces tearing the conducting ribbon

2.1.2 Early Signs of Vandalism

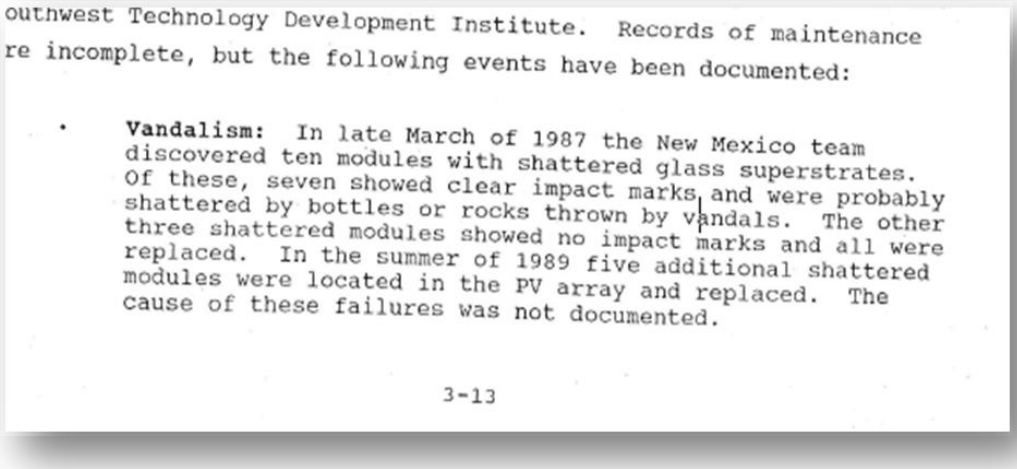

outhwest Technology Development Institute. Records of maintenance re incomplete, but the following events have been documented:

- **Vandalism:** In late March of 1987 the New Mexico team discovered ten modules with shattered glass superstrates. Of these, seven showed clear impact marks and were probably shattered by bottles or rocks thrown by vandals. The other three shattered modules showed no impact marks and all were replaced. In the summer of 1989 five additional shattered modules were located in the PV array and replaced. The cause of these failures was not documented.

3-13

Reprinted from Southwest Technology Development Institute

Figure 4- Vandalism mention from 1989 report [2]

Early reports on the Solar One plant noticed evidence of vandalism. They found that in 1987 ten modules were shattered. Seven of these modules were obviously vandalized, including three with no clear cause of breakage.

2.2 Vandalism

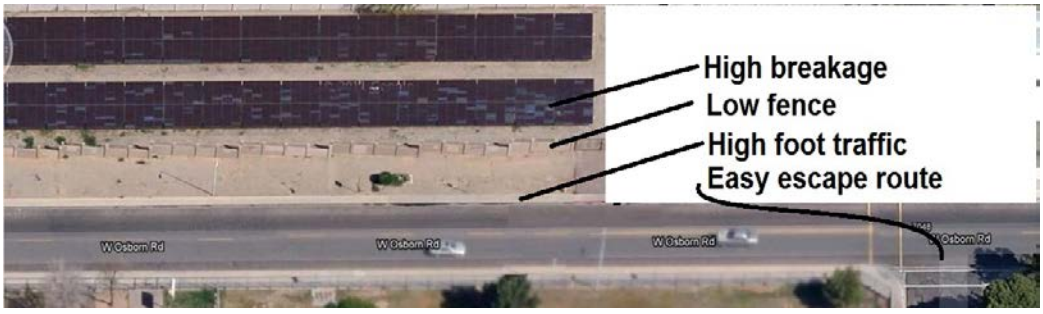

Reprinted from Google Maps

Figure 5- East Side of Array With Heavy Vandal Impact

There are a few factors that could possibly contribute to increased vandalism. A high level of pedestrian traffic creates a greater opportunity for damage. As an example, an elementary school was built directly across the street from the array around the year 2000. It is interesting to note that in Figure 5 a large number of broken modules can be seen on the south array, and especially the south east corner. These panels are closer to the fence and easier to hit with rocks or other objects tossed by vandals. Broken and replaced modules show up as the lighter color rectangles. The city of Philadelphia solar guidebook [5] states that "ground-mounted arrays are more susceptible to vandalism than pole or roof mounted systems." It also states that solar designers need to consider a safe location and that the array should be protected from vandalism without "compromising energy production."

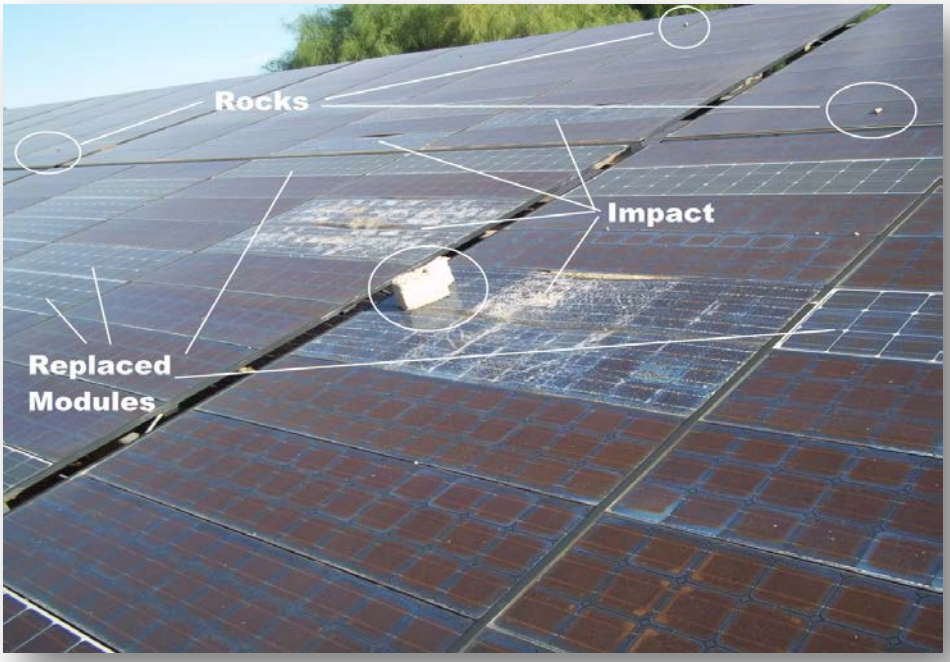

Figure 6- East Side of Array with Vandalism Evidence

Considering that there were a high number of broken and replaced modules over the years and there was a fence, a low fence would appear to lack the security necessary to prevent damage from vandalism. Perhaps a simple remedy would have been a higher fence that would obscure the array.

Figure 7- Low Fence

2.3 Module Design Flaws

The design of the panel group assembly has some inherent design issues involving the conducting ribbons [4]. Figures 20-22 show the layout of the “panel group”(PG) and how these conducting ribbons are connected. Each PV module is bonded and glued to the busbar shown in Figure 8. This glue held the conducting ribbon causing it to tear as the busbar thermally elongated. The Austin report indicated this assembly issue was a major contributor to a 30% failure rate in the first few months of operation for the Austin array.

Today's module designs and packaging enclosures are much cleaner and isolated from this old exposed power design. Modern PV solar designs account for thermal expansion and are tested for mechanical cyclic failure [6].

Figure 9 below shows details of the backside of the typical Solar One Panel Group. The busbar can be seen running down the center connecting the modules in parallel. The ribbons at the end of each panel connect to the busbar.

2.4 Incorrect Assembly Methods

The damaged modules on the array were replaced in the field. They had to be removed by cutting busbar seals and the glue holding the module in place. Correct reapplication of a new module to the panel group is important in terms of safely and premature failure. The conductive ribbon alignment is critical since thermal expansion [7] has an impact, potentially causing the ribbons to crack and eventually break into an open circuit.

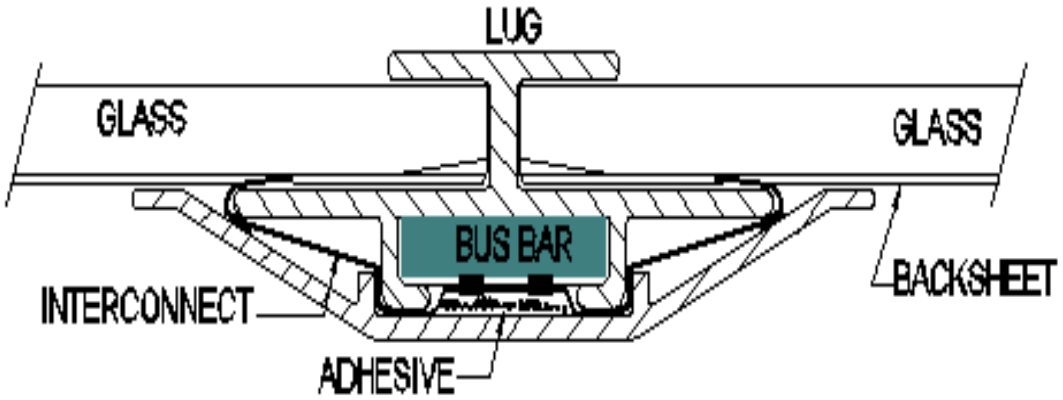

Figure 8- Cross Section of Busbar and Module Connection

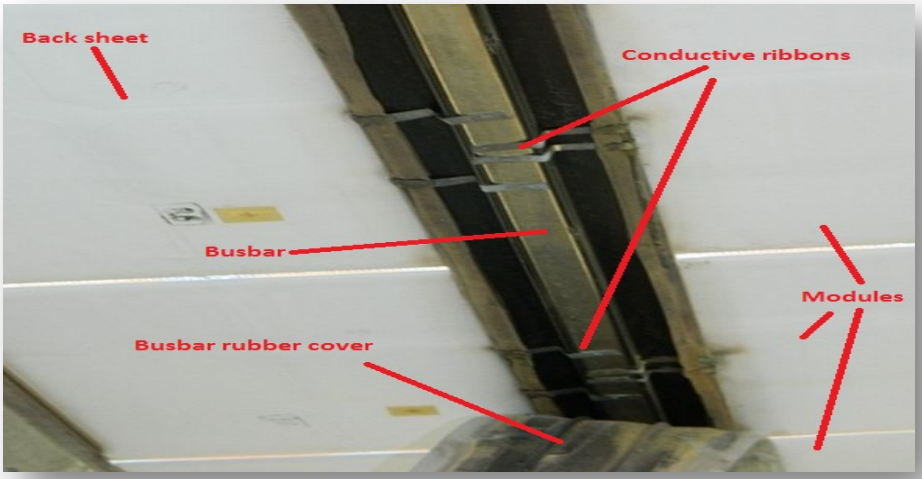

Figure 9 – A View From Under Panel Group

2.5 Degradation and Failure of Packaging Materials

Several events lead to the failure of the system components. It is difficult to assign all of the blame for ribbon failure to improper reassembly techniques since the original ribbon design was not of a structurally sound nature. However, each component and assembly method contributed to the end result, an increase in series resistance and encapsulant browning.

Figure 10 Failed Busbar Seal

A failure of the seal can be shown by the photo in Figure 10. It clearly shows that the type of seal used degraded over time and failed.

2.6 Ribbon Fatigue from Cyclic Loading

The main component that had the greatest effect on array performance is the thin connecting ribbon. Incorrect reassembly puts even greater stresses the ribbons. Once the ribbon cracks (and breaks) the current is restricted from flowing. This effectively gives a higher series resistance which had a large affect on the panel group I-V performance.

The mechanics of ribbon failure is an interesting ending to a series of effects. The choice of a thin ribbon to conduct the electrical current in place of cables with connectors does not seem to be a good choice of a conductor. Conducting materials that can flex for changing conditions would prevent this type of mechanical stress failure.

2.7 Corrosion Degradation

The busbar shown in Figure 11 is covered with a protective seal that can degrade over time. During the Arizona rain, water can intrude into and onto busbar. This seal was proven to be ineffective on the three panel groups that we examined during wet Megger testing.

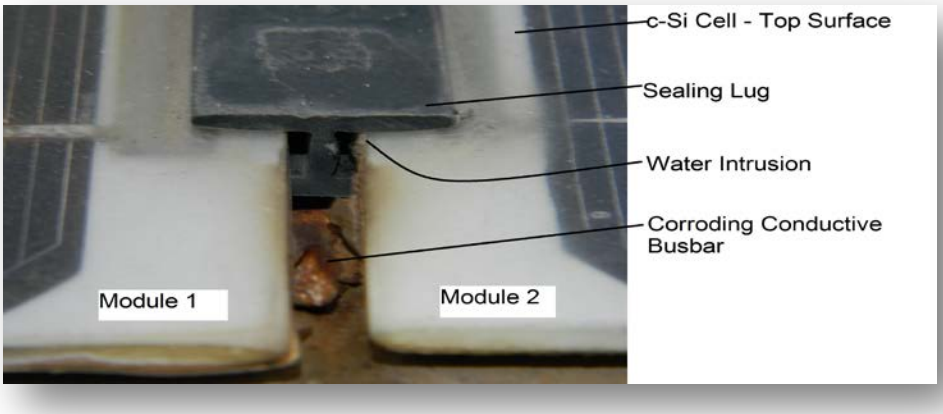

Figure 11- Busbar Sealing Lug and Corrosion

2.8 System Degradation

The overall performance degradation of any physical device or system is inevitable. Stresses can be from heat, electrical conduction, UV and other environmental conditions and can affect any part of the system.

A well-sealed crystalline silicon solar cells [8] generally has long term field life. The modules manufactured today generally have a warranty life of 20-25 years.

2.8.1 EVA Browning

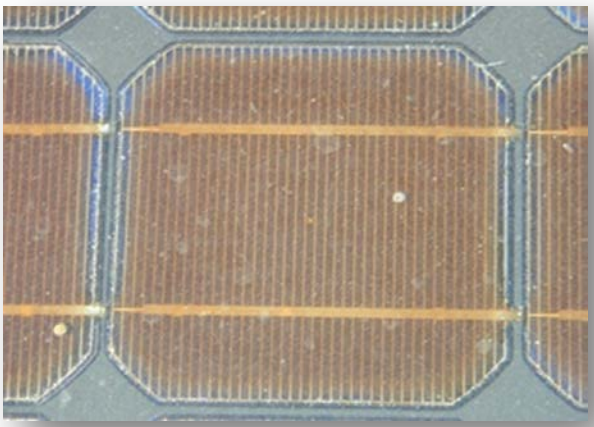

Figure 12- Typical EVA Browning

One common degradation condition comes from EVA browning. Most modules use a polymer as an encapsulate between the glass cover and the PV cells called Ethylene Vinyl Acetate (EVA.) Appropriate EVA formulation is a good choice because it can withstand UV and, transparent sealer for the solar PV cells and internal conducting ribbons. However, EVA browning becomes an effect when UV rays begin to degrade the EVA [9]. Additionally, as the EVA degrades it can form acetic acid that corrodes internal cell ribbons.

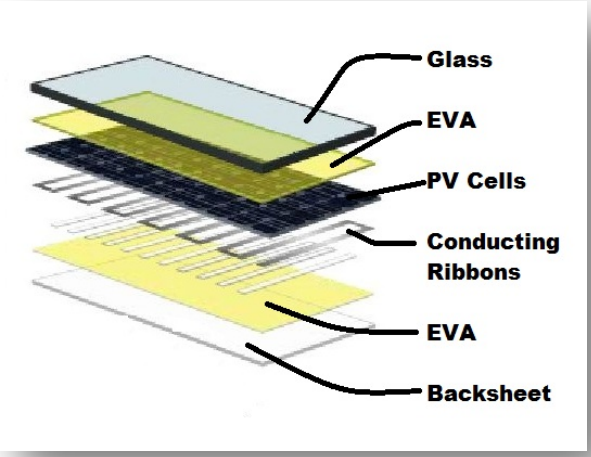

Figure 13- Typical PV Layer Construction

2.8.2 Cell Metalization

A JPL study showed that potential differences between two charged cells or between the cell and grounded frame could cause cell metallization degradation [10].

The result of this reaction is the deposition of dissolved metal and dendrites formation. Solar One has both positive and negative grounding in a bipolar system. Solar One's cells could exhibit, if significant moisture is present inside the laminate, either a plating affect from the positive ground or a corrosive effect from negative grounding.

2.8.3 Parasitic Resistances

Modules have two basic pathways for electron flow [11]. Internal series resistance in a module comes from the resistance of cell/module materials and devices. The series resistance should be as low as possible and the shunt resistance has high as possible for an efficient cell

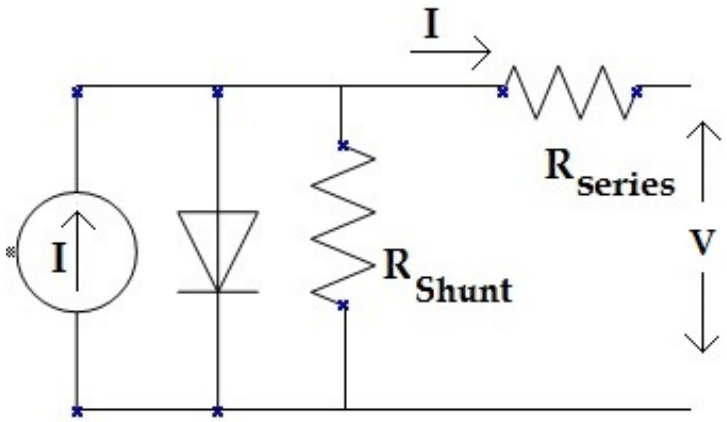

Figure 14- Example of Shunt and Series Resistance Circuit

Parasitic losses result when either the series resistance is high or when the shunt resistance is too low. The electron pathway should easily flow through the circuit and not shorted by the shunt resistance.

Figure 15 below shows an example of three IV curves. The ideal curve is compared to the typical parasitic IV curves.

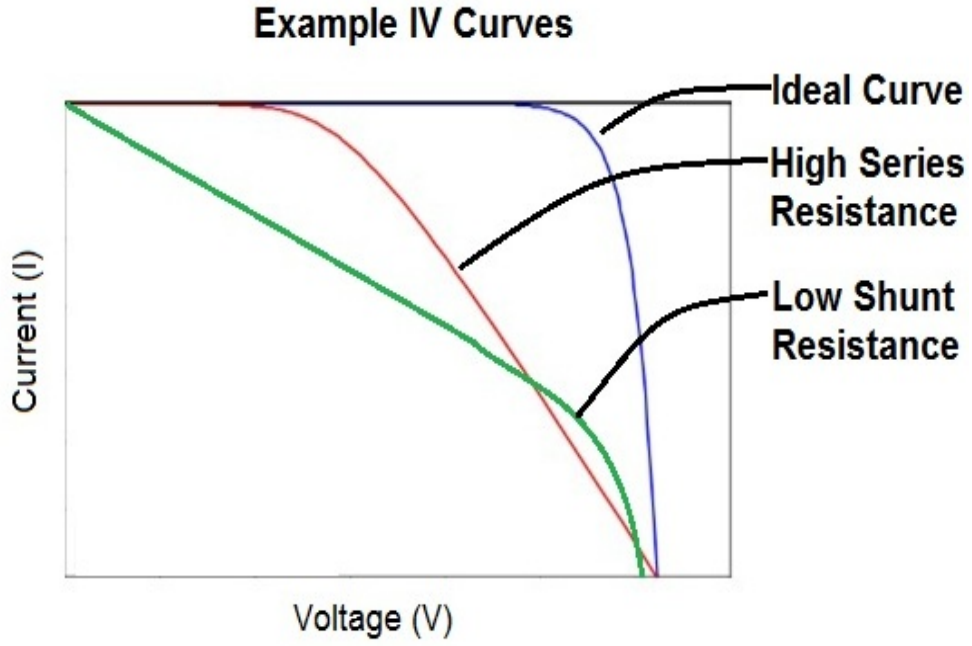

Figure 15- Example of Shunt and Series Resistance in IV curves

2.9 Bipolar Arrays

Bipolar arrays are a way to stay below the 600 volt limit set by Article 690.2 of the National Electric Code (NEC). The Solar One array was designed as a bipolar system to keep the string voltage less than 600 volts. This system was designed for a maximum voltage of +375 volts on one end of the array and -375 volts on either side of the PV array.

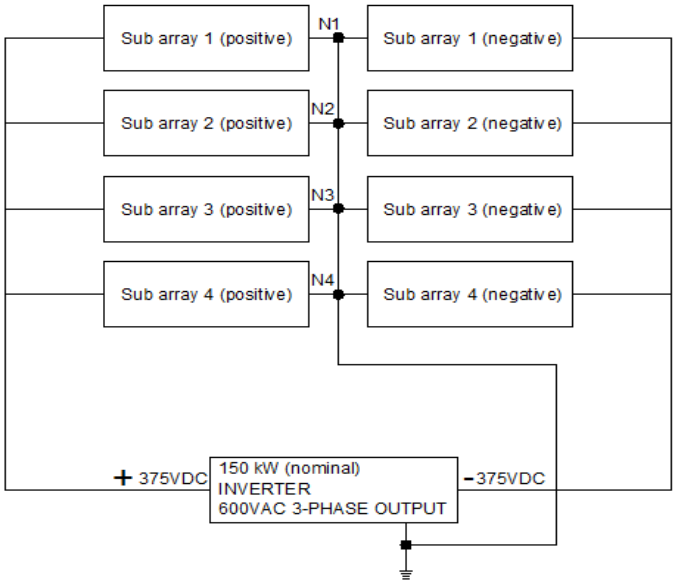

Figure 16- Single Line Diagram of the Bipolar Circuit

2.10 Potential Induced Degradation (PID) Definition

PID can occur if a PV string with positive ground is exposed to high humidity. As the string voltage increases, the voltage difference between the module frame and the module cells results in a leakage current. This flow of current from active cell layer travels through the encapsulate then along the glass surface to the frame. If PID occurs there could be large power losses.

Since the Solar One system has modules with no frames and Arizona is a dry climate PID is not a factor. This is substantiated additionally by the fact that both positive and negative grounded systems are connected within Solar One with no correlating effects.

CHAPTER 3

METHODOLOGY

3.1 Power Plant Configuration

The Solar One photovoltaic power plant system is a 200 kW DC PV array. This system was designed to produce 175 kVA (AC) 3-phase 600 volt inverter output derived from a 150 kW DC nominal inverter input from the array.

3.1.1 Bipolar Construction

The array is a bipolar circuit arrangement split into eight sub-arrays. Four of these are positive grounding and four negative grounding. The positive sub-arrays have 13 panel groups and negative sub-arrays have 12 panel groups. Sub-arrays 1 and 2 are to the south, and sub-arrays 3 and 4 are to the north.

3.1.2 Balance of System Layout

Power is fed from the array into an inverter through underground copper cables feeding into the equipment building to the west. Other balance-of-system equipment are:

- DC combiner box for the sub-arrays – one side live the other with disconnects
- Three wall mounted DC disconnects with fuses feeding the inverter
- Switchgear
- 600V to 12.5kV transformer
- Vacuum circuit breaker
- Metering cabinet

These components connect to three 50kVA transformers that supply power to the grid and in turn power the Solar One neighborhood.

Figure 17 - Solar One Array Layout

3.1.3 Inverter Characteristics

The custom Toshiba inverter built in August 1985 has a nominal input power rating of 150 kW at 375V DC; and is housed in three cabinets within the equipment building. Analog meters on one of the enclosures display instantaneous DC and AC current, voltage and power of the PV system. System status and diagnostics are read from an LED display in front of the inverter. The inverter also has a maximum power point tracking (MPPT) that can be switched to a manual mode to adjust array voltage ranging from 250V to 470V DC.

There is no ground fault detection on the DC side of the inverter and the AC side has a breaker for about 5-10 Amps of leakage current. This could be a safety concern around the array during wet conditions.

3.2 PV Modules and Panel Group Characteristics

The Power Plant is made of 4000 frameless mono-crystalline silicon PV modules. These 12” x 26” frame-less modules are glued onto a steel support beam. Several of these are mounted in groups that we call panel groups.

Table 1

Arco Module Specifications

Arco M54 module specifications at Standard Test Conditions (STC)
Open circuit voltage = 7.3 V
Maximum power voltage = 5.8 V
Maximum power current = 8.6 A
Short circuit current = 9.6 A
Rated power = 50 W
Fill factor = 0.71

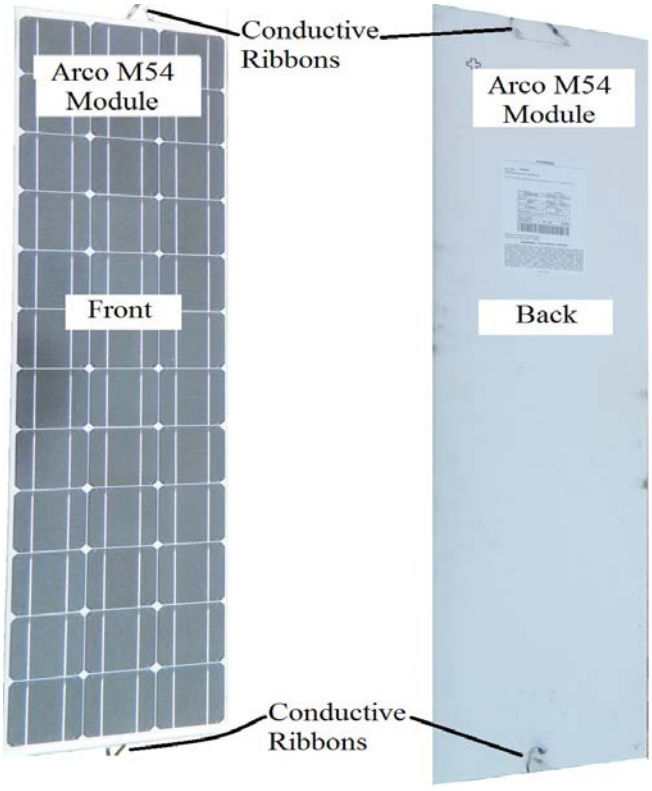

Figure 18 - Arco M54 Module

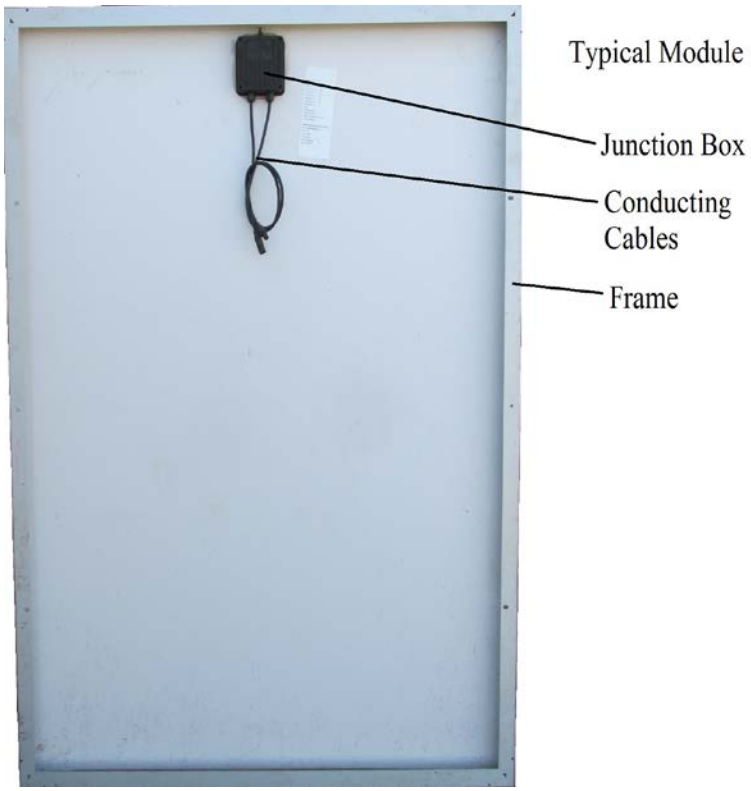

Figure 19- Typical module in 2012

3.2.1 Comparison of Arco M54 with Current Modules

The difference between these Arco modules and current modules are the connecting ribbons. Notice the difference between M54 module shown in Figure 18 compared to a typical module that is used today in Figure 19.

Today's quality testing would not allow for the ribbon design type found on the Arco modules. Cable and junction boxes are much stronger then ribbons and must pass stringent stress tests.

3.2.2 Baseline Curve Measurement

We acquired new modules which were used for replacement modules in the early 1990's. We analyzed these modules to see how they compared to the nameplate specification on the back of the module. We also determined the temperature coefficients.

3.2.3 Solar One Panel Group Construction

Ten modules are connected in parallel to form a panel. Four of these panels are connected in series to form a panel group by connecting the conducting ribbons to busbars between them. The figures below show the arrangement of the modules in the panel groups.

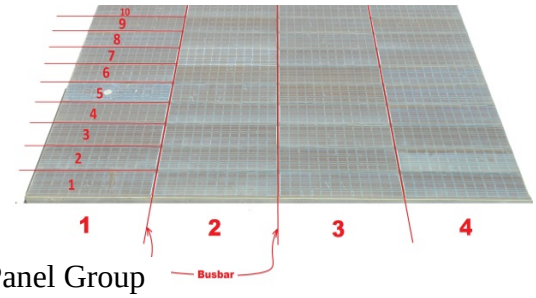

Figure 20 – Photo of Panel Group

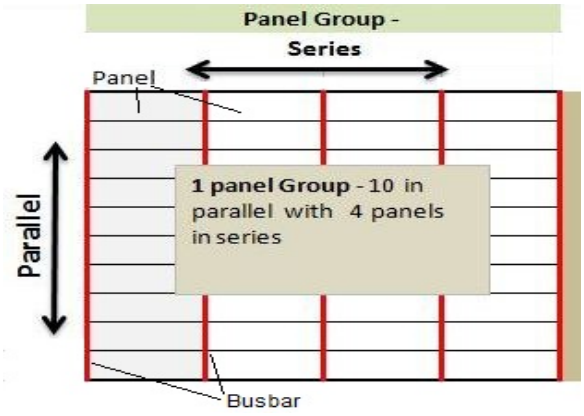

Figure 21 – Sketch of Panel Group

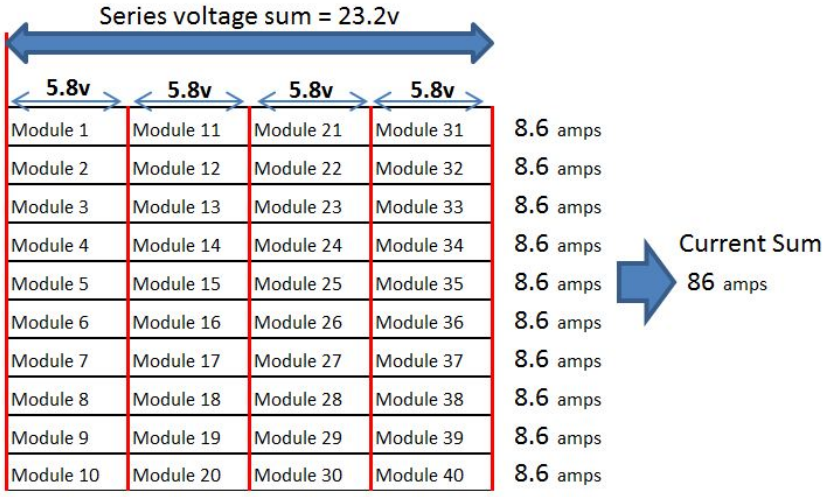

Figure 22 – Panel Group Ideal Voltage and Current

3.2.4 Panel Group Voltage and Current

The panel group voltage and current are graphically shown in Figure 20. The values listed are based on the module nameplate specifications listed in Table 1. The ideal panel group series voltage at STC would be 23 volts with the parallel module current of 86 amps.

3.2.5 Panel Group Connections

Each panel group is an independent device that can be unplugged from the array. Although this would interrupt the array power for the string, this is how we took I-V

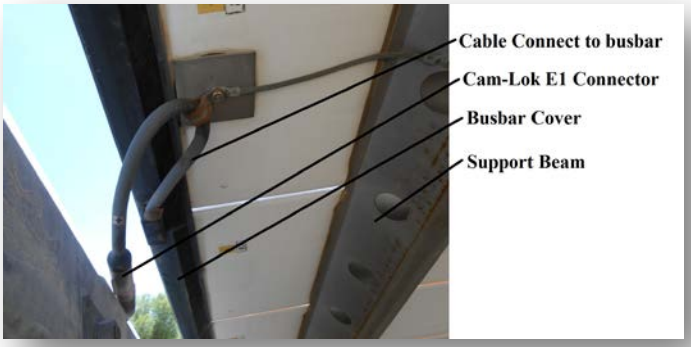

Figure 23 – Cable Interconnections Between Panel Groups

curves for each panel group. Each panel group has a Cam-Lok 15 connector that connects one panel group to another panel group in a series that make up a sub-array.

3.2.6 Module Connections

Figure 24 – Module Power Conducting Ribbons Connected To Busbar

Each module end has two flat power conducting ribbons. These copper ribbons are 0.300" wide by 0.005" thick for a cross section of 0.0015 in².

Deriving the ampacity from the busbar charts (12), using the smallest busbar in the chart we arrive with:

$$Busbar\ Ampacity = (154\ amps)/(.0625 in^2) = 2464\ \text{amps}/\ in^2$$

Therefore:

$$Ribbon\ Ampacity = [0.0015\ in^2]x\ [2464\frac{amps}{in^2}] \approx\ 3.7A$$

Where:

A= Current in Amperes

In^2 = square inches

Ampacity is the measure of the amperes that can flow through a wire. This would be the limiting factor for maximum current going through each of the conducting ribbons for the entire string. Each module has two ribbons. The total amps that can be carried is about 7.4 amps. This is less than the amp loads produced by the module of 8.6 amps at STC. The result of this is an immediate limitation of current flow at the design level. There would be no allowance for any interrupted interconnects resulting in reducing the power plant output.

The ribbons are mechanically connected to a busbar. Connections to the busbar are either rivet from factory assembly or by spot welding shown in Figure 24.

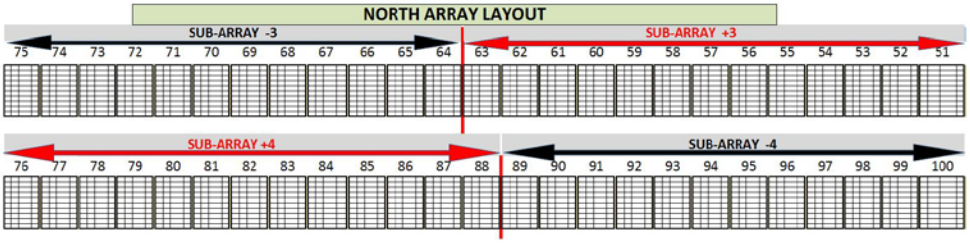

Figure 25 – North array

3.2.7 Sub-array

Panel Groups are connected together in series to form strings. Each panel group contributes to an additional sum of voltage along the string. This increase ideally would be about 23 V for each Panel Group at STC. Higher temperature operating conditions would reduce this voltage series sum.

A total of 8 sub-arrays make up the power plant; four on the north array and four for the south array.

3.3 Site Work

3.3.1 Overview of Work Performed

We performed preliminary field work to determine the performance of the PV system. This included: eight I-V curves of the sub-arrays, one hundred I-V curves of the panel groups, analysis of monthly/annual energy generated and billing reports, and a PID study. Additional tests that we performed were: visual inspections, hotspots scans, interconnect breakage determinations, temperature and wind studies and low irradiance I-V curve studies of six sample panel groups. We also tested panel groups for high potential wet/dry resistance insulation. These tests can give us an overall picture of how the system is performing and perhaps where we can concentrate some specific study. For instance visual inspections can show us various states of degradation of materials on a cellular level. I-V curves can show effects of increased series resistance or a decrease in shunt resistance.

3.3.2 Equipment Used

Table 2

Solar One Testing Equipment

Testing Equipment Used
Daystar's DS-100C I-V Curve Tracer
IVPC3.0.5 I-V Software
Mono Crystalline Silicon Calibrated Reference Cells
Special Panel Group Cables With Cam-Lok 15 Connectors Fitted With Voltage Sense Extended Wire Contacts
Fluke TI-55 Infrared [IR] Imaging Camera
Thermocouples and Micro Temp IR Thermometer
Visual Inspection Camera
Digital Multimeters
Ideal 61-795 Digital Insulation Tester
Safety Equipment For Electrical Insulation

3.3.3 Measurement Strategy

For the north sub-arrays I-V curve measurements the data was generally collected when our reference cells showed close to a value of 1000W/m^2 irradiance. This allowed

the power characteristics of the array to be at optimal performance for measurements. The standard procedures for measuring I-V curves, including normalization, were followed which included a mono-crystalline silicon reference cell set in the plane of array. The four sub-array's I-V curves were measured using the I-V curve Daystar DC-100C machine at the collection box where the entire array's wiring terminates in the equipment building. Since half of the box was live, extreme care had to be taken to avoid DC arc flash.

3.3.4 North 50 Panel Group I-V Curves Measurement

I-V curves for the 50 individual panel groups were measured and normalized to STC for a common reference point of comparison. Normalization was based on a standard setting within IVPC3 software, ASTM-E1036-96

The array I-V data obtained included:

- STC values of maximum power
- Short circuit current
- Open circuit voltage
- Fill Factor

3.3.5 Analysis Of Monthly And Annual Energy Billing Report

We organized the data that was accumulated from monthly billing reports. This data began in 1988 and continued to 2010. We compared this data with the measurements made in 2011. From this information we were able to determine the annual degradation rate shown in chapter 4.

3.3.6 Potential Induced Degradation (PID) Study

As a result of our data collection, we noticed an unusual power drop on the east side of the array. Initially it was thought that Potential Induced Degradation (PID) could have been the cause but as it is explained in Section 2.10 Arizona condtions are not ideal for PID.

Since both east and west arrays have 2 positive sub-arrays and 2 negative sub-arrays each, it was easy to rule out the possibility of PID since there was no pattern that could be associated with it. High humidity linked with high negatively biased arrays along with silicon nitride antireflective coated cells are generally potential conditions for PID. This is not the case for the titanium dioxide antireflective coated cells in the relatively arid environment of Phoenix. Both positively and negatively biased sub-arrays on the east side of the PV array were observed to have degraded considerably compared to the sub-arrays on the west.

3.3.7 Visual Inspection

After I-V measurements were completed a detailed visual inspection of the entire array was carried out using the visual inspection checklist developed at ASU-PRL. A table of failure modes was developed from the information obtained from the visual inspection.

This visual inspection included:

- broken modules
- cracked cells
- back sheet delamination

- cell corrosion
- metal blossoming
- interconnect breakage
- hotspot

3.3.8 Hotspots Scan

A localized heating occurrence within a PV module is called a hot spot. This happens when the module current is greater than the short circuit current of the lowest current producing cell. This cell then becomes reverse biased and heats up like a resistor.

Although there is no apparent shading of solar cells at Solar One, all panel groups have steel support framing behind the modules which prevented adequate ventilation of the solar cells directly above them. These cells operated at higher cell temperatures than the rest of the cells in the panel groups and this thermally induced performance non-uniformity between the cells in a module could be partly responsible for performance degradation of the PV system. These effects are shown in chapter four using the infrared camera on the front surface of the panel groups under load.

3.3.9 Interconnect Ribbon Breakage

Our visual inspection found that some busbar covers were opened, making the module ribbon connections to the busbar visible. Some of these ribbons were fully or partially broken. This finding prompted us to investigate the entire array for broken ribbons.

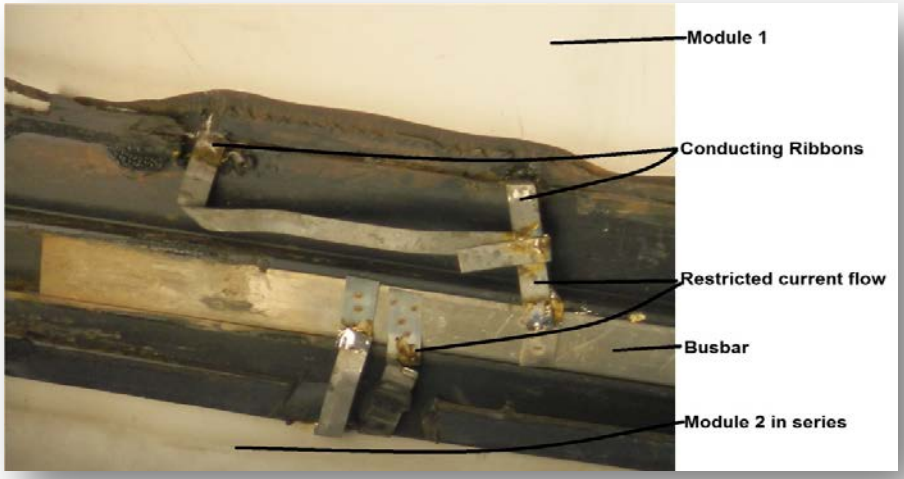

Figure 26 – Example of Incorrect Ribbon Connection

The method devised was to use an IR camera to scan the topside of the module back. Heated ribbons shown through with elevated temperatures while an open circuit showed no temperature rise. So if current is flowing through the connection it shows up as a hot spot. This method was very useful in finding broken interconnects without the need to break open any busbar covers within the PV array.

3.3.10 Low Irradiance I-V Measurements of Sample Panel Groups

When a solar cell is exposed to low light intensity, the effect of the shunt resistance becomes important. When there is less light generated the current equivalent resistance or the characteristic resistance of the solar cell approaches the shunt resistance, increasing the fractional power loss due to shunt resistance [5].

The low irradiance experiment was conducted by using calibrated mesh screens to partially block the sunlight. These were laid on the panel groups before I-V curves were taken in order to reduce irradiance to about 150-200 W/m^2.

During these measurements, the reference cell was not covered with mesh screen to avoid the non-uniformity issue on the small area (4 cm^2) cell. A high irradiance IV-curve was taken immediately after the mesh screen was removed in order to compare results.

3.3.11 Gradient Array Temperature

Since c-Si module voltage is affected by temperature determining the temperature under the array is important. Typically, the temperature along an array increases with the wind direction. Testing for this condition is necessary to see if it could partly explain the power difference between the east and west arrays.

Since we did not have a lot of time or resources for doing a large in-depth ambient temperature study it was decided we needed a method to quickly collect data.

3.3.12 Objects Reflect Average Ambient Temperatures

Thermalization is the process of an object that reaches thermal equilibrium through energy interaction. In our case equilibrium is through energy convection or conduction of the surrounding air just under the array. Thus, it can be said that an object will represent the average ambient temperature of the surrounding air. In this case, the steel support beams represented the heated air directly above them. Data was quickly gathered by walking along array and measured with an infrared (IR) sensor using the following method.

- The two measurement locations on each Panel Group was similar for all measurements
- The measuring location was similar in distance for each measurement
- The measuring location was entirely shadowed from the sun
- A total of 100 measurements were scanned on the north and south arrays within 15 minutes

Figure 27 – Temperature Measuring Locations

The temperature readings were taken on two successive days at approximately the same time of day. For this to be a more representative study, several days of temperature collection would have been necessary.

3.3.13 Wet And Dry Insulation Test

An insulation test was conducted to verify the effectiveness of the module and array packaging material. These materials isolate the components and electrical connections from water that can degrade the module or pose a safety hazard. The PV array had several broken modules, cracked cells and delaminated back sheets. These defects could potentially create a conductor to a ground. Since the array operated at high voltages and currents, personnel safety became a concern with the array particularly during wet conditions of rain and morning dew.

The test approach was to use an Ideal 61-795 digital insulation tester, and connect according to Figure 41. A dry test and a wet insulation test were conducted. The results obtained are reported in chapter 4.

CHAPTER 4

RESULTS AND DISCUSSION

4.0 Application of this Study

This chapter outlines the important aspects of this power plant in terms of degradation and reliability. Studying this power plant was important in many respects. Much of what we found is a relevant reference for today's application for solar PV. In addition, we completed the task that was assigned to us by SRP; to determine the state of the current array.

The following is a summary of the applicable aspects of our study.

Safety

- Electrical hazard of this system
    - Extreme caution should be exercised with wet modules.

Current State of the Array

PV Application

- Mechanical movement is not good for a reliable PV system
    - This system illustrates when mechanical principles of expansion are not considered, systems fail.
    - Sturdy cable designs are important to reduce reliability failure.
- The data collected can be applied as a reference for future systems
    - Importance of temperature influence
        - Mechanical stresses
        - Hot spot generated from obstructions

- Fences for protection but not obstruction to airflow
- Overall degradation rate and how it applies to other systems
- Cellular aging as a comparison to today's modules
- Wind effect on gradient array temperatures
- Possible wind turbulent effect on module performance and longevity
    - Uniquely amplified from the modular / panel design of Solar One
- Reinforces current studies and results of PID effects
    - PID is not a factor in dry environments

4.1 I-V Testing

The following information is a result of several months of testing various electrical characteristics that began in the fall of 2011. We began testing on a large scale and worked our way down to the near module level.

4.1.1 Performance of 4 South and 4 North Sub-Arrays

The first step of our investigation was to take I-V curves of 4 north sub-arrays. This led us to an interesting first finding. These first tests show that there was less power being produced in the east array compared to the west. Figure 28 summarizes the sub-array differences. The case was similar for the four south sub-array. This early discovery helped propel our search and helped direct our research.

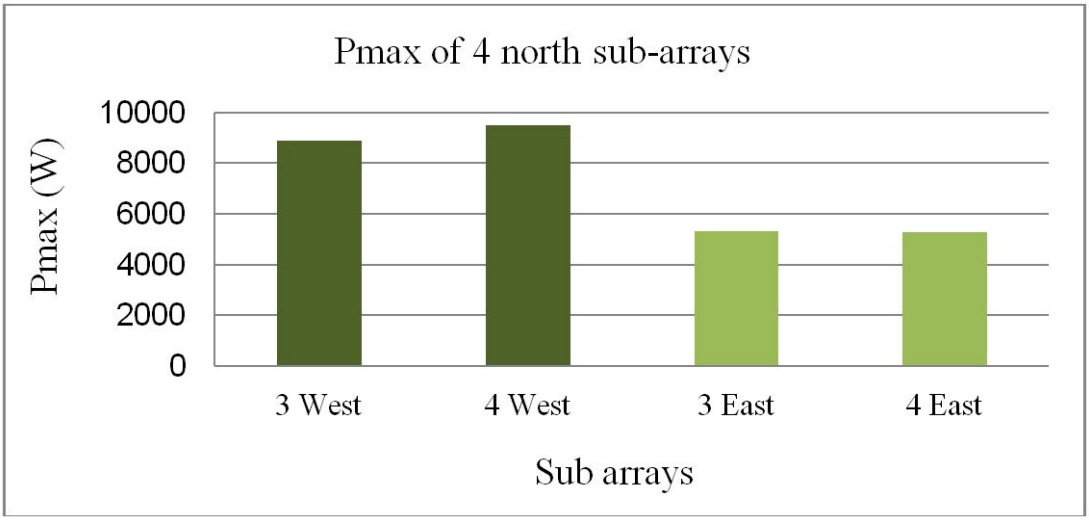

Figure 28 – I-V Power of Four North Sub-Arrays

The measurements of the performance for the four sub-arrays were taken on the 12th of October 2011 at the Solar One power plant around 10:35 am and 11:15 am.

Table 3

Results of 4 North Sub-Arrays Measurements

	SUB-ARRAY NUMBER	NUMBER OF PG'S	STC ISC A]	STC VOC [V]	STC PMAX [W]
NORTHWEST ARRAY	3-negative	12	65	316	11,139
	4-positive	13	67	344	12,427
Average			66	330	11,783
Total	2	25			23,566
NORTHEAST ARRAY	3-positive	13	55	340	6,833
	4-negative	12	57	315	6,572
Average			56	327	6,702
Total	2	25			13,405

From table 3 above it can be said that:

- We recorded greater power output from the west sub-array than east sub-array

- North array output = 37 kW
- Northwest sub-array = 24 kW
- Northeast sub-array = 13 kW
- Northeast sub-array = 54% of northwest sub-array power output
- South array output = 39 kW
- Combined total Solar One array output = [37+39] = 76 kW
- Inverter reading for total array STC output = 62.1 kW
- The total eight sub-arrays mismatch losses = [76 – 62.1 / 76]= 18%

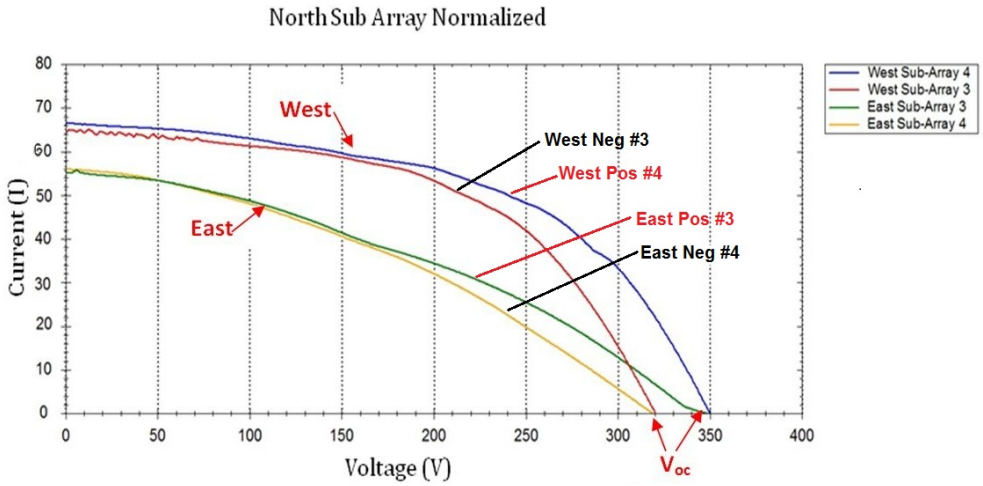

Figure 29 – North Sub-Array Normalized I-V Curves

Figure 29 above shows some interesting effects. The current on the Y-axis shows that west sub-arrays have more current and a resulting greater power. Reviewing the figure we see:

- West sub-arrays have similar higher I_{sc} values
- East sub-arrays have similar reduced I_{sc} curves
- Negative sub-arrays have lower V_{oc} because of one less panel group
- Lower I_{sc} in east sub-arrays is due to a greater number of broken module ribbons

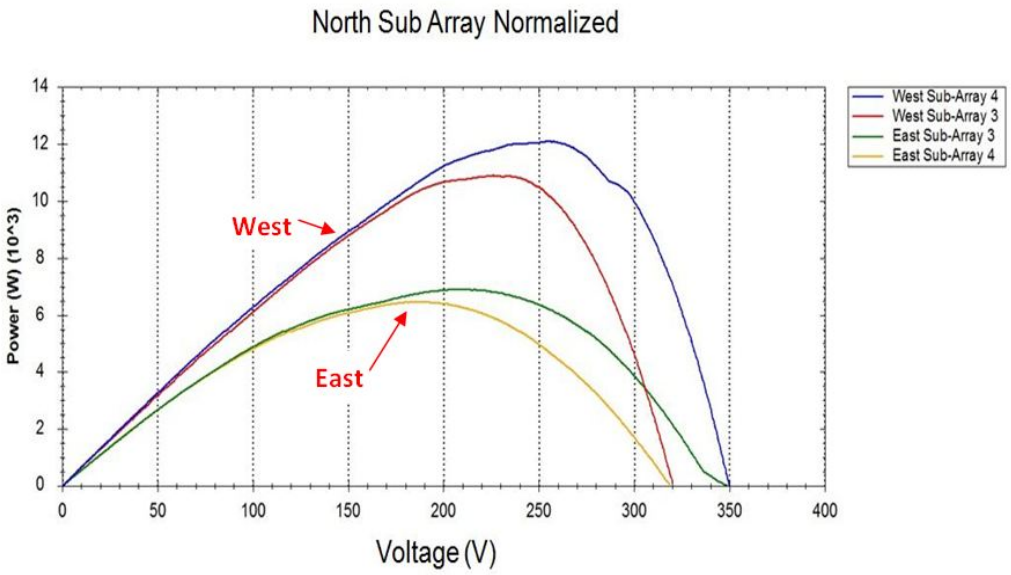

Figure 30 – North Sub-Array Power Curves

4.1.2 I-V Curves of 50 North Panel Groups

I-V curves of north panel groups were taken on the 26th of October 2011. We began measuring at 11 am and concluded measuring at 2 pm. Figure 31 below gives the summary of power measurements obtained for the north array.

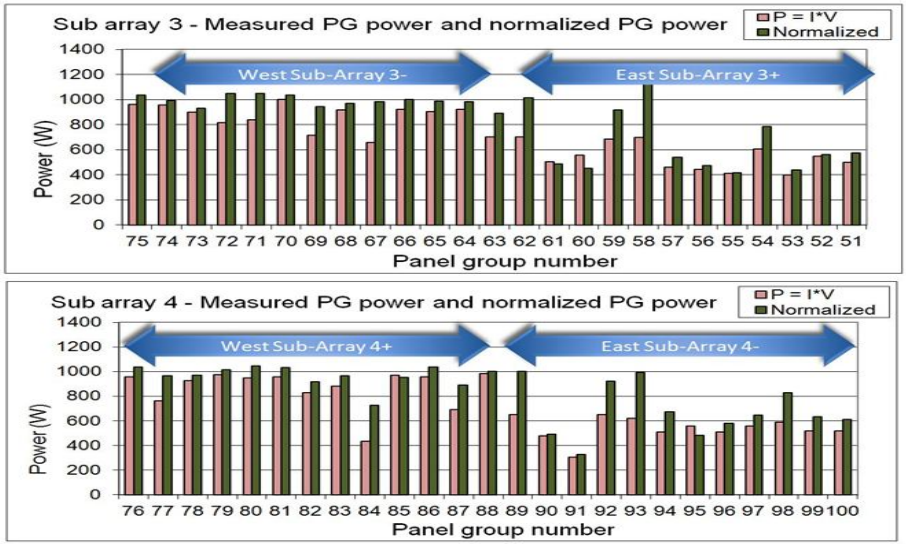

Figure 31 – North Array Measured and Normalized Power Summary

Studying Figure 31 above results in the summary of:

- Pmax total of all 50 panel groups at STC = 41 kW
- Pmax total of 4 sub-arrays at STC = 37 kW
- Panel group mismatch loss = [[41 - 37] / 41] = 11%
- Lowest performing panel group PG 91 = 325 W [north east]
- Most panel groups in the west performing close to 1kW
- Most panel groups in the east perform close to 0.6kW

4.1.3 Annual Degradation of the System

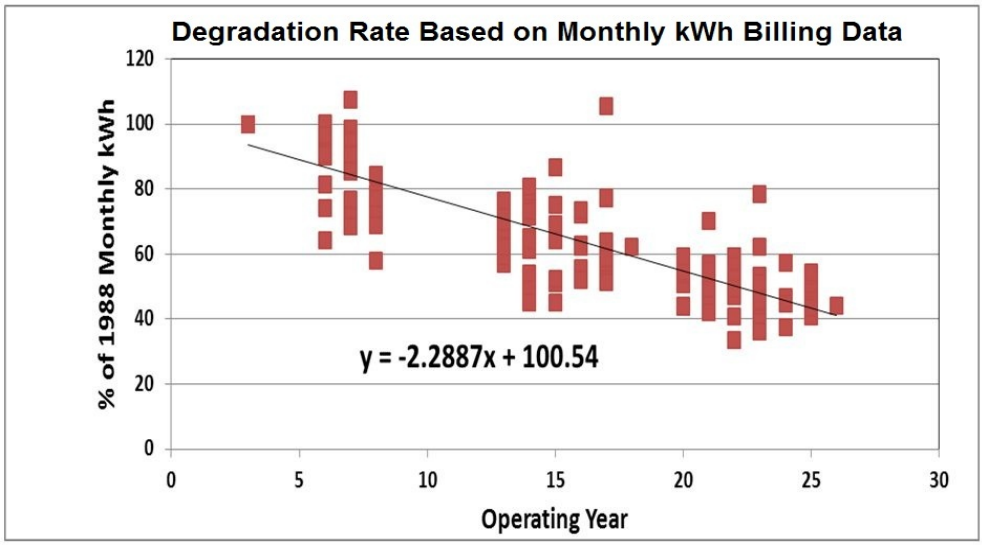

Figure 32 – Solar One Array Degradation Rate is 2.3% Per Year

Figure 32 above is derived from accumulated utility bills. A linear equation was derived from the scatter plot showing approximately a negative 2.3 slope. This degradation of 2.3% is almost three-four times greater than average degradation rates typically reported in literature for the current modules.

- Average annual energy production is about 112 MWh for the past 10 years
- Annual energy production 1988 = 321 MWh

4.2 Low Irradiance Affects

A Fill Factor (FF) is a way to measure the relative performance derived from an I-V curve. It is the area under the curve of the I-V with respect to the ideal absolute I_{sc} x V_{oc} curve.

Low irradiance measurements help to characterize solar cells in terms of series and shunt resistance effects. We can use low light I-V curves to measure to measure these effects resulting from shunt or series resistance.

Table 4

Results Of High and Low Irradiance

Panel Groups with increased Fill Factor			
PG91	**PG97**	**PG55**	**PG14**

Panel Groups with decreased Fill Factor
PG58

The fill factor increases with reduced series resistance issue at low light levels due to lower current generation. Higher irradiance conditions results with higher current flow thus causing a higher series resistance. This results with a higher voltage drop thus decreasing the fill factor.

The output of both high and low irradiance measurements were normalized and provided in Table 5 and Figure 33 below.

Table 5 - Results Of High and Low Irradiance Measurements

HIGH IRRADIANCE @STC					
	Lowest Performance	Low FF	Low FF	Average FF	Best FF
Panel Group	**PG91**	**PG97**	**PG55**	**PG58**	**PG14**
Fill Factor [FF%]	23.4	38.4	24.8	43.7	54.8
I_{sc} (A)	51.0	54.4	58.5	85.0	73.8
V_{oc} (V)	29.1	28.6	28.1	28.3	28.9
Peak Power (W)	347.7	597.3	407.9	1053.2	1165.5
I_{peak} (A)	28.3	33.7	24.8	51.2	55.1
V_{peak} (V)	12.3	17.7	16.4	20.6	21.1
Irradiance (W/m^2)	1,000	1,000	1,000	1,000	1,000
Cell Temp	25	25	25	25	25
LOW IRRADIANCE					
Fill Factor	35.7	49.5	64.8	18.6	66.7
I_{sc}	12.2	12.9	8.3	49.1	13.3
V_{oc}	25.6	25.8	21.6	24.7	25.0
Peak Power	111.3	164.4	115.6	225.9	221.6
V_{peak}	17.3	19.6	14.8	19.0	19.5
I_{peak}	6.4	8.4	7.8	11.9	11.3
Irradiance	200	200	200	200	200
Cell Temp.	25	25	25	25	25

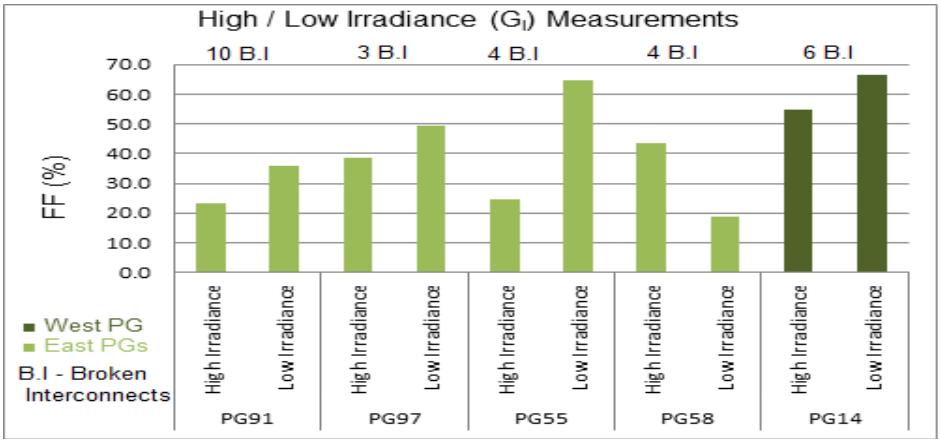

Figure 33 – Effect of Low Irradiance on Panel Group Fill Factor

The results of the low irradiance testing showed:

- Reduced series resistance
- Fill factor is better due to reduced series resistance interconnect failure – showing result of broken ribbons.
- PG58 has unusually high I_{sc} at low irradiance responsible for fill factor drop

4.3 Visual Inspection Analysis

4.3.1 Degradation or failure modes observed

We took a visual survey using visual inspection checklist developed at ASU-PRL and collected our observations based on the following conditions. We found:

- Replaced modules (7% in south array)
- Glass breakage
- Cell/metallization corrosion
- Encapsulant browning
- Cell cracks
- Back sheet delamination
- Broken interconnects

Figure 34 below shows the failure modes from the north array.

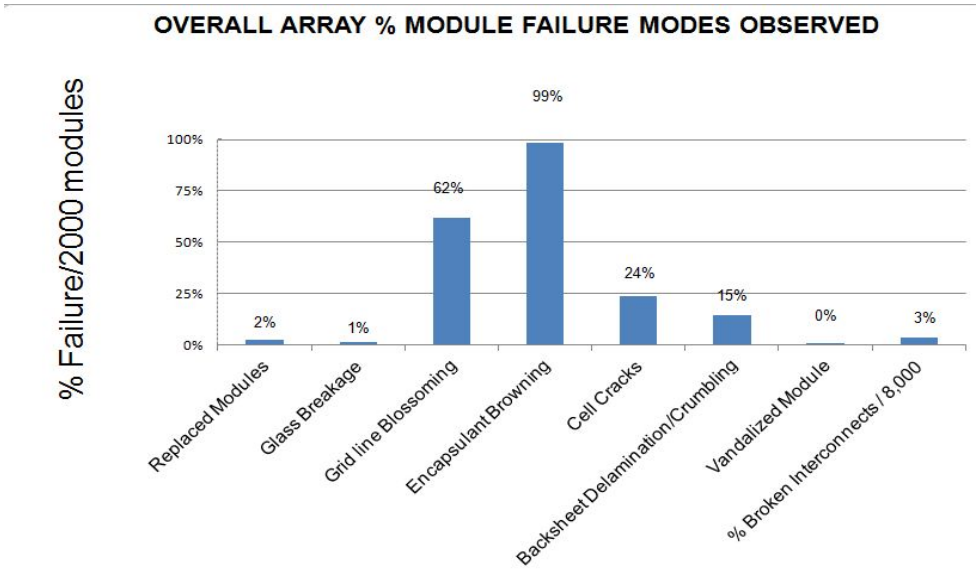

Figure 34 – Summary of Physical Defects

4.3.2 Visual Survey of Broken Interconnect

As reviewed in chapter 3, the interconnect ribbons carry the full current load of the array. Each module has 4 interconnect ribbons making a total of 8000 ribbons for the north array.

The photo in Figure 34 below shows evidence of the broken interconnect problem at the Solar One site. This shows that it is more than a metal fatigue problem but also a shearing stress problem resulting from the sealer restricting movement.

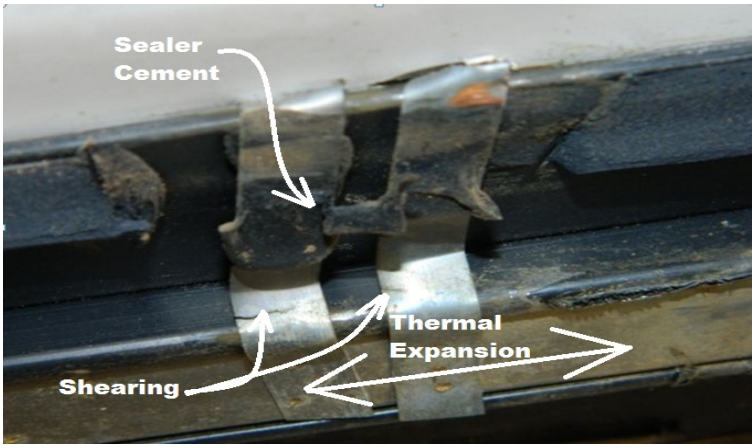

Figure 35- Busbar Expansion and Conducting Ribbon Failure

Figure 36- Examples of Busbar Seal Failure

During our inspection, we found that some busbar covers were hanging loose, making the module interconnecting ribbons visible. Some ribbons were completely or partially broken. A non-intrusive IR scanning image pinpointed broken ribbons. If a ribbon was connected, the resulting heat from current flow would show up in the IR images as a hotspot. Conversely, an open circuit would not show up on an IR image. After the entire array was captured in the IR images, it was found that the east sub-arrays have more broken interconnects than the west sub-arrays. The cause for this imbalance in ribbon breakage was not clear. Since vandals have broken a greater number of modules in the east it is possible that the method of module replacement with intrusive repair (onsite soldering the ribbons-instead of factory riveting-along with onsite workmanship issue during site repairing) could have accelerated the failure. A possible explanation could be due to improper sealing of the back cover, since the sealing cement would accelerate the ribbon shear. Additionally, since alignment of the ribbons would be critical, any field work would be more difficult to properly adjust the components. Also an improper seal would expose the ribbon to moisture and the associated corrosive effects of heat and electricity. There would also be a compounding effect when greater current is forced through fewer interconnections causing higher series resistances.

The broken interconnect summary below shows the results of the IR count. The high number of broken east ribbons explains the reason why the west array is performing better than the east array as subsections of the north array. It was found that this was also the case for the east and west subsections of the south array.

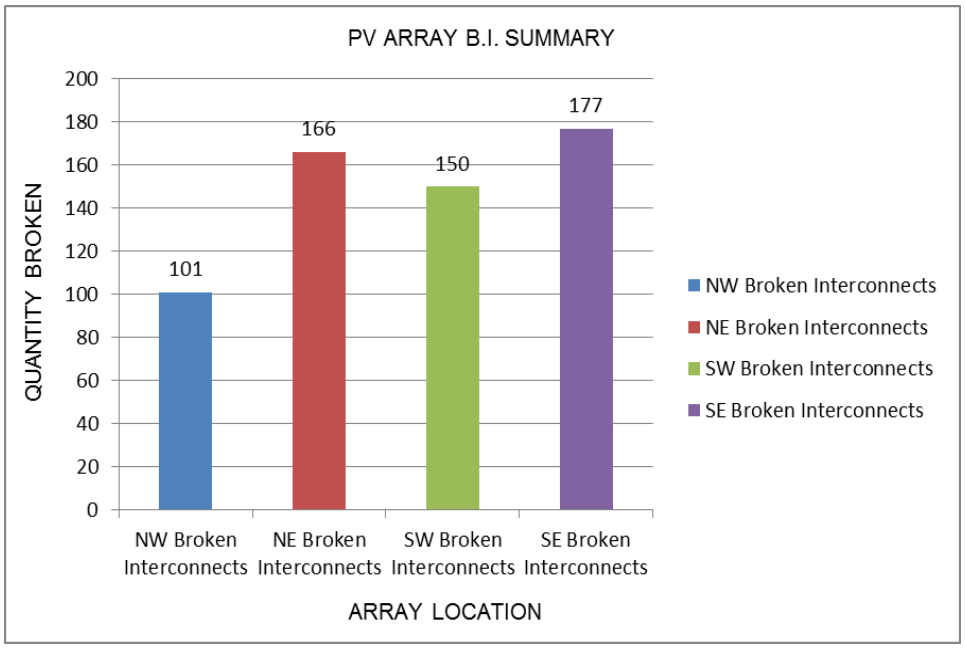

Figure 37- Summary of Broken Interconnects on PV Array

4.3.3 Broken Ribbon Interconnects Effects on P_{max}, I_{sc} and FF

Open circuits have obvious consequences on electrical output. Broken ribbons significantly reduce the power output of the Solar One power plant. Although the quantity of the broken ribbon interconnects has an effect on the power, more specifically it is actually the number of broken ribbon interconnects in each panel in series that matters. Each panel acts like a gate since the entire current of the string passes through these remaining interconnects.

Figure 37 shows that panel groups in the east array have lower fill factors than the panel groups in the west side of the array. The following figures show various comparisons of the broken interconnects within each panel group. It can be observed that the trend declines as the quantity of the broken interconnects increases.

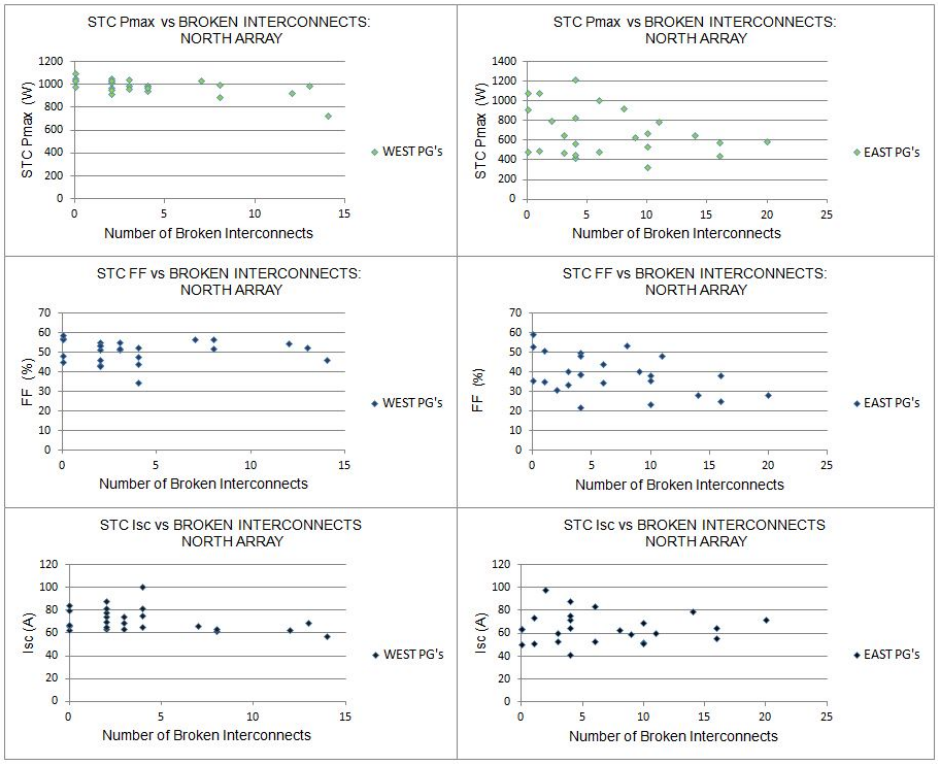

Figure 38- Failure Modes Interactions on PV Array

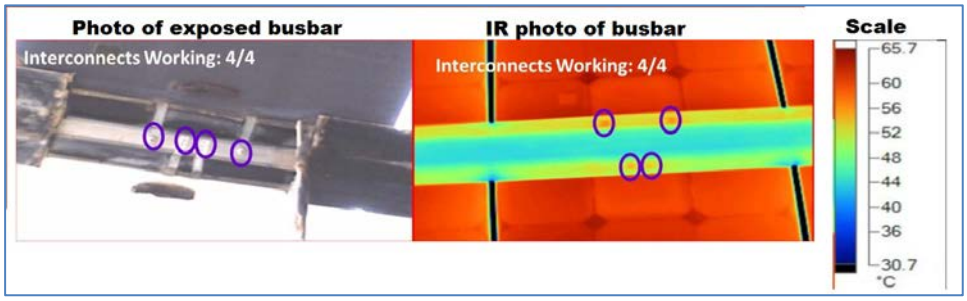

Figure 39- Photo and IR of Four Interconnects Working

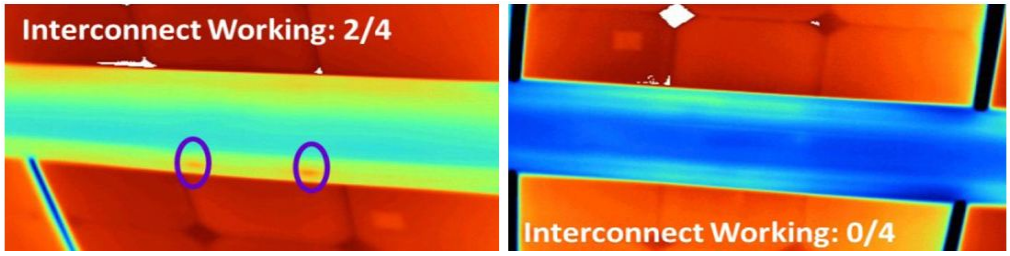

Figure 40 - Broken Interconnect Comparison

4.4 Panel Group Bypass Diodes

The system was designed to have two bypass diodes that are externally wired into the panel group as shown graphically in Figure 41 below. If there is a malfunction or a mismatch, the bypass diode will be activated, re-routing the power around it.

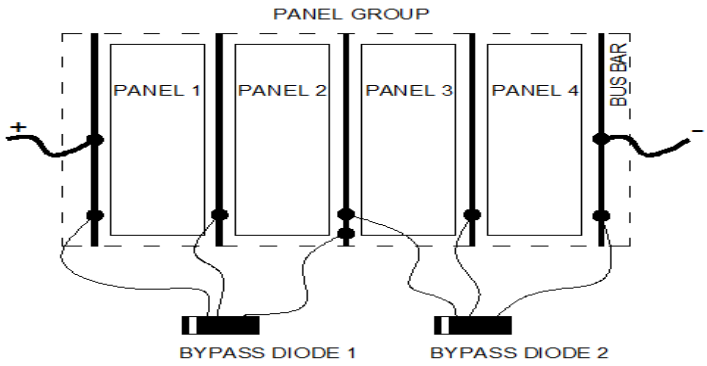

Figure 41- Bypass Diode Wiring Schematic

Table 6

Activated Bypass Diodes

Panel Groups with Activated Bypass Diodes					
PG53	PG69	PG77	PG84	PG87	PG91

4.5 Panel Group Voltages

The busbars were probed to determine panel voltages. This gave us a closer look at each panel group and how it was functioning with respect to voltage. The figure above shows the bypass diodes and points of contact for finding voltages across the panels. A digital multimeter was used to take voltage measurements by probing into the wire on each panel with respect to the center tap to the end of the sub-array.

The recorded voltages can be seen on Figure 42. Each circled panel voltage in the table shows where a diode has triggered a bypass. Notice that there is an unusual voltage

drop, including a triggered diode, for Panel Groups from 52 to 57. A possible explanation is reviewed in section 4.6

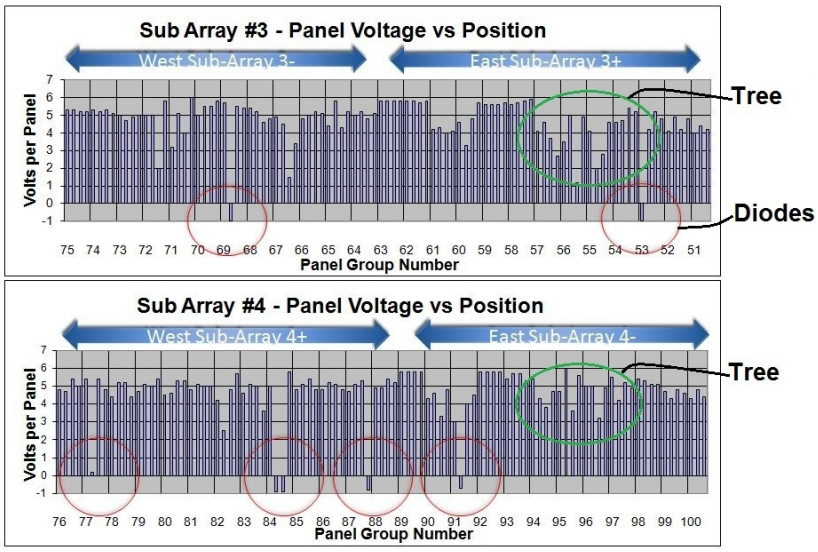

Figure 42- North Array Panel Voltages and Possible Turbulent Effect

4.6 PV North Array Temperatures

The graphs below show the results of the measurements taken for the successive two day period. The two days of temperatures along the array are similar implying a repeatable trend. The temperature measurements were taken on:

- Day 1 – MAY 3 At 1:08 pm , wind speed 5 mph
- Day 2 – MAY 4 At 12:40 pm ,wind speed 5 mph

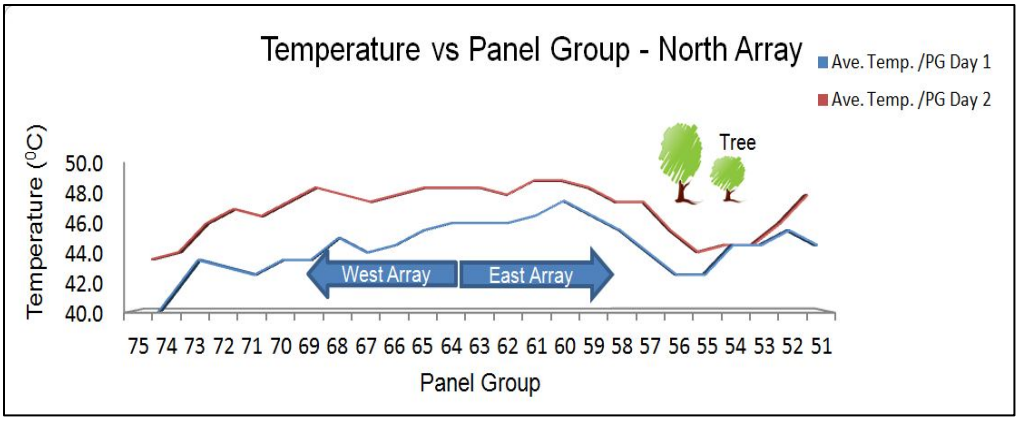

Figure 43- North Array Temperatures

4.6.1 North Array Construction for Air Flow

The construction of the north array has some air flow restrictions with Figures 44 and 45 showing details of these restrictions. Low ground clearance to the south, a 17° tilt and a wall on the north with trees all affect the air flow in different ways.

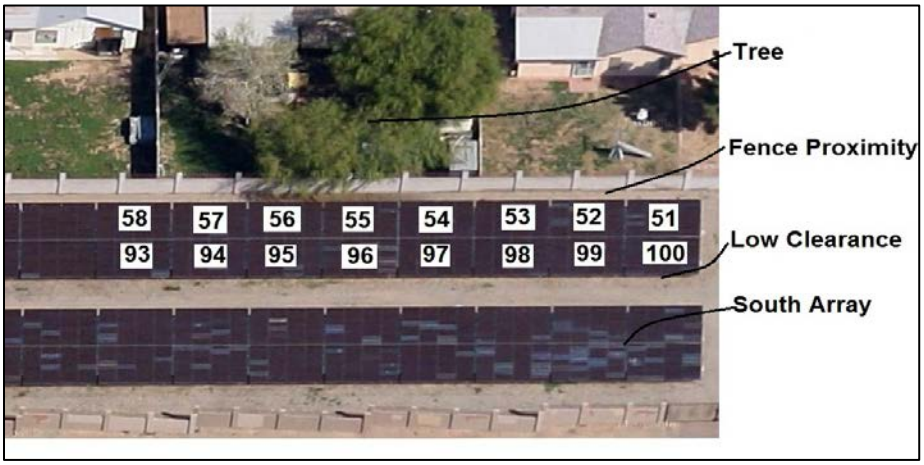

Figure 44- North Array Temperature and Tree Area

4.6.2 Gradient Temperatures and Possible Turbulent Wind Effects

The prevailing wind direction is out of the south west. The result of this wind direction shows an increasing temperature gradient along the array from west to east.

This gradient increase drops suddenly as a result of the trees located behind Panel Group 56-54. It seems that turbulent air surrounding the trees may have an effect on the ambient air temperature on several east modules.

Figure 45- East End View of North Array

The side view of the north array is shown in Figure 45. Notice the wall, the one foot gap at the bottom of the array and how the trees overhang the wall.

4.6.3 Unique Possible Turbulent Effects of Solar One

As described earlier, the unique ribbon design is highly susceptible to thermal expansion. Any temperature fluctuation increases destructive movement and mechanical failure. This would be the result from any cooling or heating effect, especially from a variable turbulent air flow. Since the tree effect can be shown to cool the array in a 5 mph wind it could be assumed that it will follow a gradient increase without wind.

Turbulence would not be restricted to the tree effect but would also result at the end of the array. Table 7 shows the susceptible turbulent wind panel groups.

Table 7

Turbulent Wind Panel Groups

Panel Groups Subjected to Turbulent Wind							
PG51	PG52	PG53	PG54	PG55	PG56	PG57	PG58
		PG75	PG74	PG73	PG72		

Figure 46 shows a possibility that the turbulent air flow is associated with increasing interconnect failure. See how the voltage reduces while the broken interconnects increase with the suspect Panel Group locations. Notice the large percentage of broken interconnects associated with these turbulent wind regions.

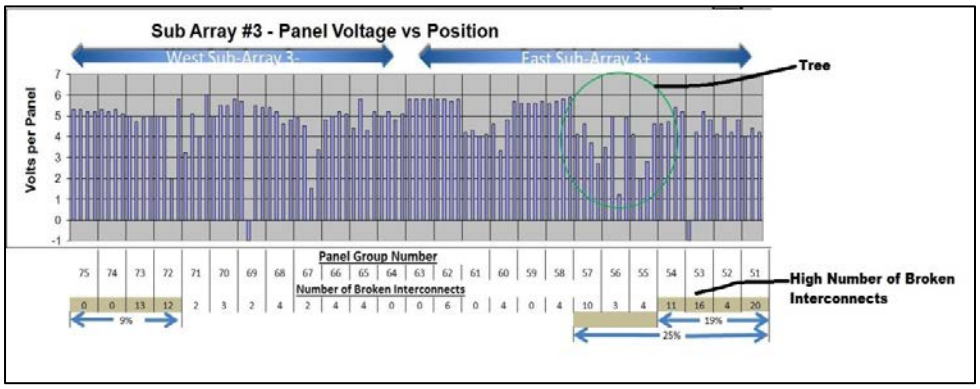

Figure 46- Panel Group Voltage Broken Interconnect Comparison

4.7 Hot Spots

An infrared (IR) image of every panel group was taken during full sun conditions. Mismatched cells begin to heat up and show as a hot spot. Hot spots were observed mostly in low voltage producing panel groups.

Table 8

Panel Groups with Hot Spots

Panel Groups with Hot Spots			
PG5	PG69	PG84	PG91

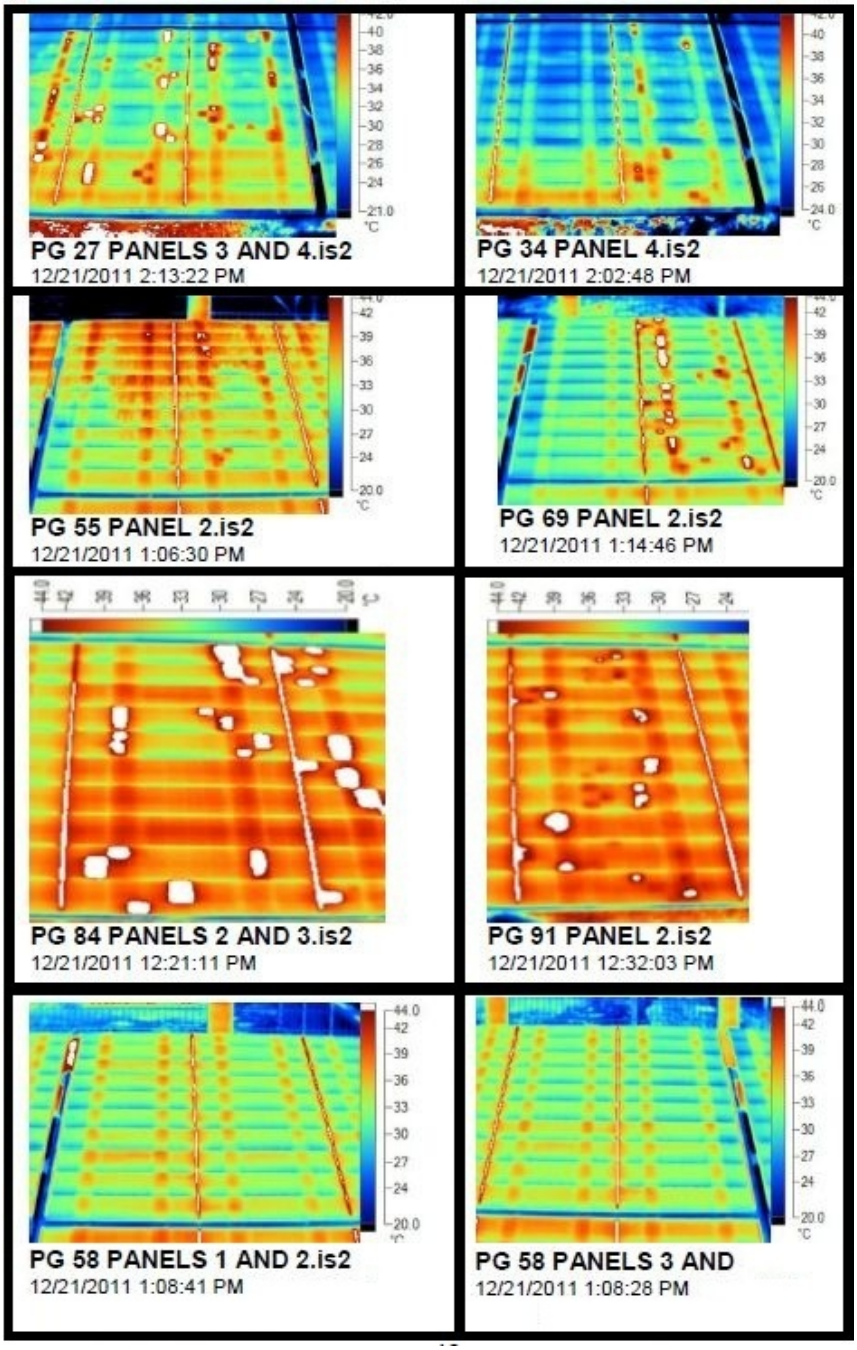

Figure 47 - Hot Spots Shown in Infrared

In Figure 47 panels with severe hot areas are shown. By comparison Panel Group 58 has mild hot spots.

4.7.1 Insulated Hot Spots

In addition to the mismatched hot spots there are hot areas also generated by the back of the module being insulated by the support beams. The support beam below the module acts as an insulator as shown in the hot spot areas shown in Figure 47.

4.8 High Voltage Insulation Test

4.8.1 Basic Standards Electrical Insulation Test

Electrical Insulation Testing, also known as High Potential Testing, is derived from IEC 61730 and UL 1703. These are the basic standards that cover requirements for construction and safety of photovoltaic modules, covering conditions that could lead to electrical shock or fire hazards. A high voltage is connected to one of the leads on the module and the other to the ground. High Potential tests are conducted to see if there was any current leakage of the PV array in wet or dry conditions. In our test, a wet condition was simulated by throwing water from buckets onto the panel group. The results in are shown in Table 9 below. Broken glass reduces the resistances in Panel Group 14 and 55. The end result shows a high leakage current and low resistance making the array unsafe during wet conditions.

Table 9

Hi-Pot Test Current and Resistance Output

HIGH POTENTIAL TESTING: CURRENT IN MILLI AMPS (mA)

PGs TESTED	DRY CONDITION M +	DRY CONDITION M-	VERY WET CONDITION M +	VERY WET CONDITION M-	MILD WET CONDITION M +	MILD WET CONDITION M-
*14	0.0026	0.0013	35.714	250.000	-	-
97	0.0015	0.0026	14.286	33.333	-	-
4	0.0024	0.0020	10.417	6.250	-	-
*55	0.0028	0.0028	-	-	0.038	0.014
91	0.0027	0.0022	-	-	0.010	0.011
58	0.0028	0.0028	-	-	0.048	0.008

HIGH POTENTIAL TESTING: RESISTANCE IN MEGA OHMS (MΩ)

PGs TESTED	DRY CONDITION M +	DRY CONDITION M-	VERY WET CONDITION M +	VERY WET CONDITION M-	MILD WET CONDITION M +	MILD WET CONDITION M-
*14	192.5	371	0.014	0.002	-	-
97	330	190	0.035	0.015	-	-
4	209.4	244.5	0.048	0.08	-	-
*55	177	181	-	-	13.3	36.56
91	183	232	-	-	48	44
58	179	176	-	-	10.5	63.8

* Panel Group has one module with broken glass

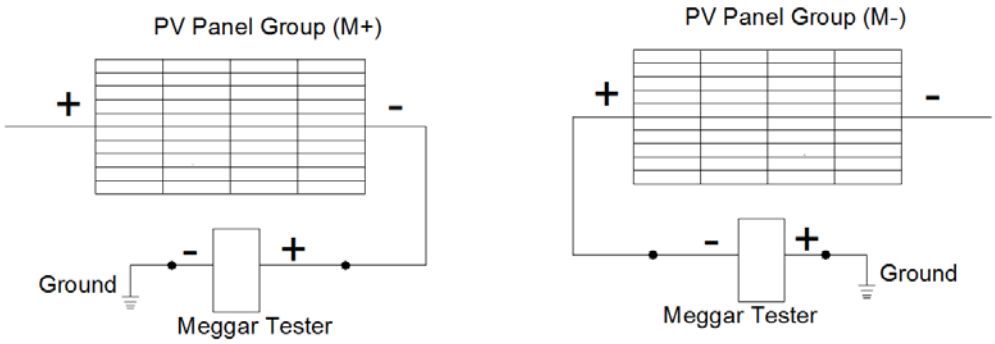

Figure 48- High Potential Testing Setup

4.9 I-V Before and After Repair

Figure 49 shows the results of an interesting experiment. The I-V curve at the top is representative of a new panel group as it was installed in 1985. The second I-V line below that shows the best panel group 14 with no ribbon breakage was performing at

58% of the original power. This indicates that the power drop (42%) is primarily caused by encapsulant browning and series resistance increase probably due to solder bond fatigue of the cells.

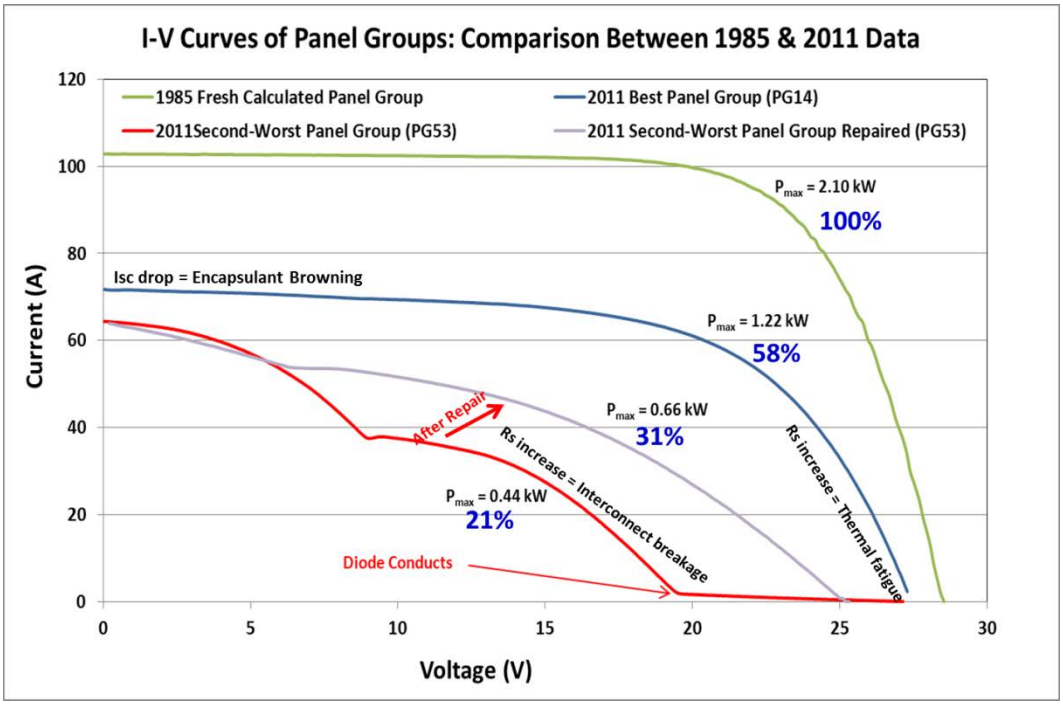

Figure 49- IV Comparison and Repair Experiment

The experiment was to repair some of the broken ribbon interconnects on poor performing Panel Group 53. Before the repair the panel group only had 21% of original power. After the repairs Panel Group 53 increased its power by 50%. This further substantiates that fact that ribbon failure is a large contributing factor in the overall system degradation.

CHAPTER 5

CONCLUSION

This report discussed and presented findings regarding the Solar One PV system's overall condition. Through visual inspection, various electrical tests and summary data analysis we were able to determine the system degradation and failure modes. We reviewed this in terms of both energy output and the physical array condition.

The array was found to be degrading at a rate of about 2.3% per year. Part of this can be attributed to the degradation of the Ethylene Vinyl Acetate material resulted in browning on the solar cell surface reducing light transmission. This reduction of light causes a loss of short circuit current and maximum power point current effectively reducing the power output for the array. All the original modules without replacement modules at Solar One have a high degree of browning. Even the best panel group with no ribbon breakage indicated a power drop of 42%. This power drop is primarily attributed to the encapsulant browning and series resistance increase probably due to solder bond fatigue of the solar cells.

We saw that heat transfer can be restricted by structural configurations on small and large scales. Thermal effects cannot be taken lightly. Heat not only reduces the efficiency of c-Si modules but thermal cycling and the resulting material fatigue can have a detrimental effect on the life of a system. Negative effects can be seen by localized heating from enclosures and array wind flow restriction.

Ribbon reliability failure was primarily responsible for the reduction of output power for the entire array. Many modules were replaced due to vandalism. It is believed that

module design, incorrect reassembly methods and sealing materials accelerated the failure. The ultimate failure was a result of interconnect ribbon breakage resulting from thermal expansion and contraction from a connecting busbar. Metal fatigue in the ribbon was a result of this cyclic thermal loading. As the ribbons broke, the parallel pathways for current were reduced resulting in a 40% power difference between the lower performing east array and the better performing west array.

We observed some unusual array cooling effects resulting from turbulent flow around trees on the north side. The normal gradient temperature increase on the east was interrupted in this tree zone. In the early days, trees were absent from the fence line. Turbulent cooling effects could have accelerated the ribbon metal fatigue. Array protection from vandalism is important since it was the cause of module replacement. A fence that conceals the array might have reduced the number of occurrences of broken modules. It is very important also to consider the location and the possible effect from increased vandalism from high traffic and highly visibility.

Although it was first suspected, Potential Induced Degradation (PID) effect was eliminated as a cause of panel deterioration as soon as we could compare the data from our panel group I-V curves from both positive and negative sub-arrays. Humidity and type of antireflective coating on the cells (titanium dioxide versus current silicon nitride) a strong factor for PID; and the dry conditions of Arizona and titanium dioxide AR coating do not seem to be favorable for PID.

This study showed that design parameters which regulate system reliability and durability, and safe array configurations are essential to the longevity and bankability of a

PV system. The Solar One study also showed that array configurations can be adversely affected by installation methods, vandalism and Arizona's environmental conditions. It is my expectation that these findings will help contribute to future improvements in the development of solar energy hardware and installations.

REFERENCES

[1] Campen, G. L. "An Analysis of the Harmonics and Power Factor Effects at a Utility Intertied Photovoltaic System." *Power Apparatus and Systems, IEEE Transactions on* PAS-101.12 (1982): 4632-9. Print.

[2] Russell, M. C. & Kern, Jr., E. C. (1990). *Lessons learned with residential photovoltaic systems*. Waltham, Massachusetts: IEEE Photovoltaic Specialists Conference. Print.

[3] Salt River Project (1993). *Solar One Subdivision Photovoltaic System Ownership Analysis*, - Salt River Project, Arizona. Print.

[4] City of Austin Texas Electric Utility Department. Solar Energy Research Institute under contract to the U.S. Department of Energy. "Photovoltaic Module Reliability Workshop." *Module Field Experience With Austin's PV Plants*. N.p., 25 Oct. 1990. Print.

[5] City of Philadelphia. *Guidebook for Solar Photovoltaic Projects in Philadelphia.* 2nd ed. N.p.: n.p., 2011. *Phila.Gov/Green/Solar.* Mar. 2011. Web.

[6] Jeong, Jae-Seong, Nochang Park, and Changwoon Han. "Field Failure Mechanism Study of Solder Interconnection for Crystalline Silicon Photovoltaic Module." *Microelectronics Reliability* 52.9–10 (2012): 2326-30. Print.

[7] McEvily, Arthur J. *Metal Failures - Mechanisms, Analysis, Prevention*. John Wiley & Sons Print.

[8] TamizhMani G., Kuitche J. (2012) *"Background Review and Analysis on: Accelerated Lifetime Testing of Photovoltaic Modules,"* Solar ABCs Study Report

[9] Kempe, Michael D., et al. "Acetic Acid Production and Glass Transition Concerns with Ethylene-Vinyl Acetate used in Photovoltaic Devices." Solar Energy Materials and Solar Cells 91.4 (2007): 315-29. Print.

[10]G.R. Mon, "Module Voltage Isolation and Corrosion Research," Reliability and Engineering of Thin-Film Photovoftaic Modules: Research Forum Proceedings, JPL Publication 85-73, JPL Document 5101264, DOE/JPL-1012-111, pp. 197-234, Jet Propulsion Laboratory, Pasadena, California, October 1, 1985. Print.

[11] Pysch, D., A. Mette, and S. W. Glunz. "A Review and Comparison of Different Methods to Determine the Series Resistance of Solar Cells." Solar Energy Materials and Solar Cells 91.18 (2007): 1698-706. Print.

[12] "DC Copper Busbar Ampacities." Copper Development Association Inc. Copper Development Association Inc, n.d. Web. 2013. <http://www.copper.org/applications/busbar/ampacity/busbar_ampacities.html>.

[13] Tatapudi, Sai Ravi Vasista. "Potential Induced Degradation (PID) of Pre-Stressed Photovoltaic Modules: Effect of Glass Surface Conductivity Disruption." M.S. Arizona State University, 2012. Print.United States -- Arizona: .

APPENDIX A

Testing Equipment Used
Daystar's DS-100C I-V Curve Tracer **IVPC3.0.5 I-V Software** http://www.daystarpv.com/curvetracer2.html
Mono Crystalline Silicon Calibrated Reference Cells Calibrated irradiance measuring cells
Special Panel Group Cables With Cam-Lok 15 Connectors **Push lock connectors found in electrical connectors** **Fitted With Voltage Sense Extended Wire Contacts To prevent IR drop the leads of a volage checking device need to be located near the source**
Fluke TI-55 Infrared [IR] Imaging Camera **Fluke.com**
Thermocouples and Micro Temp IR Thermometer Omega.com
Visual Inspection Camera
Digital Multimeters
Ideal 61-795 Digital Insulation Tester idealindustries.com
Safety Equipment For Electrical Insulation **http://www.asiarcflashsolutions.com/**

APPENDIX B

TABLE A1 - RESULTS OF SOLAR ONE ARRAY MEASUREMENTS

[PANEL GROUP	STC Isc (A)	STC Voc (V)	STC Pmax (W)	PANEL GROUP	STC Isc (A)	STC Voc (V)	STC Pmax (W)
1	69.7	28.9	507.6	51	71.9	28.9	584.5
2	58.6	27.4	551.5	52	71.8	27.2	571.9
3	62.8	27.4	564.9	53	64.3	27.2	438.2
4	67	27.6	851.2	54	59.7	27.1	784.6
5	59.9	27.2	683.2	55	40.8	26.8	421.2
6	60.9	27.4	761	56	52.8	27	475.1
7	49.3	27.3	568.9	57	51.6	27.3	539.8
8	57.2	27.4	663.4	58	88	27.6	1213.8
9	70.8	27.3	1130.2	59	63.7	27.3	919
10	82.4	27.3	561.2	60	75.7	27.2	452.2
11	58.3	27.3	543.2	61	50.4	27.1	487.2
12	69.9	27.4	1047.4	62	83.6	27.5	1012.6
13	74.9	28.9	1142	63	64	28.4	1083.4
14	71.7	27.3	1223.9	64	63.1	27.2	984.1
15	100	27.4	1225.7	65	81.5	27.5	987.9
16	71.5	27.4	1122.3	66	75.5	27.4	984.8
17	65.8	27.4	863.9	67	63.7	27.5	968.2
18	65.3	27.3	1088.1	68	65.2	27.4	943.2
19	79.8	27.4	1178.1	69	87.8	27.2	1035.4
20	71.2	27.4	1182.3	70	74.9	27.2	1047.4
21	72.5	27.5	1138.7	71	74.8	27.2	1048
22	72.6	27.6	1210	72	63	26.9	928.7
23	70.1	27.2	1194.9	73	68.9	27.4	990.7
24	99.7	27.2	1194.1	74	66.1	27.6	1034.5
25	69.4	27.5	1221.5	75	67.1	27.7	1100.7
26	63.9	27.2	903.8	76	66.2	27.6	1036.3
27	57.4	27	795.7	77	100.8	27.6	967.7
28	69	26.9	1034	78	69.4	27.4	984.8
29	72.8	27.4	1046.3	79	70.2	27.1	1015.5
30	65.2	27.3	1057.1	80	80.1	27.2	1048.6
31	65.2	27.3	1157.8	81	84	27.2	1031.6
32	67.4	27.2	1119.1	82	78.1	27.5	917.3
33	74.5	27	1069.5	83	63.6	27.5	965.7
34	62.9	27.2	914.6	84	57.1	27.6	725.6
35	99.9	27.2	1153	85	65.1	27.4	953.7
36	65.5	27.2	1157.7	86	81.8	27.4	1036.7
37	70	27.1	1027.8	87	62.2	27.5	890.4
38	68.9	27.1	1164.2	88	63.9	27.6	1000.4

39	79.4	28.9	1167	89	74	28.6	1083.8
40	62.9	27.3	682.4	90	51.3	27.1	492
41	55.2	27.1	591.6	91	51	26.9	325.3
42	67.5	27	1153.2	92	62.9	27.3	924
43	51.8	27.2	577.6	93	98.4	26.6	804.3
44	64.8	27.2	757.6	94	69.4	27.2	675.2
45	62.1	27.2	784	95	52.9	26.7	484.7
46	57.1	27	583.8	96	55.6	27.2	582.3
47	60.3	27.4	771.4	97	60.2	26.8	648.7
48	63.2	27.2	651.3	98	64.5	26.7	827.8
49	69.7	27	665.7	99	58.8	25	634.8
50	81.1	28.4	648	100	79.1	28.8	648.8

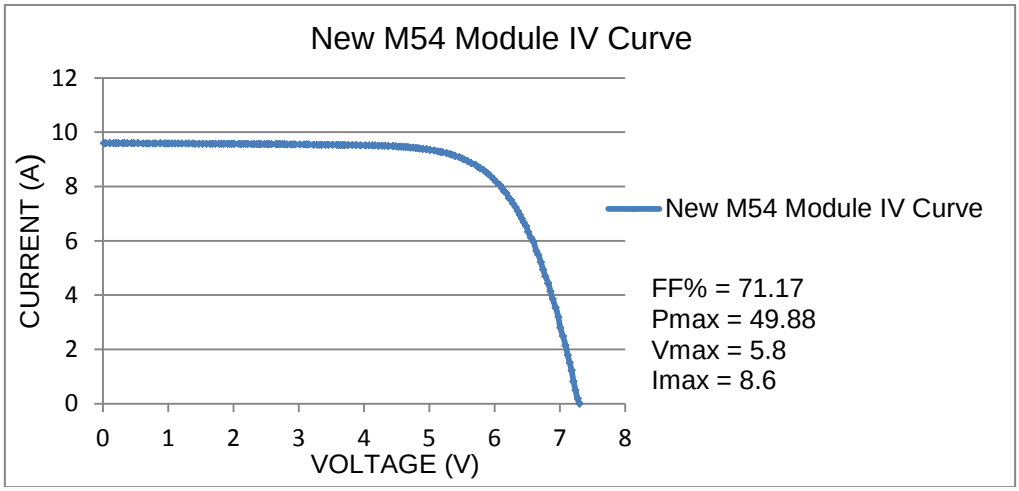

Figure A1 New M54 Module IV Curve

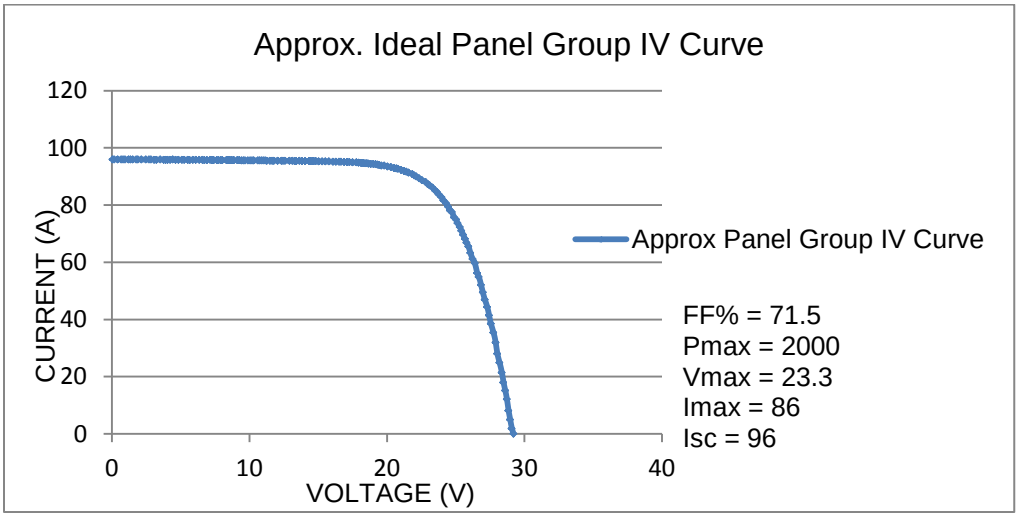

Figure A2 New Ideal Panel Group IV Curve – Generated from Figure A1

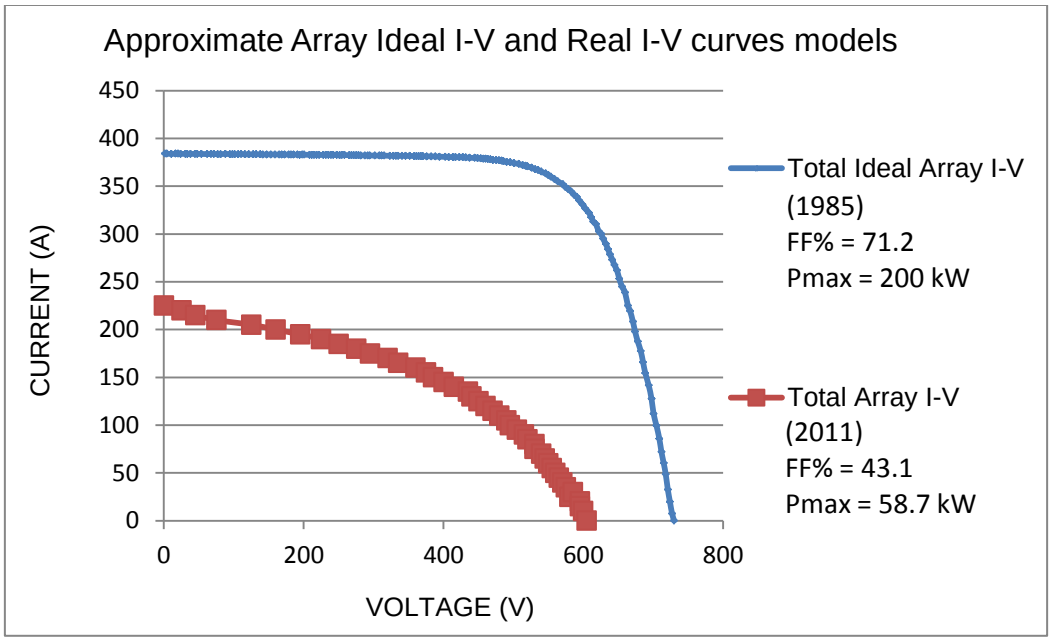

Figure A3 New Ideal Complete Array IV Curve – Generated from Figure A2 – Compared to Measured Total Array IV

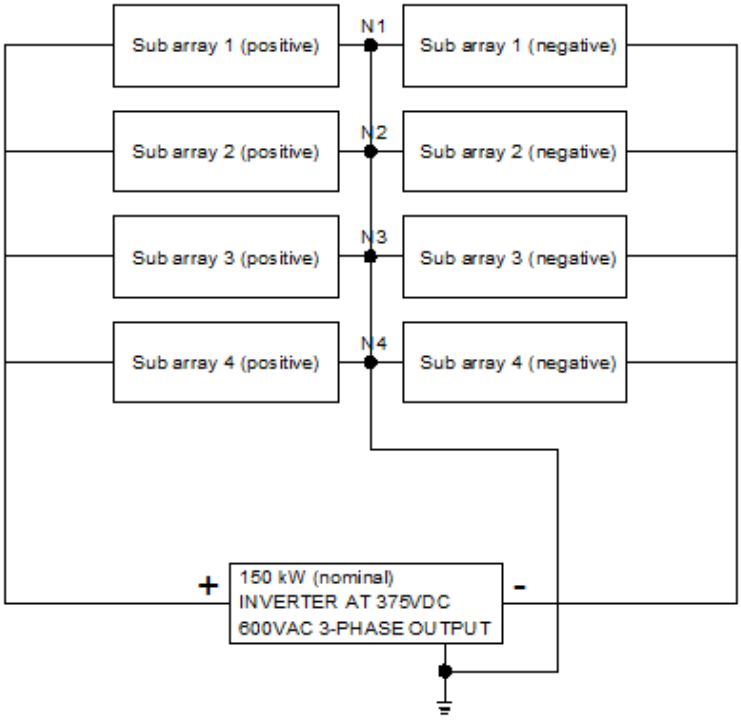

Figure A4 Bipolar array layout of Solar One

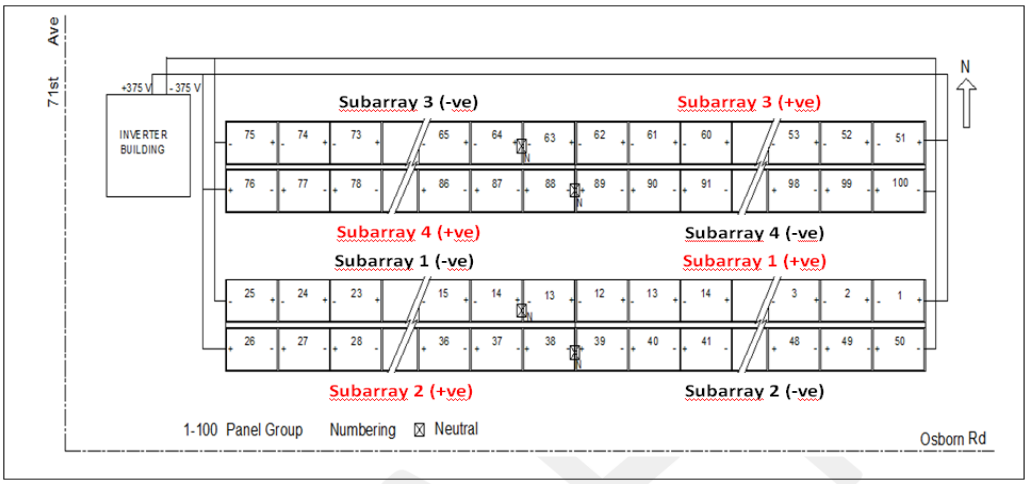

Figure A5 Sub-array layout of Solar One

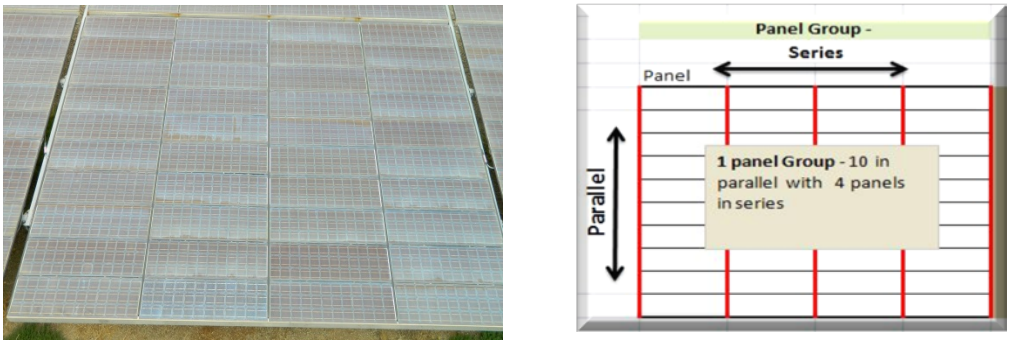

Figure A6 Panel Group Photo and Layout of Solar One

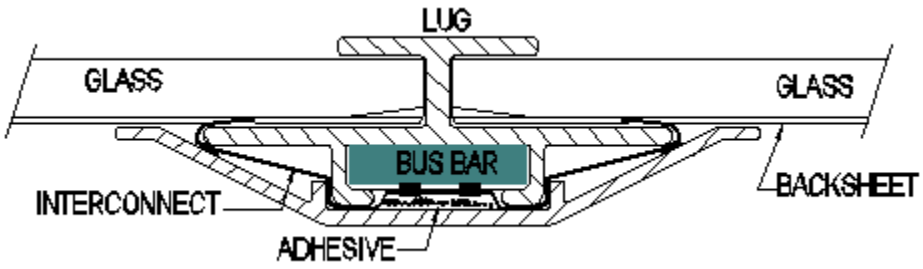

Figure A7 Typical Panel Group Busbar Assembly Cross section

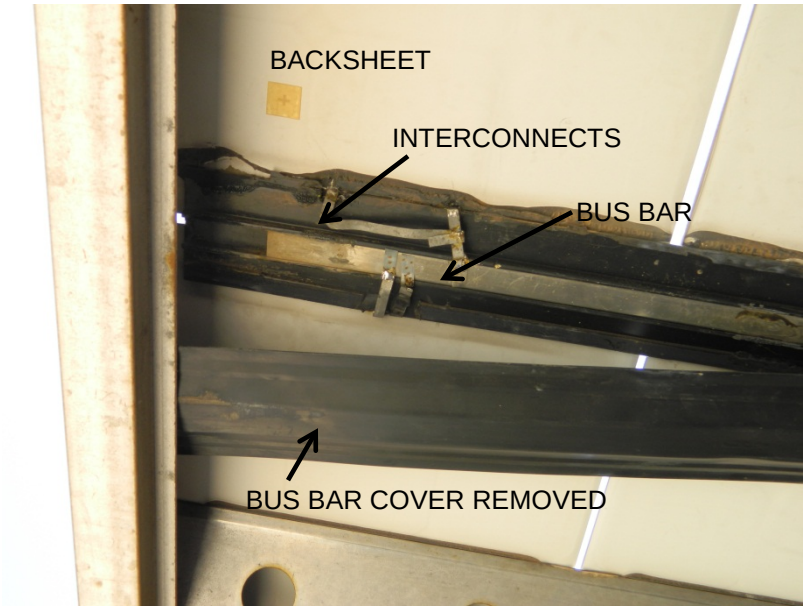

Figure A8 Photo Under Panel Group Busbar Assembly

Table A2 Temperature coefficients of 8 new sample modules

Results of Electrical Performance and Temperature Coefficient Test on 9/23/2011

Module Power Rated @ STC	10.34	7.3	9.45	5.8	73.4	55.0

Module S/N	Performance Measured at STC (1000W/m^2, 25°C)						Temperature Coefficients at Measured at STC (25°C)					
	Isc	Voc	Imp	Vmp	FF	Pm	Isc	Voc	Imp	Vmp	FF	Pm
	A	V	A	V	%	W	A/°C	V/°C	A/°C	V/°C	%/°C	W/°C
1955	9.97	7.2	9.10	5.7	72.2	51.9	0.0025	-0.0283	-0.0059	-0.0287	-0.1499	-0.2913
1957	9.95	7.2	9.02	5.7	71.7	51.4	0.0018	-0.0275	-0.0017	-0.0299	-0.1432	-0.2782
1971	10.09	7.2	9.03	5.8	71.8	52.3	0.0029	-0.0285	0.0031	-0.0330	-0.1389	-0.2830
1974	10.18	7.3	9.23	5.8	71.9	53.1	0.0010	-0.0310	-0.0063	-0.0313	-0.1413	-0.3241
2031	9.95	7.4	9.05	5.8	72.2	52.9	0.0008	-0.0351	-0.0046	-0.0373	-0.1761	-0.3611
2033	9.81	7.4	8.99	5.8	72.6	52.3	0.0035	-0.0289	-0.0041	-0.0294	-0.1519	-0.2836
2038	9.85	7.1	9.00	5.6	71.1	50.0	0.0027	-0.0229	-0.0049	-0.0214	-0.1059	-0.2159
2046	10.09	7.2	9.21	5.6	71.4	51.6	0.0026	-0.0263	-0.0033	-0.0276	-0.1409	-0.2697

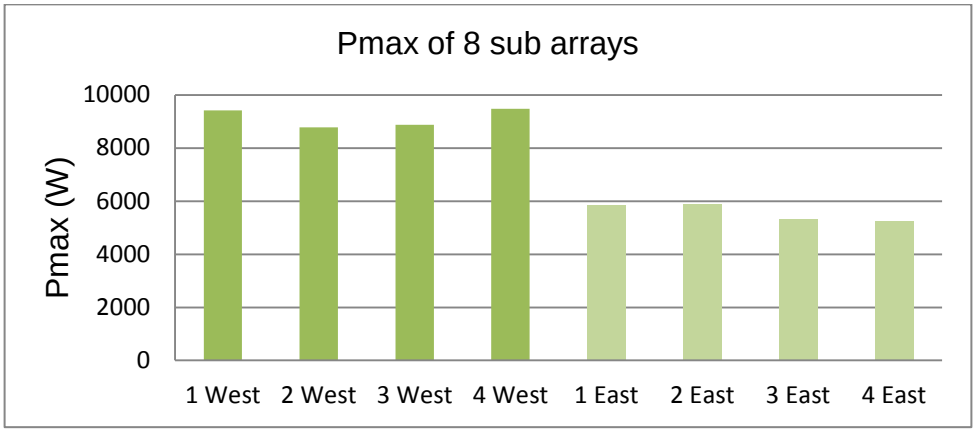

Figure A9 Sub-arrays output power summary

Table A3 Result of 8 Sub-Arrays Measurements

	SUB-ARRAY NUMBER	NUMBER OF PG'S	STC ISC A)	STC VOC (V)	STC PMAX (W)
WEST ARRAY	3-negative	12	65	316	11,139
	4-positive	13	67	344	12,427
	1-negative	12	68	320	12,155
	2-positive	13	66	343	11,672
Average			67	331	11,848
Total	4	50			47,393
EAST ARRAY	3-positive	13	55	340	6,833
	4-negative	12	57	315	6,572
	1-positive	13	58	342	7,628
	2-negative	12	61	316	7,443
Average			58	328	7,119
Total	4	50			28,476

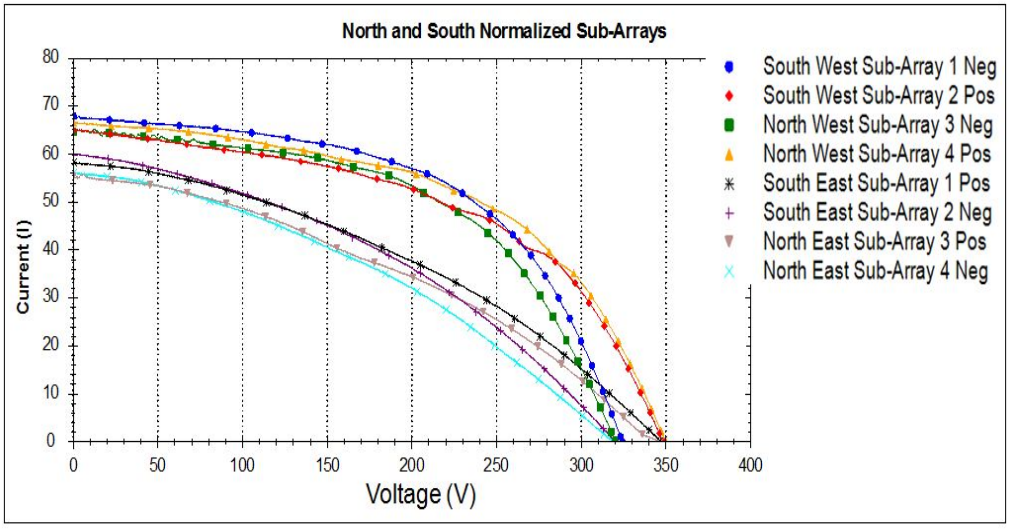

Figure A10 Sub-arrays I-V and P-V curves summary [IVPC3]

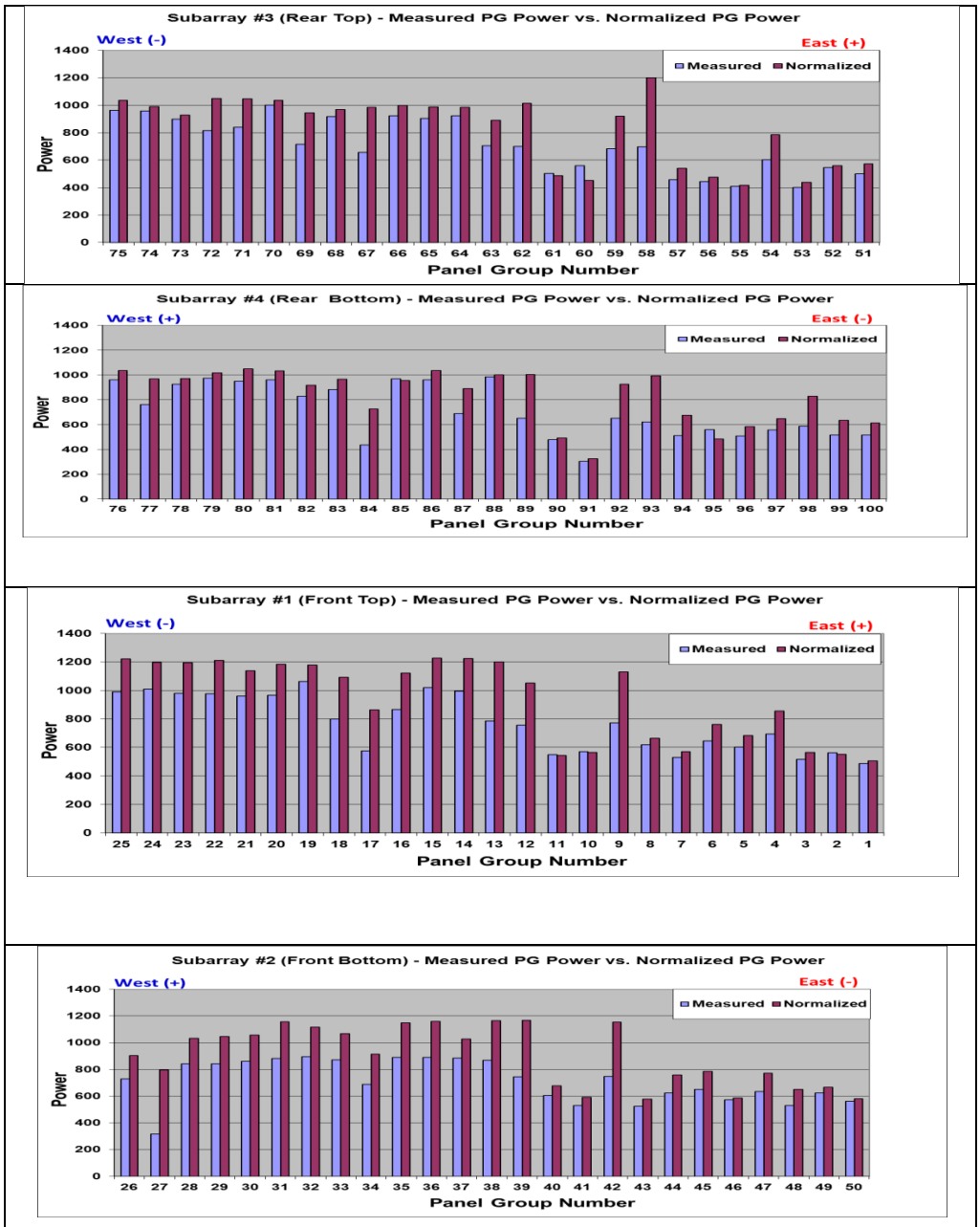

Figure 5:

Figure A11 Power vs. Panel Group for All Subarrays

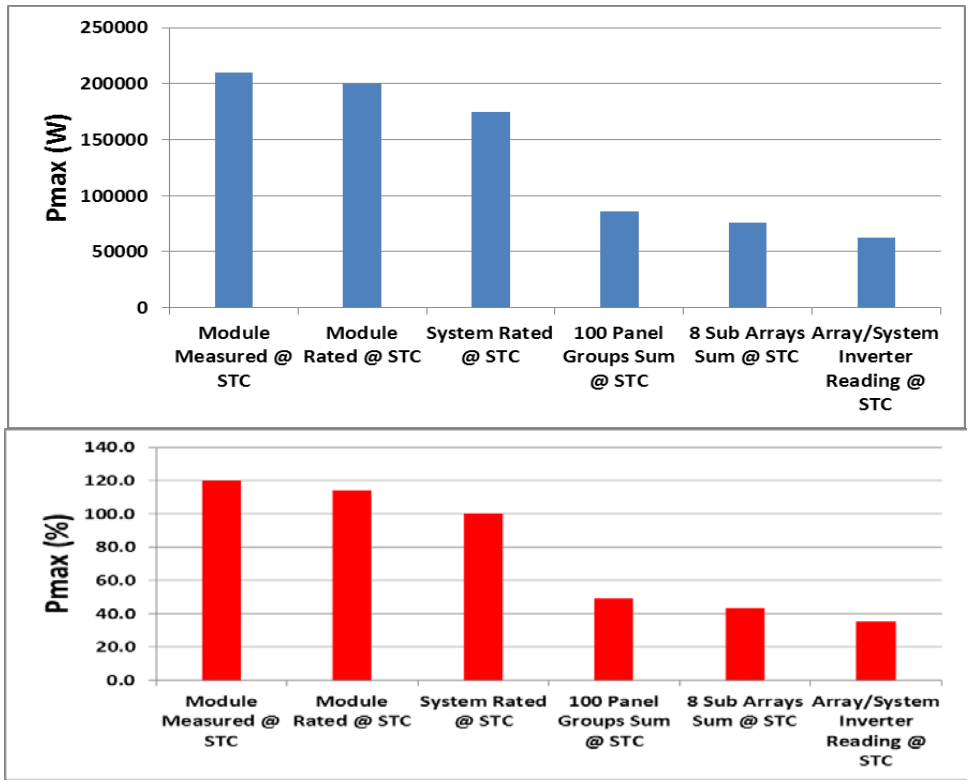

Figure A12 Pmax Values of Ideal and Actual Measured Values

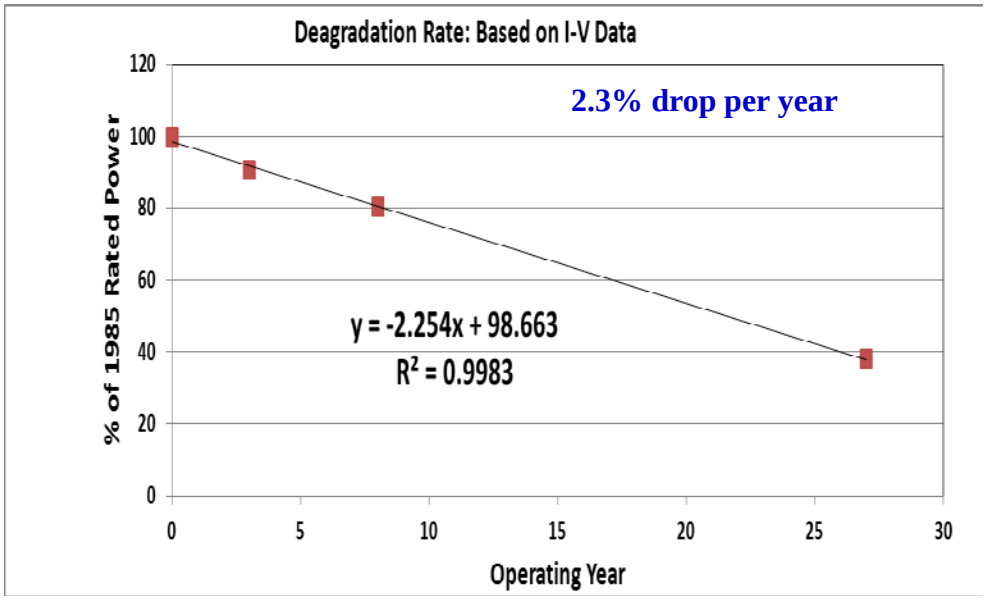

Figure A13 Degradation Plot Using Current and Past I-V Data

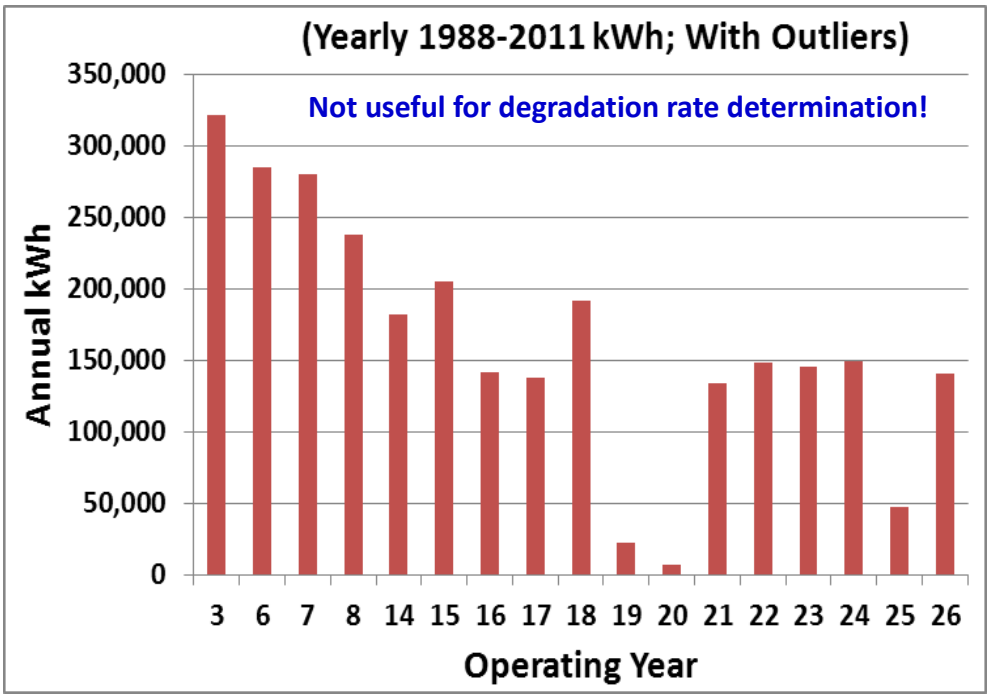

Figure A14 Yearly Inverter Power Meter Output Values Generated From Billing Records

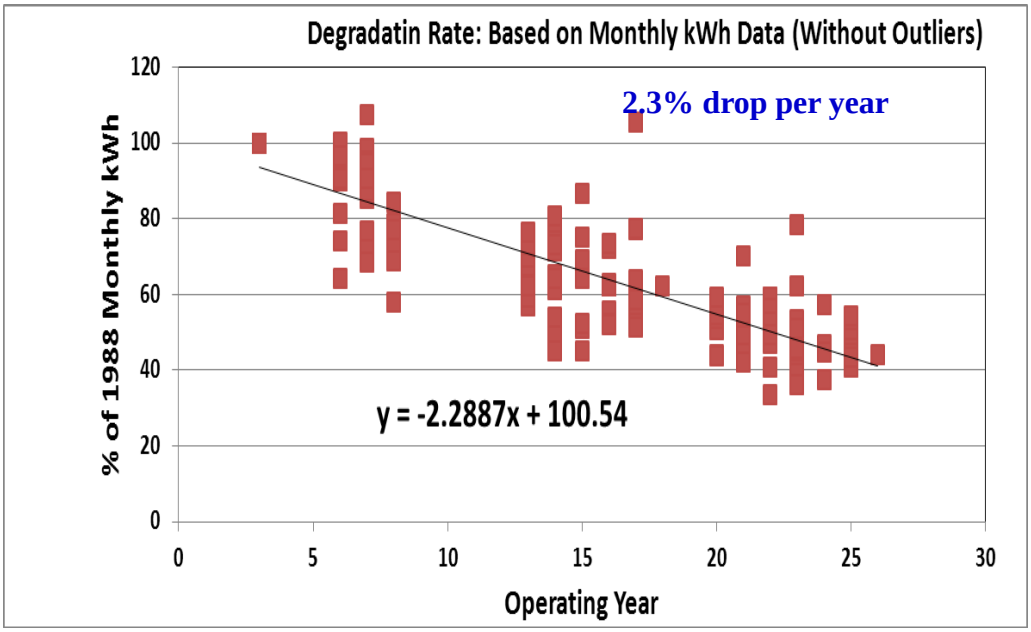

Figure A15 Linear Plot of Yearly Inverter Power Meter Output Values Generated From Billing Records with Outliers Removed

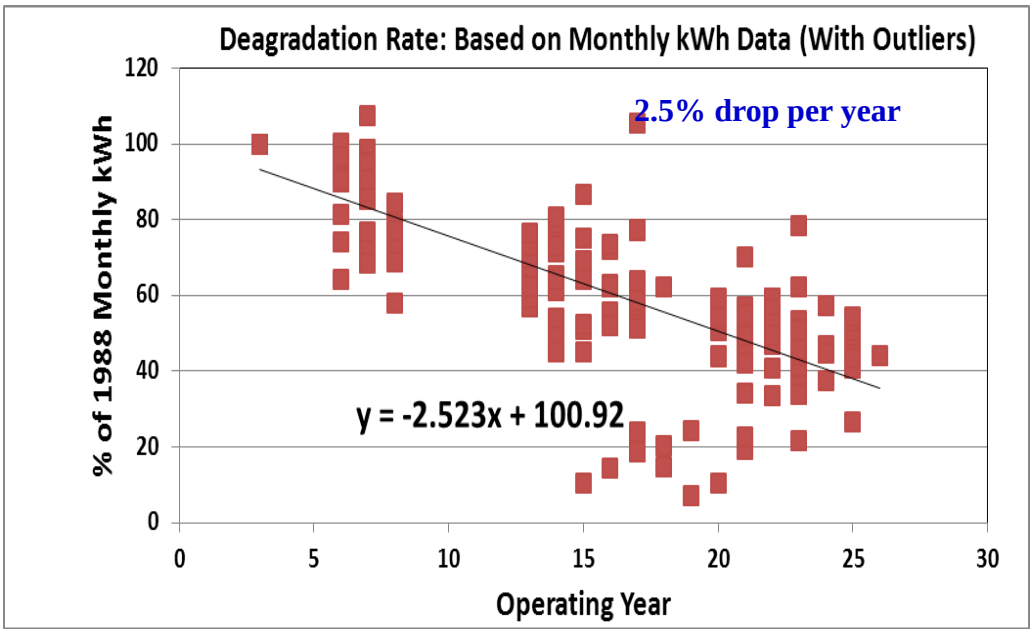

Figure A16 Linear Plot of Yearly Inverter Power Meter Output Values Generated From Billing Records with Outliers

Table A4 Result of High and Low Irradiance Measurements.

HIGH IRRADIANCE					
Panel Group	**PG91**	**PG97**	**PG55**	**PG58**	**PG14**
Voc	29.1	28.6	28.1	28.3	28.9
Isc	51.0	54.4	58.5	85.0	73.8
Fill Factor	23.4	38.4	24.8	43.7	54.8
Peak Power	347.7	597.3	407.9	1053.2	1165.5
Vpeak	12.3	17.7	16.4	20.6	21.1
Ipeak	28.3	33.7	24.8	51.2	55.1
Irradiance	1,000	1,000	1,000	1,000	1,000
Cell Temp.	25	25	25	25	25
LOW IRRADIANCE					
Voc	25.6	25.8	21.6	24.7	25.0
Isc	12.2	12.9	8.3	49.1	13.3
Fill Factor	35.7	49.5	64.8	18.6	66.7
Peak Power	111.3	164.4	115.6	225.9	221.6
Vpeak	17.3	19.6	14.8	19.0	19.5

Ipeak	6.4	8.4	7.8	11.9	11.3
Irradiance	200	200	200	200	200
Cell Temp.	25	25	25	25	25

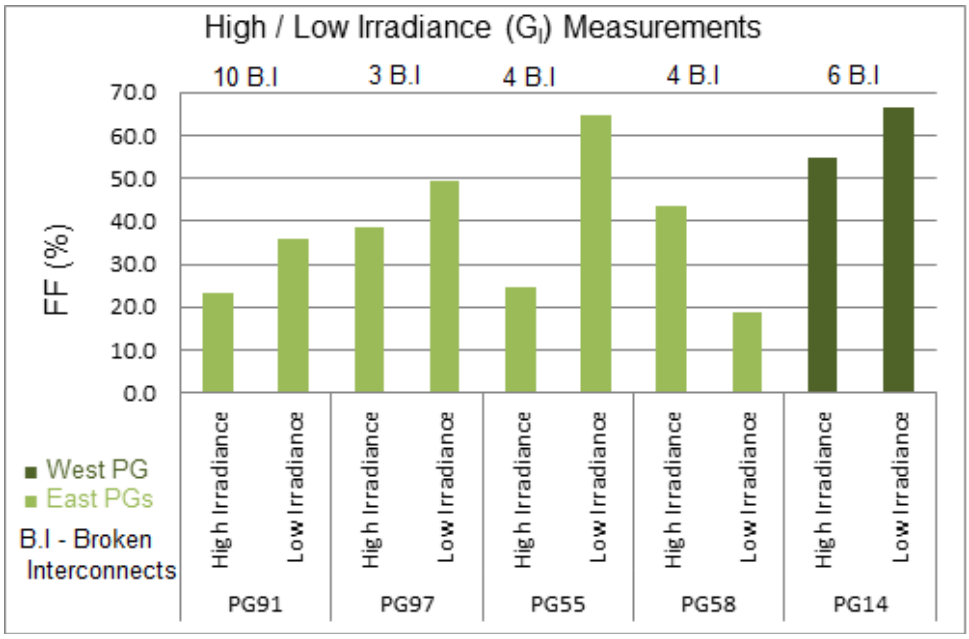

Figure A17 Effect of Low Irradiance on PG's Fill Factor

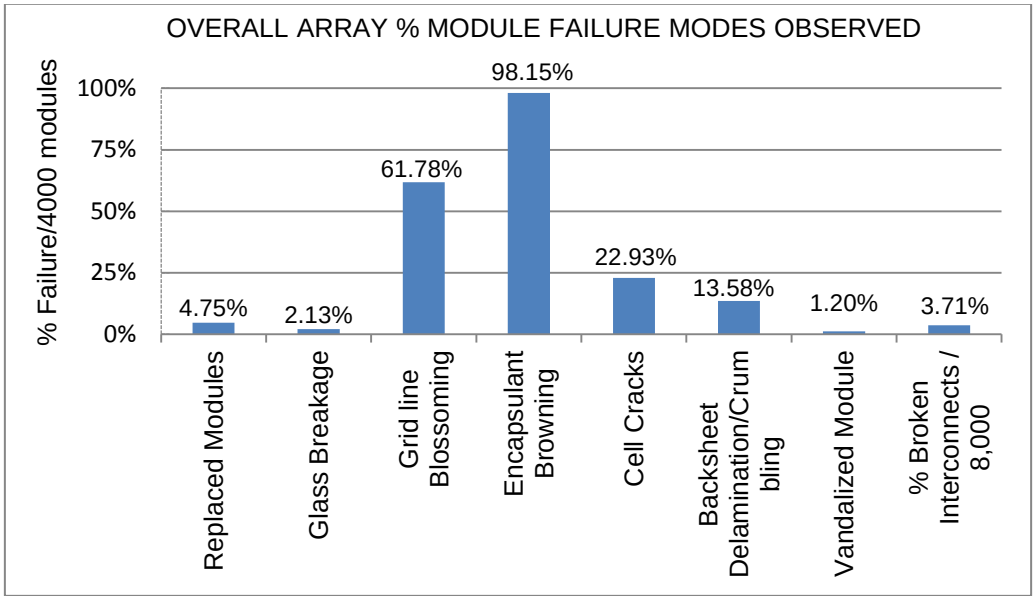

Figure A18 Summary of Physical Defects Counted on PV Array

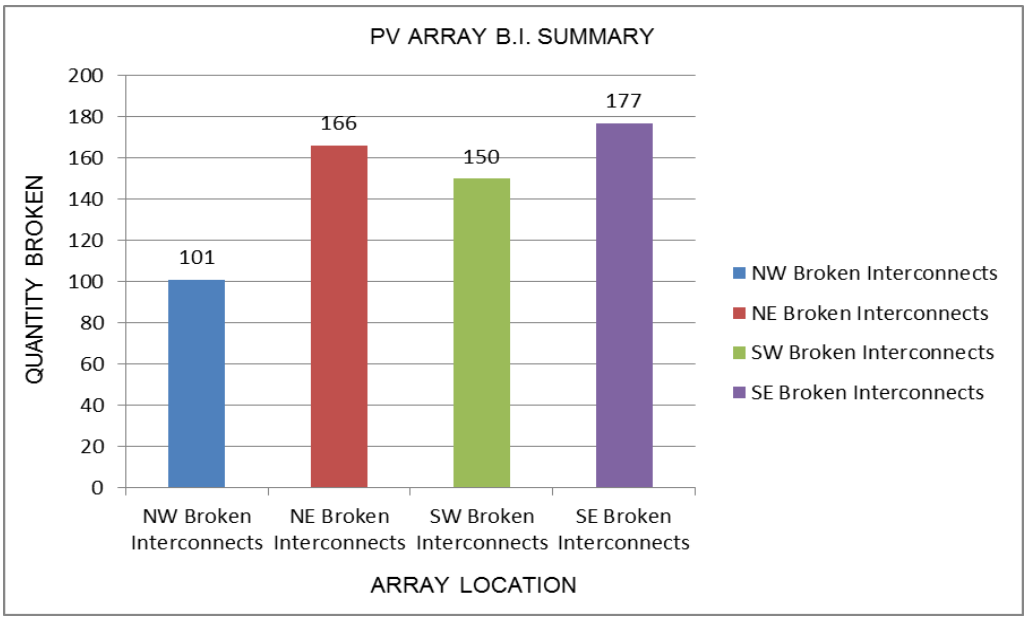

Figure A19 Summary of Broken Interconnects on PV Array

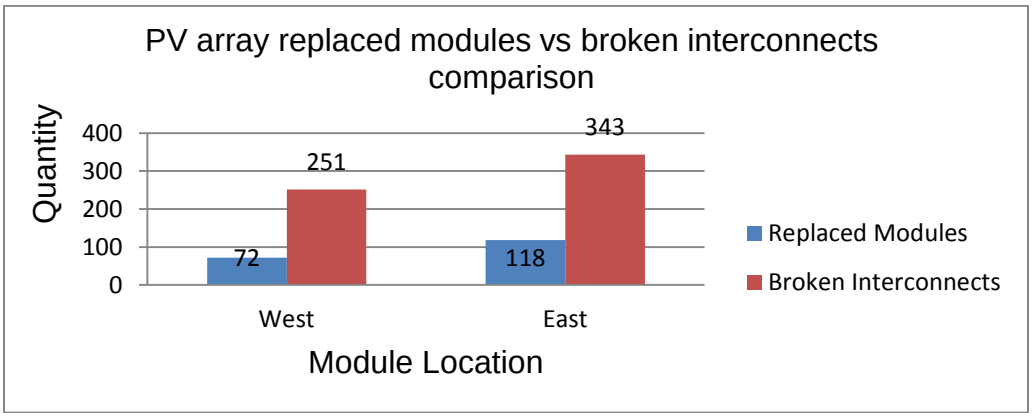

Figure A20 PV Array Replaced Modules Vs Broken Interconnects Location

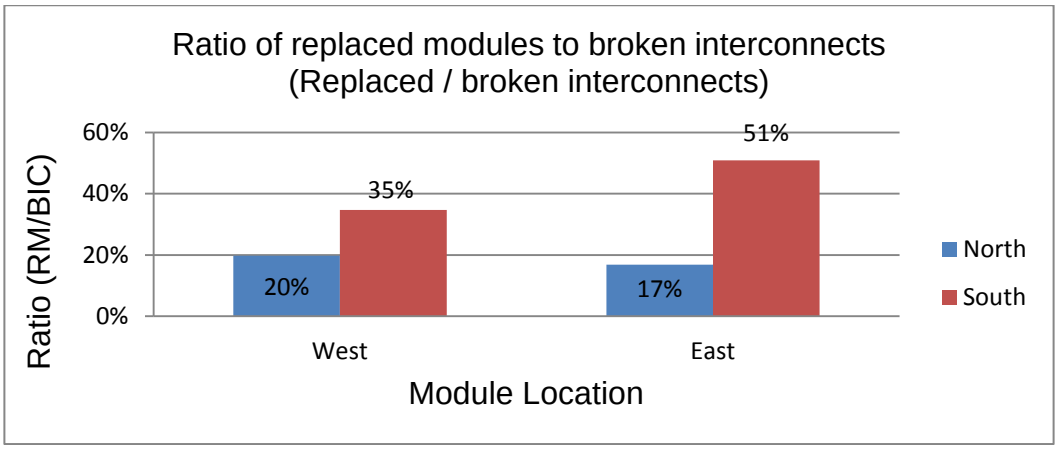

Figure A21 PV Array Ratio of Replaced Modules Vs Broken Interconnects Location

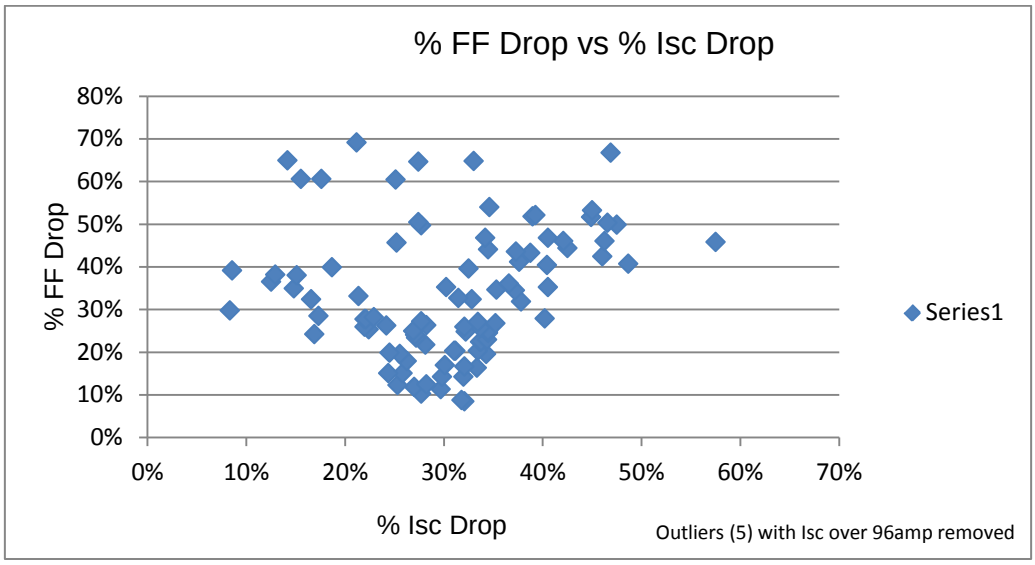

Figure A22 % FF Drop vs % Isc Drop

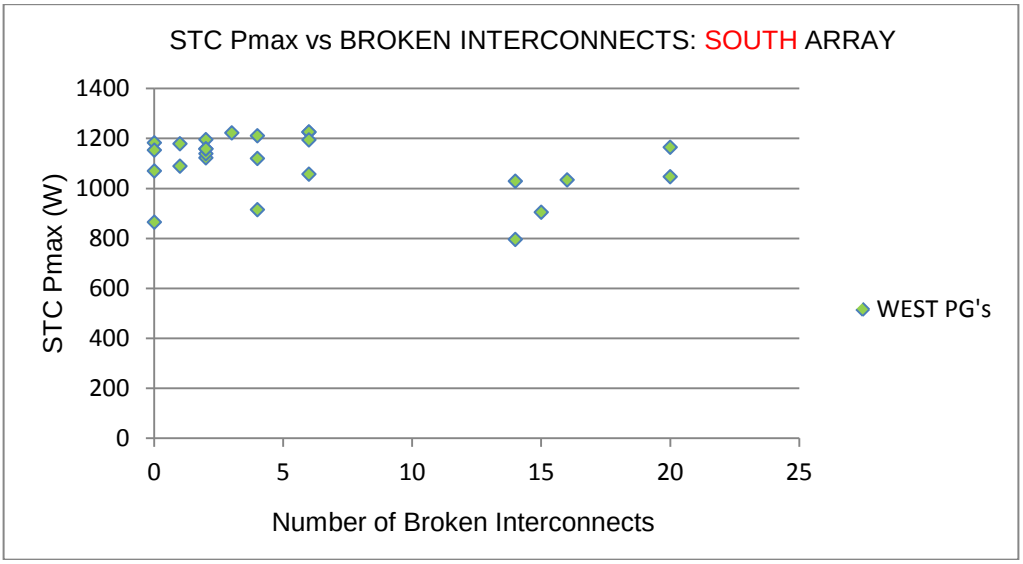

Figure A23 STC Pmax Vs Broken Interconnects: South West Array

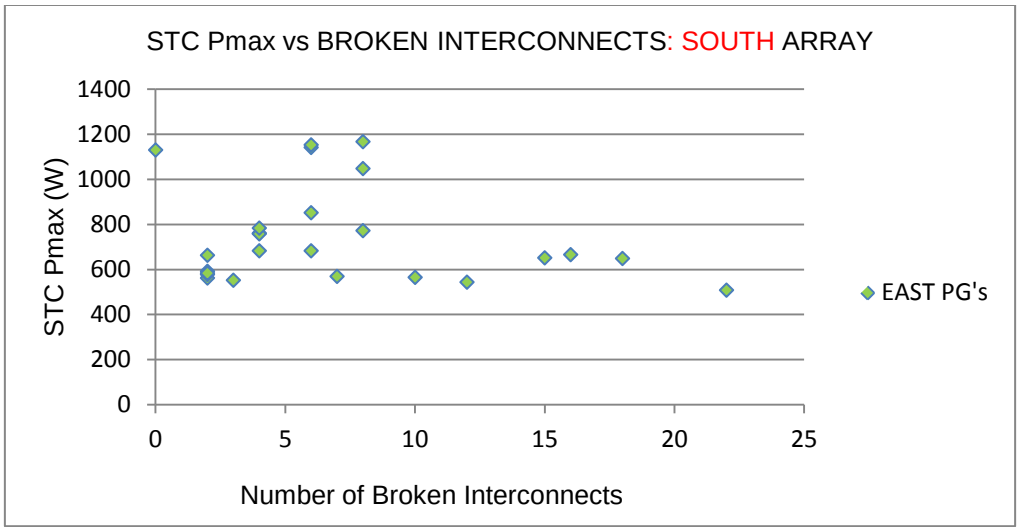

Figure A24 STC Pmax Vs Broken Interconnects: South East Array

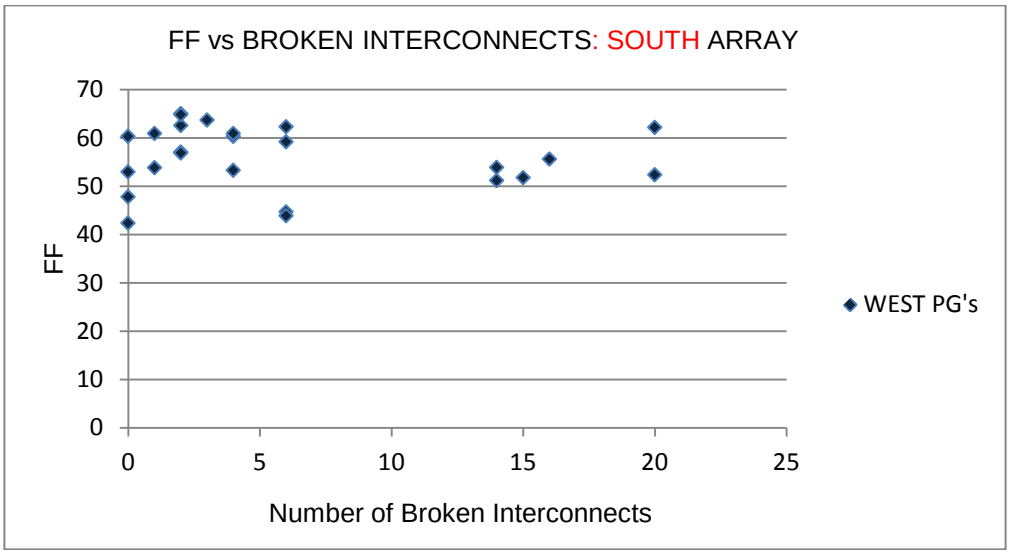

Figure A25 FF Vs Broken Interconnects: South West Array

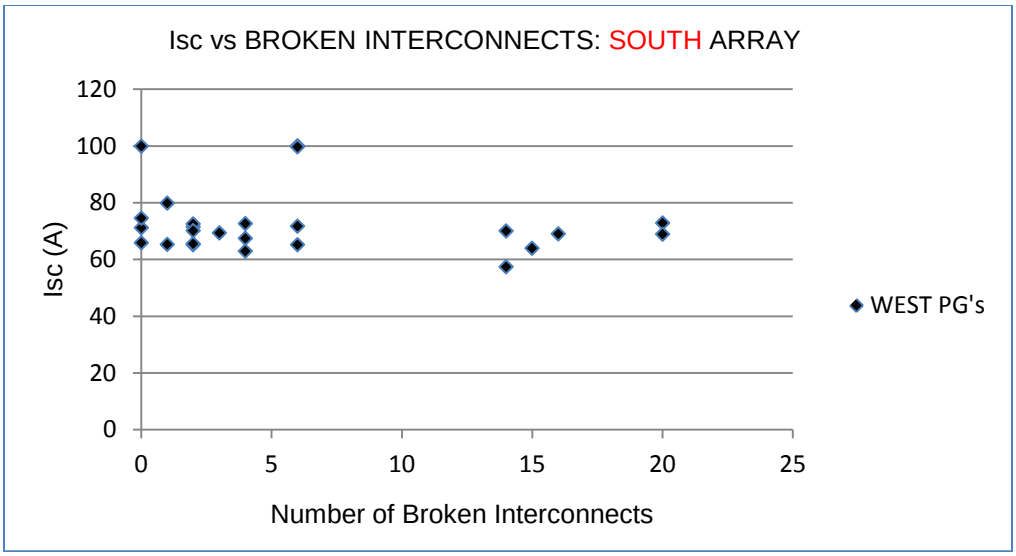

Figure A26 Isc vs Broken Interconnects: South West Array

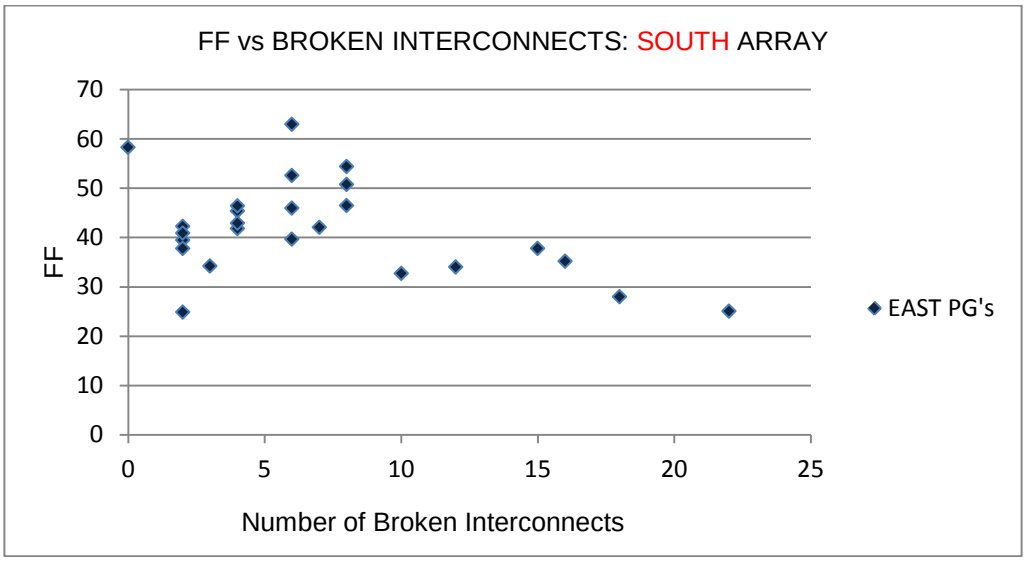

Figure A27 FF Vs Broken Interconnects: South East Array

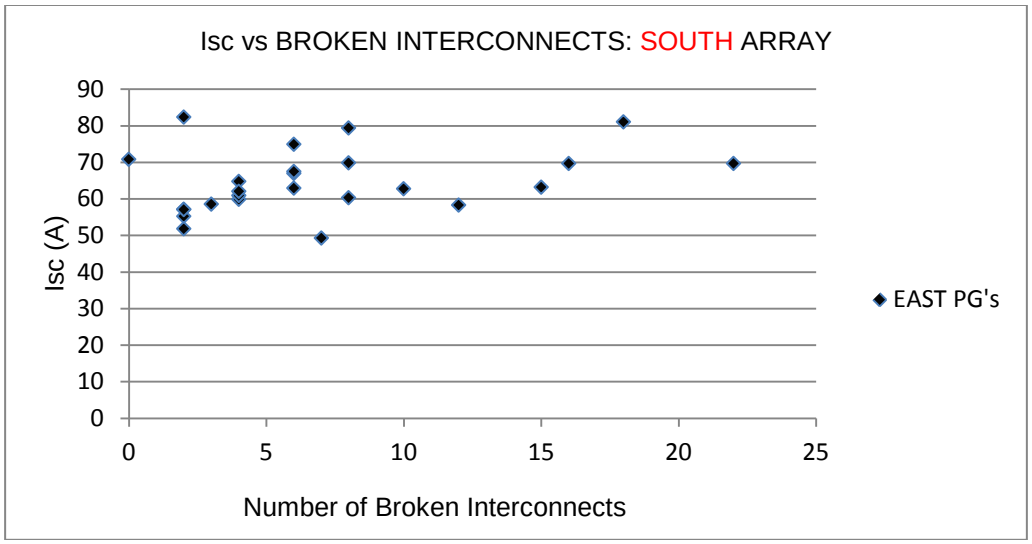

Figure A28 Isc vs Broken Interconnects: South East Array

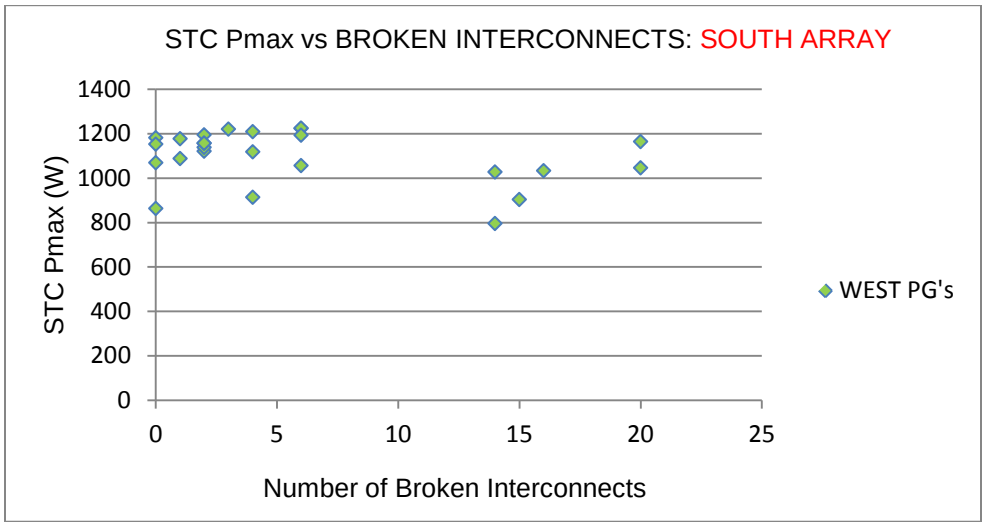

Figure A29 STC Pmax Vs Broken Interconnects: South West Array

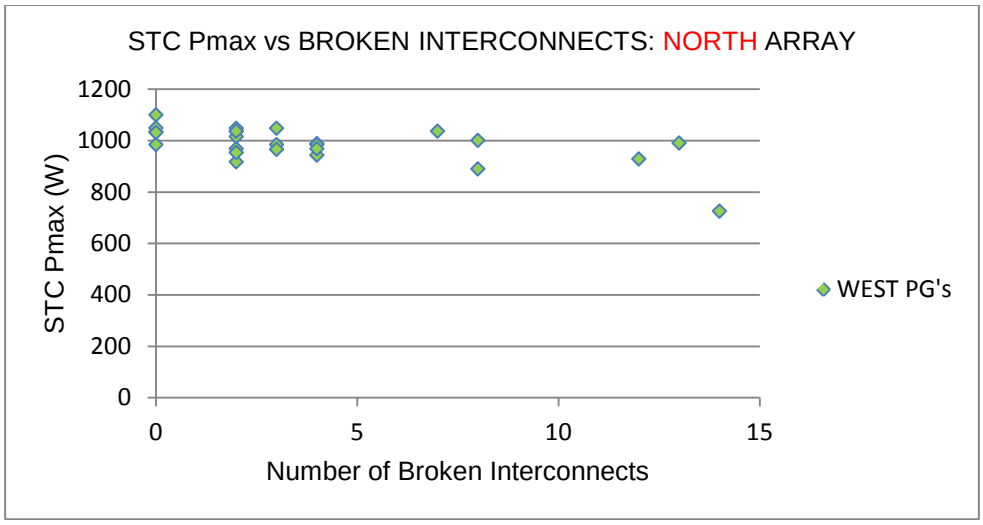

Figure A30 STC Pmax Vs Broken Interconnects: North West Array

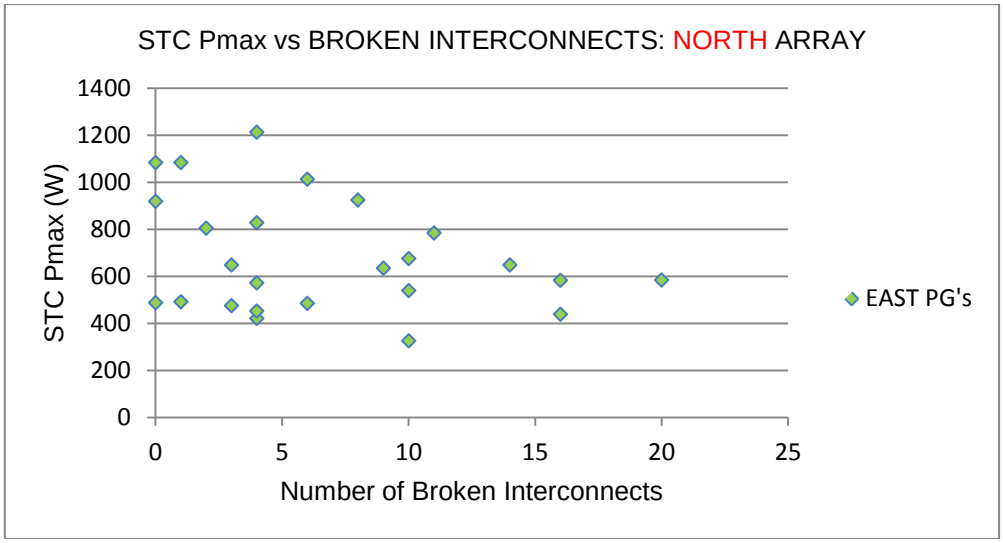

Figure A31 STC Pmax Vs Broken Interconnects: North East Array

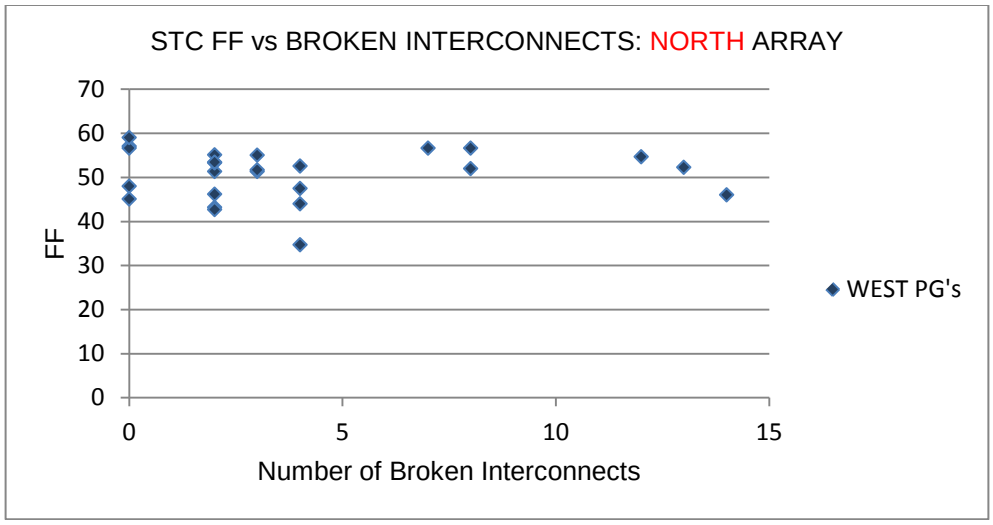

Figure A32 FF Vs Broken Interconnects: North West Array

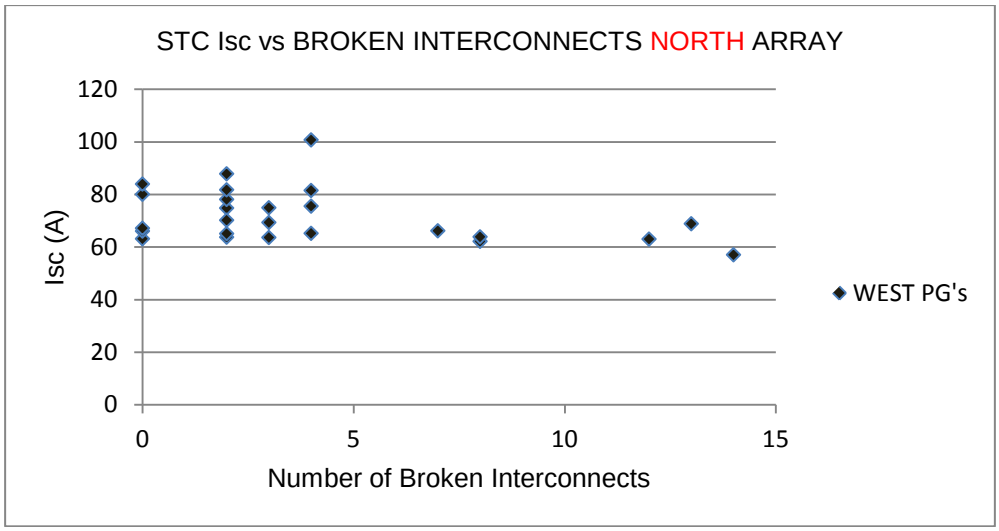

Figure A33 Isc vs Broken Interconnects: North West Array

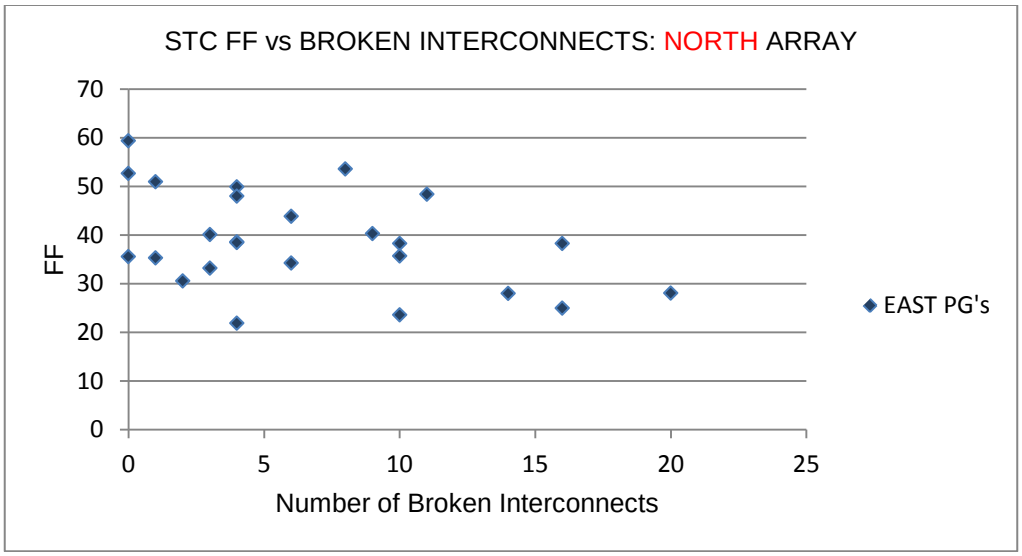

Figure A34 FF Vs Broken Interconnects: North East Array

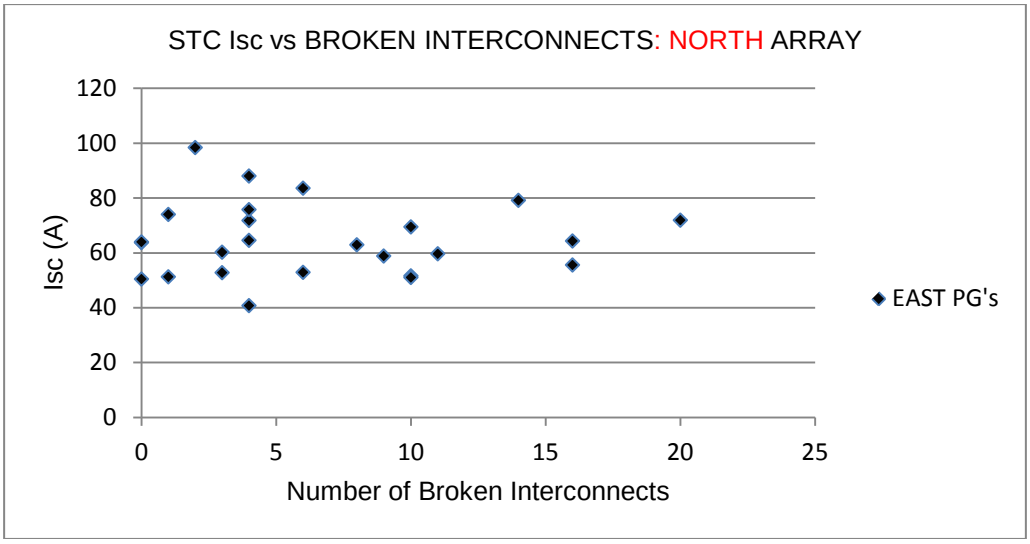

Figure A35 Isc vs Broken Interconnects: North East Array

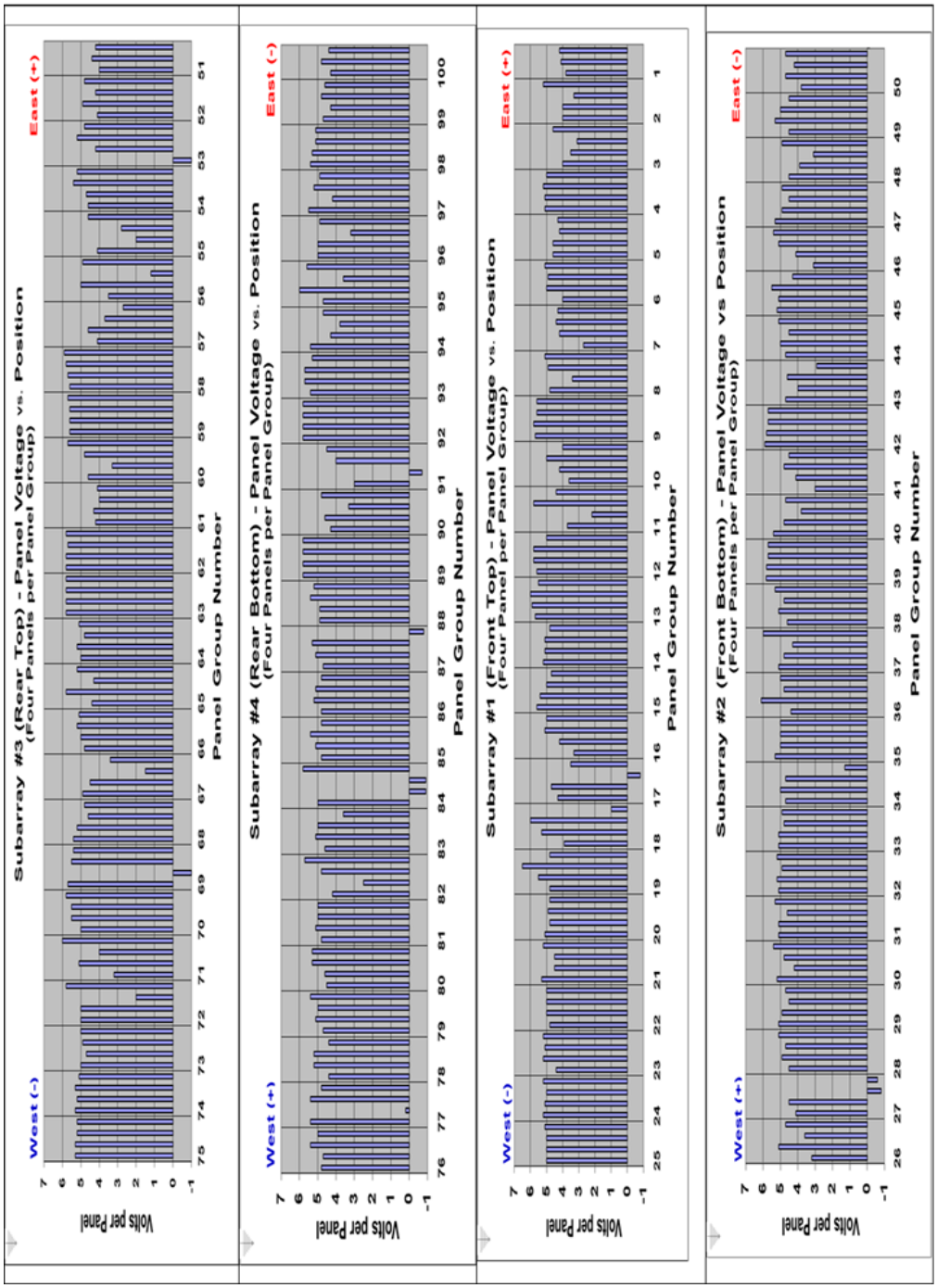

Figure A36 South Array Panel Voltages Measured Under Load

Table A5 Result of Array Temperature Measurements

North Array PG's Average Ambient Temperatures																											
DATE	WEST AVERAGE	West - Sub array 3 PG's - Top Beam IR												East - Sub array 3 PG's - Top Beam IR													EAST AVERAGE
		75	74	73	72	71	70	69	68	67	66	65	64	63	62	61	60	59	58	57	56	55	54	53	52	51	
Day 1 05/03/2012		39.1	40.0	44.0	42.0	42.0	43.0	43.0	45.0	43.0	44.0	45.0	46.0	46.0	46.0	47.0	47.0	46.0	46.0	45.0	43.0	42.0	43.0	44.0	46.0	44.0	
		38.0	42.0	43.0	44.0	43.0	44.0	44.0	45.0	45.0	45.0	46.0	46.0	46.0	46.0	46.0	48.0	47.0	45.0	43.0	42.0	43.0	46.0	45.0	45.0	45.0	
	43.4	38.6	41.0	43.5	43.0	42.5	43.5	43.5	45.0	44.0	44.5	45.5	46.0	46.0	46.0	46.5	47.5	46.5	45.5	44.0	42.5	42.5	44.5	44.5	45.5	44.5	45.1
Day 2 05/04/2012		44.0	44.0	46.0	47.0	46.0	47.0	48.0	48.0	47.0	48.0	48.0	49.0	48.0	48.0	48.0	49.0	48.0	48.0	48.0	45.0	44.0	44.0	44.0	46.0	47.0	
		43.0	44.0	46.0	47.0	47.0	48.0	49.0	48.0	48.0	48.0	49.0	48.0	49.0	48.0	50.0	49.0	49.0	47.0	47.0	46.0	44.0	45.0	45.0	46.0	49.0	
	47.0	43.5	44.0	46.0	47.0	46.5	47.5	48.5	48.0	47.5	48.0	48.5	48.5	48.5	48.0	49.0	49.0	48.5	47.5	47.5	45.5	44.0	44.5	44.5	46.0	48.0	47.0
OVERALL AVERAGE	45.2																										46.0

South Array PG's Average Ambient Temperatures																											
DATE	WEST AVERAGE	West - Sub array 1 PG's - Top Beam IR												East - Sub array 1 PG's - Top Beam IR													EAST AVERAGE
		25	24	23	22	21	20	19	18	17	16	15	14	13	12	11	10	9	8	7	6	5	4	3	2	1	
Day 1 05/03/2012		47.0	47.0	47.0	46.0	47.0	46.0	46.0	46.0	46.0	47.0	46.0	45.0	46.0	46.0	48.0	47.0	48.0	47.0	47.0	47.0	47.0	47.0	47.0	45.0	45.0	
		50.0	47.0	47.0	47.0	47.0	46.0	46.0	46.0	46.0	46.0	46.0	46.0	48.0	48.0	47.0	47.0	47.0	47.0	47.0	47.0	48.0	45.0	47.0	45.0	44.0	
	46.5	48.5	47.0	47.0	46.5	47.0	46.0	46.0	46.0	46.0	46.5	46.0	45.5	47.0	47.0	47.5	47.0	47.5	47.0	47.0	47.0	47.5	46.0	47.0	45.0	44.5	46.7
Day 2 05/04/2012		44.0	44.0	44.0	44.0	45.0	45.0	44.0	44.0	45.0	44.0	44.0	44.0	45.0	45.0	45.0	45.0	45.0	45.0	45.0	46.0	45.0	45.0	46.0	46.0	48.0	
		44.0	43.0	44.0	44.0	44.0	45.0	44.0	44.0	44.0	45.0	44.0	44.0	45.0	45.0	45.0	45.0	45.0	45.0	46.0	45.0	46.0	45.0	45.0	45.0	47.0	
	44.2	44.0	43.5	44.0	44.0	44.5	45.0	44.0	44.0	44.5	44.5	44.0	44.0	45.0	45.0	45.0	45.0	45.0	45.0	45.5	45.5	45.5	45.0	45.5	45.5	47.5	45.4
OVERALL AVERAGE	45.3																										46.0

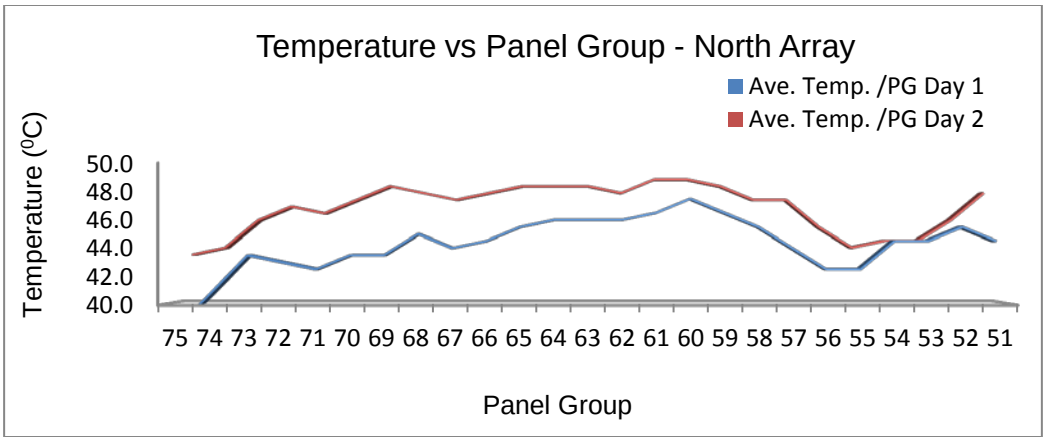

Figure A37 Temperature vs Panel Group - North Array

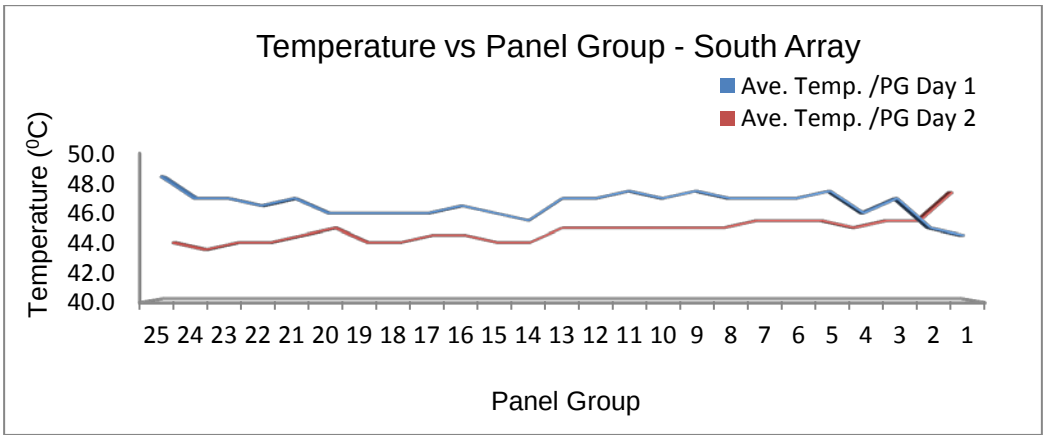

Figure A38 Temperature vs Panel Group - South Array

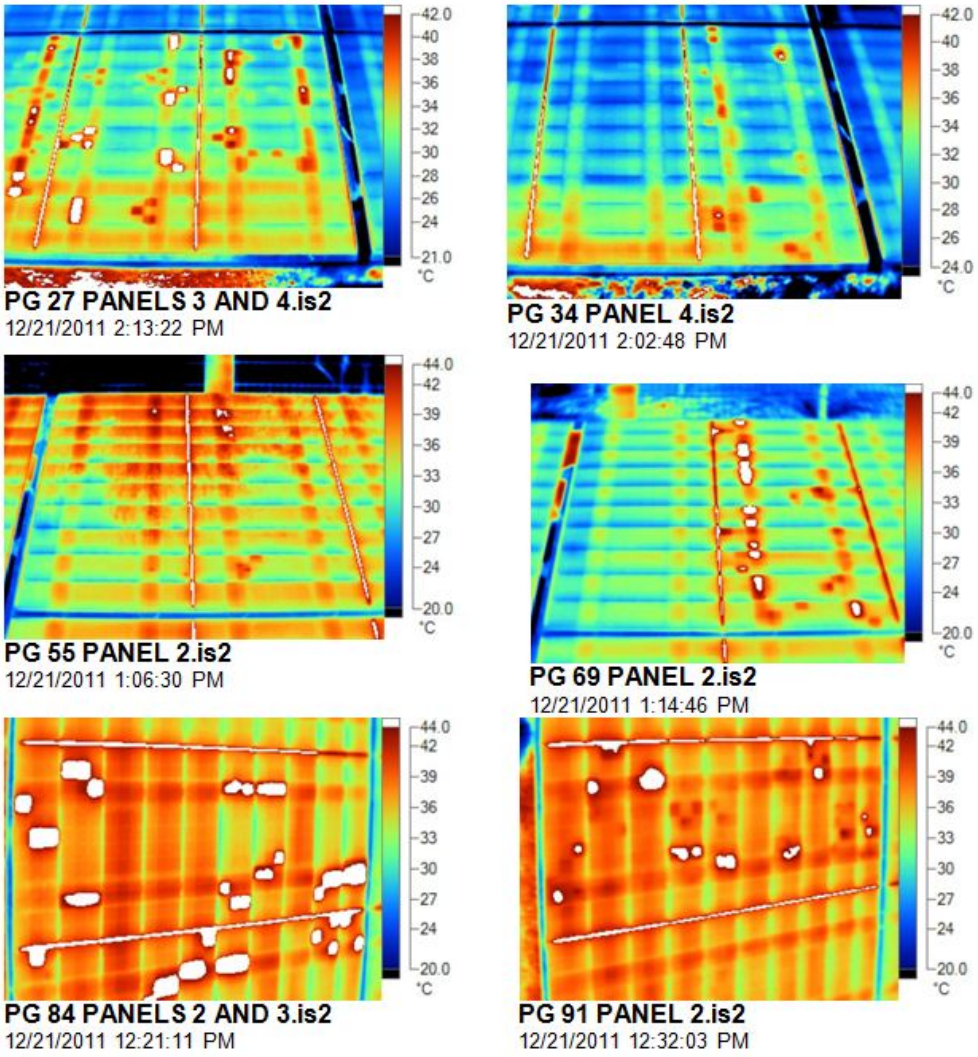

Figure A39 Infrared Photos Showing Hot Spots

Table A6 High Potential Test Resistance Output in mega Ohms (MΩ)

PGs TESTED	DRY CONDITION		VERY WET CONDITION (RAIN)		MILD WET CONDITION (DEW)	
	M +	M-	M +	M-	M +	M-
*14	192.5	371	0.014	0.002	-	-
97	330	190	0.035	0.015	-	-
4	209.4	244.5	0.048	0.08	-	-
*55	177	181	-	-	13.3	36.56
91	183	232	-	-	48	44
58	179	176	-	-	10.5	63.8

Table A7 High Potential Test current Output in milliamps (mA)

PGs TESTED	DRY CONDITION		VERY WET CONDITION (RAIN)		MILD WET CONDITION (DEW)	
	M +	M-	M +	M-	M +	M-
*14	0.0026	0.0013	35.714	250.000	-	-
97	0.0015	0.0026	14.286	33.333	-	-
4	0.0024	0.0020	10.417	6.250	-	-
*55	0.0028	0.0028	-	-	0.038	0.014
91	0.0027	0.0022	-	-	0.010	0.011
58	0.0028	0.0028	-	-	0.048	0.008

* Panel Group has one module with broken glass

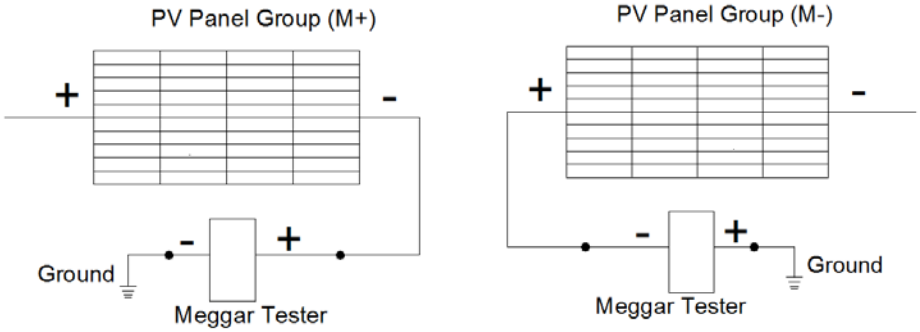

Figure A40 Hi-Pot Insulation Test Wiring for Positive (Left) and Negative (Right) Polarities Above Ground

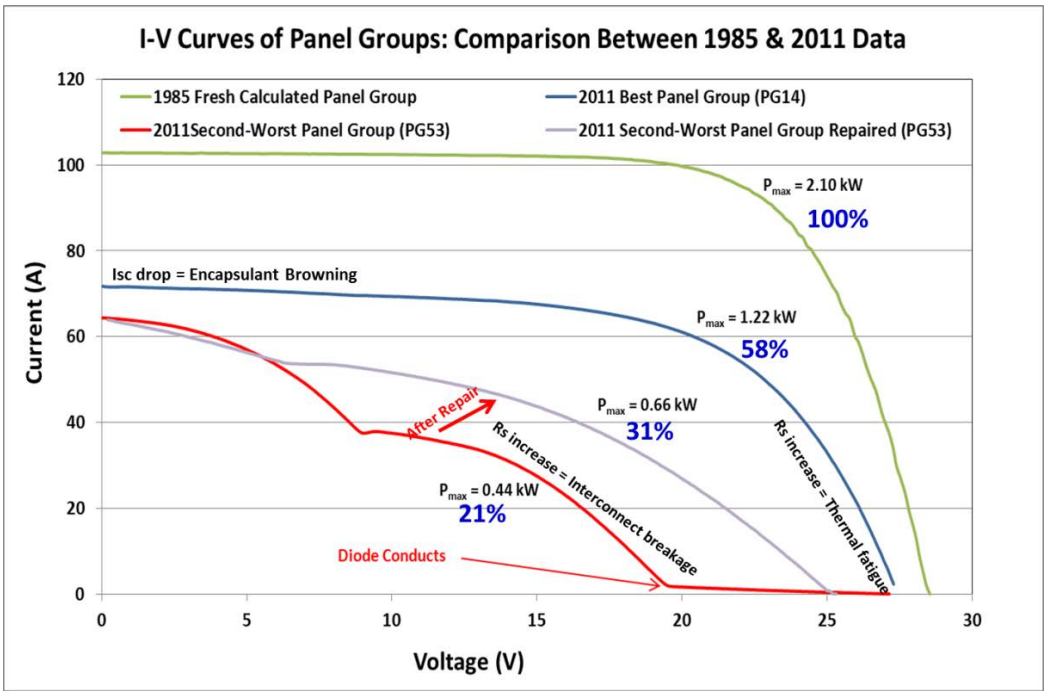

Figure A41 I-V Before and After Interconnect Repair

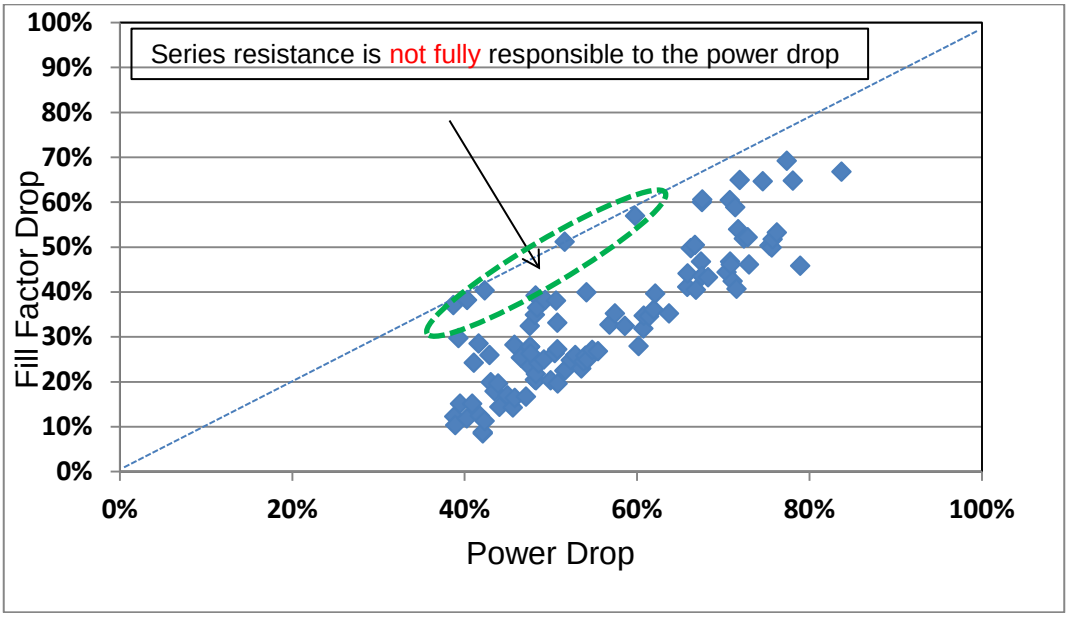

Figure A42 Power One Array FF vs Power Drop

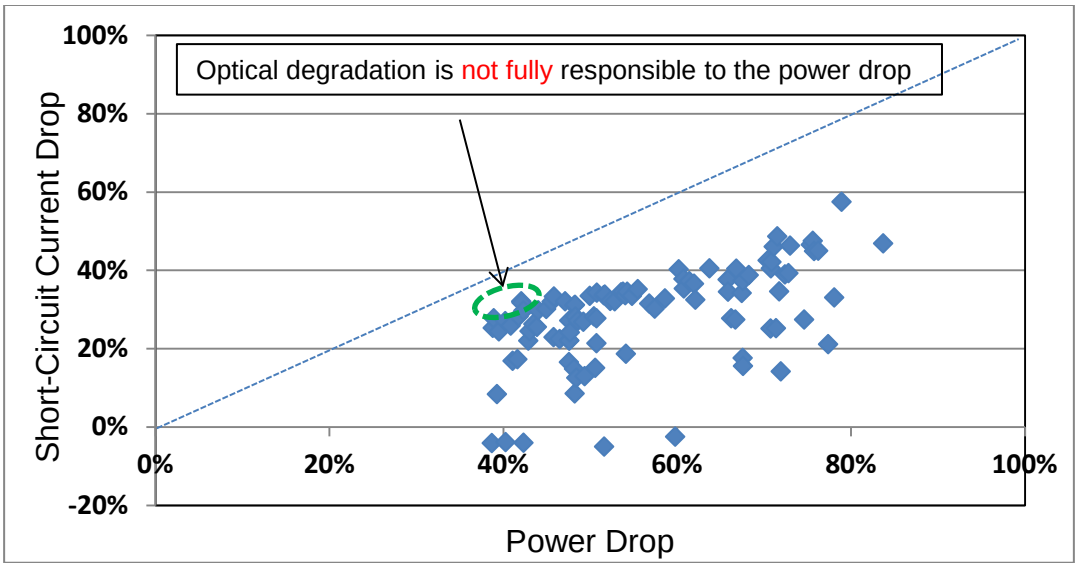

Figure A43 Power One Array Isc vs Power Drop

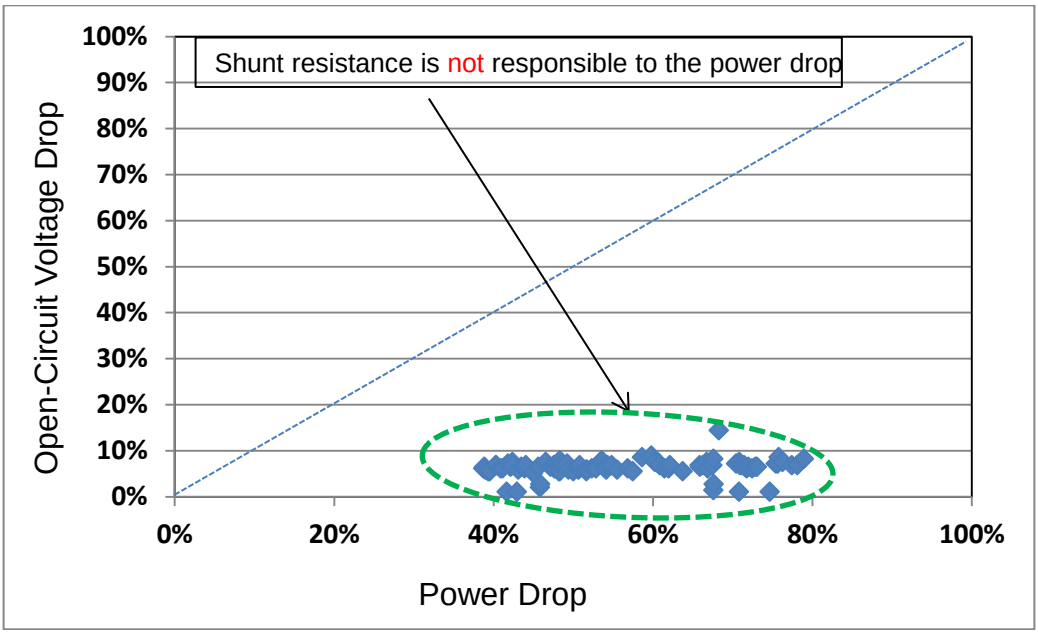

Figure A44 Power One Array Voc vs Power Drop

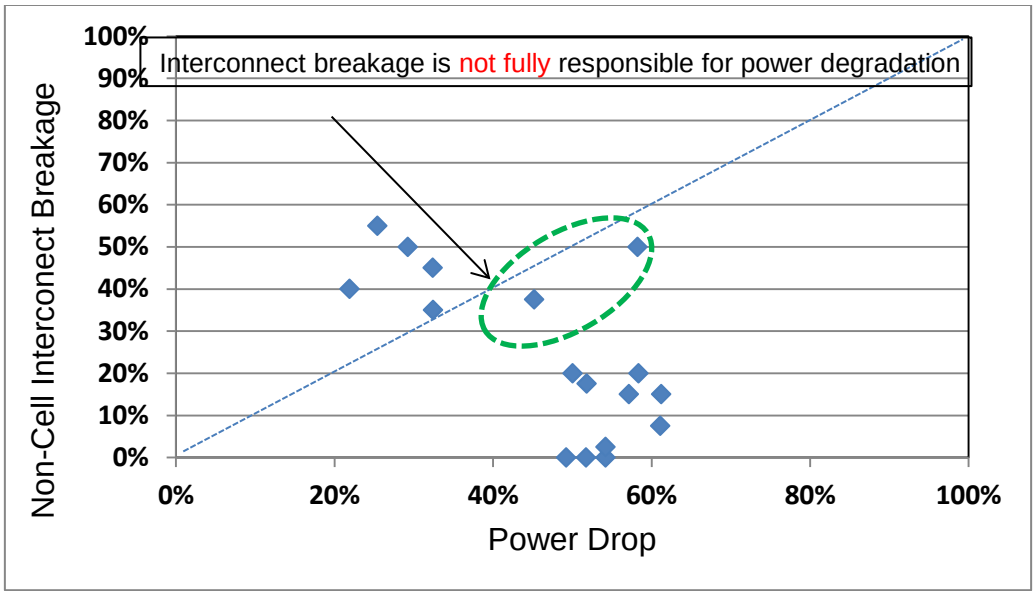

Figure A45 Power One Array Interconnect Breakage vs Power Drop

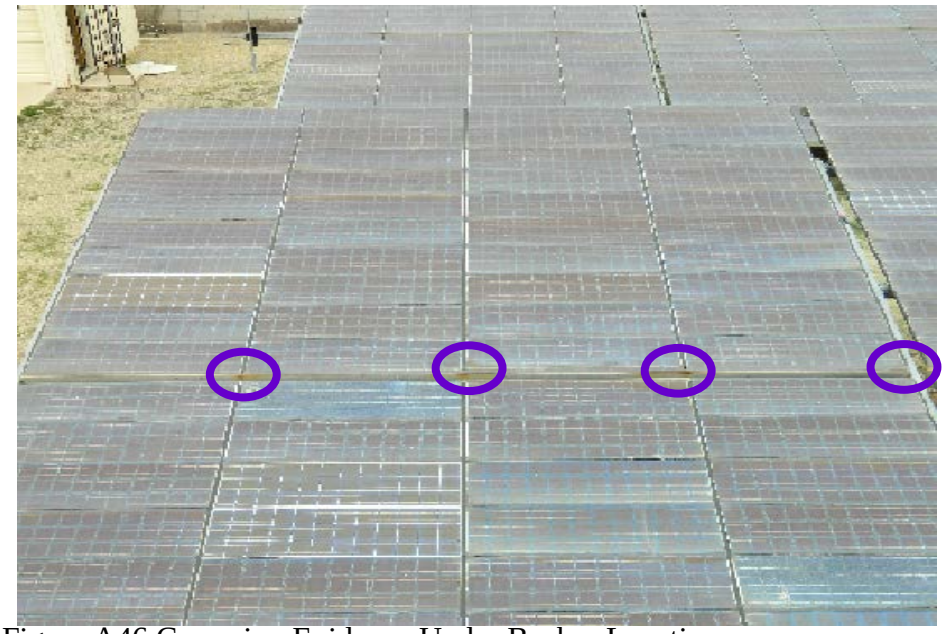
Figure A46 Corrosion Evidence Under Busbar Locations

Table A8 Result of Array Temperature Measurements

Number of Units	Number of Subunits per Unit	Parallel or Series Connection
1	System	NA
2	Arrays per system	Parallel
4	Subarrays per array	Parallel
12 or 13	Panel groups per subarray	Series
4	Panels per panel group	Series
10	Modules per panel	Parallel
Total number of modules = 1x2x4x13x4x10 = 4000		
Voltage of each module = 7.3 V		
Sytem Voltage = 13x4x7.3 ~ 375 V (4 positive and 4 negative as shown below)		

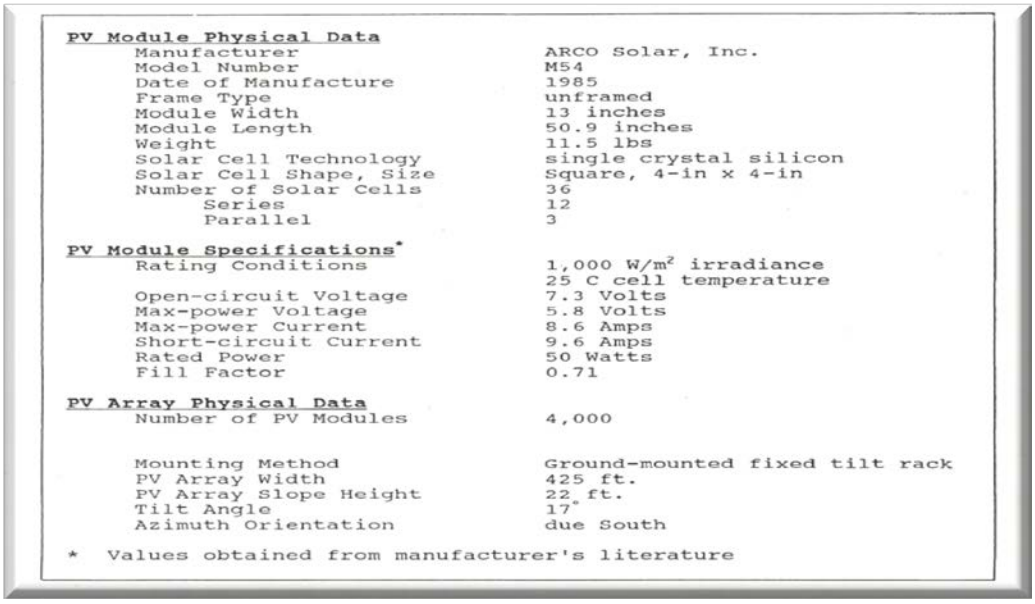

PV Module Physical Data

Manufacturer	ARCO Solar, Inc.
Model Number	M54
Date of Manufacture	1985
Frame Type	unframed
Module Width	13 inches
Module Length	50.9 inches
Weight	11.5 lbs
Solar Cell Technology	single crystal silicon
Solar Cell Shape, Size	Square, 4-in x 4-in
Number of Solar Cells	36
Series	12
Parallel	3

PV Module Specifications*

Rating Conditions	1,000 W/m² irradiance 25 C cell temperature
Open-circuit Voltage	7.3 Volts
Max-power Voltage	5.8 Volts
Max-power Current	8.6 Amps
Short-circuit Current	9.6 Amps
Rated Power	50 Watts
Fill Factor	0.71

PV Array Physical Data

Number of PV Modules	4,000
Mounting Method	Ground-mounted fixed tilt rack
PV Array Width	425 ft.
PV Array Slope Height	22 ft.
Tilt Angle	17°
Azimuth Orientation	due South

* Values obtained from manufacturer's literature

Figure A47 Module and Array Specification [2]

Table A9: Measured Pmax of West Sub-arrays

West Subarray	Panel Groups	Pmax (kW)	Irradiance (W/m^2)	Tamb (^oC)	Tarray (^oC)
Subarray 3 (-ve)	12	8.88	903	33.8	55
Subarray 4 (+ve)	13	9.48	867	35.1	55
Subarray 1 (-ve)	12	9.43	877	34.6	54
Subarray 2 (+ve)	13	8.78	855	32.9	54
Average		9.1425	875.5	34.1	54.5
Total	50	36.57			

Table A10: Measured Pmax of East Sub-arrays

East Subarray	Panel Groups	Pmax (kW)	Irradiance (W/m^2)	Tamb	Tarray
Subarray 3 (+ve)	13	5.32	859	34.3	55
Subarray 4 (-ve)	12	5.27	904	34.4	54
Subarray 1 (+ve)	13	5.83	853	33.5	54
Subarray 2 (-ve)	12	5.88	898	35.4	54
Average		5.575	878.5	34.4	54.25
Total	50	22.3			

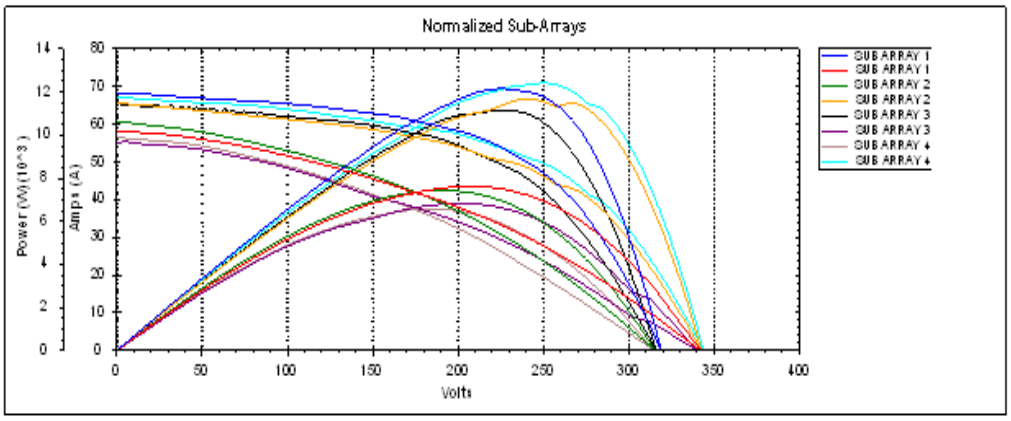

Figure A48 I-V and P-V Curves of 8 Sub-Arrays at STC

Table A11 STC Pmax of West Sub-Arrays

West Subarray #	Panel Groups	Date	Pmax	Isc	Voc	Imax	Vmax	FF
			(W)	(A)	(V)	(A)	(V)	%
Subarray 3 (-ve)	12	10/12/2011	11,139	65	316	50	224	54
Subarray 4 (+ve)	13	10/12/2011	12,427	67	344	49	251	54
Subarray 1 (-ve)	12	10/12/2011	12,155	68	320	54	225	56
Subarray 2 (+ve)	13	10/12/2011	11,672	66	343	49	240	52
Average			11,848	67	331	51	235	54
Total	50		47,393					

Table A12 STC Pmax of East Sub-Arrays

East Subarray #	Panel Groups	Date	Pmax	Isc	Voc	Imax	Vmax	FF
#			(W)	(A)	(V)	(A)	(V)	%
Suarray 3 (+ve)	13	10/12/2011	6,833	55	340	34	199	36
Suarray 4 (-ve)	12	10/12/2011	6,572	57	315	35	185	37
Suarray 1 (+ve)	13	10/12/2011	7,628	58	342	37	206	38
Suarray 2 (-ve)	12	10/12/2011	7,443	61	316	39	192	39
Average			7,119	58	328	36	196	38
Total	50		28,476					

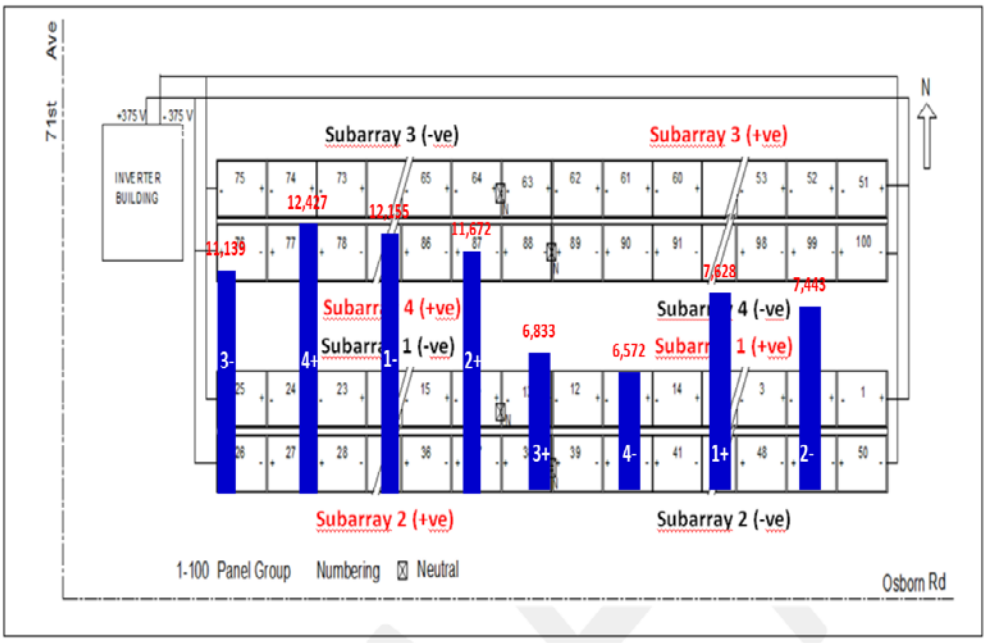

Figure A49 Power vs Location of 8 Sub-Arrays

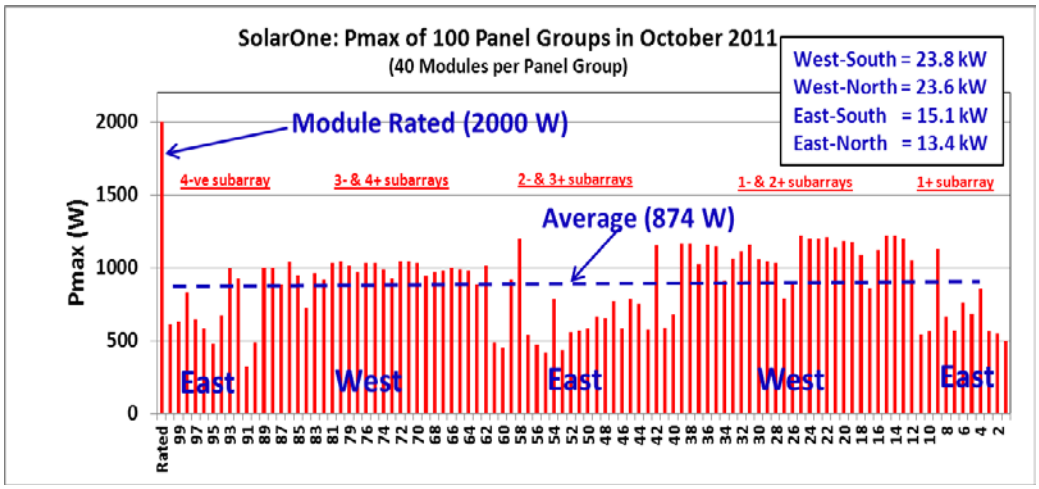

Figure A50 Panel Group Number versus STC Pmax Plot

John F Long

Reprinted by authorization of John F. Long Foundation

Figure A51 John F. Long with GE Representative Ronald Regan

Figure A 52 Team Working Under North Array

Figure A53 Team Working Under South Array with Scorpion Mascot